

# Comprehensive Review of Climate Change and the Impacts on Cryosphere, Hydrological Regimes and Glacier Lakes

## Authors

A.F. Lutz, MSc.  
Dr. W.W. Immerzeel  
Dr. M. Litt  
Dr. S. Bajracharya  
Dr. A.B. Shrestha

December 2015

# Summary

The climate, cryosphere and hydrology of the Hindu Kush Himalaya (HKH) region have been changing in the past and will change in the future. In this literature review, the state of knowledge regarding climate change and its connections to changes in the cryosphere and hydrology has been investigated, with a specific focus on impacts for hydropower development.

From historical trends in climate it is clear that air temperature has been increasing in the HKH region over the past decades. Rates of increase are different for daily mean air temperature, maximum air temperature and minimum air temperature. Temperature in the higher elevations increased more over time than temperature in lower elevations. Historical precipitation trends on the other hand show no significant increasing or decreasing trends overall, but the trends vary locally.

Projections of future climate are made using dynamically or statistically downscaled General Circulation Models and Regional Climate Models. The current state of knowledge indicates that climate warming is likely to continue during the 21<sup>st</sup> century. The projections of precipitation change are uncertain as the climate models project a wide range of possible futures, including strong precipitation increases and precipitation decreases. An increase in precipitation is most likely for the upstream Ganges and Brahmaputra, but the magnitude is highly uncertain. Precipitation projections for the upstream Indus show increases as well as decreases with large uncertainties related to the projections. Extreme precipitation events are likely to be more severe and occur with higher frequency. For the Indian summer monsoon precipitation totals, precipitation intensity, inter-annual variability in monsoon strength, and inter-daily variability are likely to increase. It is important to note that the current state-of-the-art climate models have significant difficulties in simulating the complex climate in the HKH region. Only a limited number of models can satisfactorily simulate the monsoon dynamics and no single model is able to simulate all important features in the HKH precipitation regimes.

In the past years, much knowledge has been gathered regarding the cryosphere in the HKH region. Glaciers in most of the HKH region are losing mass in response to climate warming, but glaciers in the Karakoram region have been growing in recent years. The reason for this “Karakoram anomaly” is not yet fully understood. Despite scientific progress, estimates of total ice volume vary considerably because of the difficulties of estimating ice volumes in situ or from remote sensing products. No strong trends in snow cover changes have been observed. Minor increases or decreases have been reported for different areas. Little is known about the distribution of permafrost in the HKH region. Thus its importance for the regional hydrology remains unclear as well. Estimates of future glacier volumes and areas are uncertain and are hampered because modelling of ice flow is restricted to catchment scale studies. However, strong decreases in glacier volume and area are projected for the HKH region as a whole.

As a result of glacier retreat, the number of proglacial lakes is increasing rapidly and existing lakes are increasing in area and volume. The lakes are often dammed by moraines, which can be unstable. Dam failure can result in glacial lake outburst floods (GLOF) which can have devastating downstream effects. Glacial lakes are being monitored more extensively, but proper mitigation remains challenging.

In summary, consistent trends of climate change related impacts on hydrology in the HKH region are recognized, but detailed analyses at catchment scale remains necessary for proper

assessment of climate change induced hydrological risks for candidate hydropower development sites. These analyses should also consider other factors influencing suitability for hydropower development, such as health, safety and security, environmental and social factors.

It is recommended that ICIMOD jointly with Statkraft develop a research program that focuses more strongly on the understanding of impacts of climate change at catchment level, and specifically in those catchments which are candidates for hydropower development. Such a joint research program will have to be based on a well thought through design to address the spectrum of research requirements that became apparent in this review.

# Table of contents

|          |   |           |
|----------|---|-----------|
| <b>1</b> | <b>Introduction</b>   | <b>9</b>  |
| 1.1      | Background and regional context   | 9         |
| 1.2      | Hydropower issues in the HKH  | 9         |
| 1.3      | Hydropower potential in the Himalayan region                                      | 10        |
| 1.4      | Criteria for hydropower development   | 12        |
| 1.5      | About this review   | 13        |
| 1.6      | Geographic scope  | 14        |
| 1.7      | Thematic scope  | 14        |
| <b>2</b> | <b>Climate Change and its Variability</b>   | <b>16</b> |
| 2.1      | Historical trends and variability   | 16        |
| 2.2      | Climate change studies  | 20        |
| 2.2.1    | Climate modeling and climate change scenarios                                     | 20        |
| 2.2.2    | Downscaling techniques  | 22        |
| 2.3      | Future climate change and variability in the Indus, Ganges and Brahmaputra basins | 26        |
| 2.4      | Performance of climate models   | 29        |
| 2.4.1    | Monsoon dynamics  | 29        |
| 2.5      | Summary remarks   | 32        |
| <b>3</b> | <b>Cryosphere Dynamics</b>  | <b>33</b> |
| 3.1      | Cryosphere components distribution  | 33        |
| 3.1.1    | Glaciers  | 33        |
| 3.1.2    | Snow cover  | 35        |
| 3.1.3    | Permafrost  | 35        |
| 3.2      | Approaches to measure cryosphere components                                       | 36        |
| 3.2.1    | In-situ   | 36        |
| 3.2.2    | Remote Sensing  | 39        |
| 3.2.3    | Modelling   | 41        |
| 3.3      | Results   | 43        |
| 3.4      | Glacier observations  | 43        |
| 3.4.1    | Indus   | 44        |
| 3.4.2    | Ganges  | 45        |
| 3.4.3    | Brahmaputra   | 46        |
| 3.5      | Glacier simulations   | 47        |
| 3.6      | Snow cover  | 49        |
| 3.7      | Key limitations   | 50        |
| 3.8      | Summary remarks   | 51        |
| <b>4</b> | <b>Hydrological Regime</b>  | <b>52</b> |
| 4.1      | Approaches to quantifying the hydrological regime                                 | 52        |
| 4.1.1    | Types of models   | 52        |
| 4.1.2    | Driving input data for hydrological models  | 52        |
| 4.1.3    | Process representation  | 52        |
| 4.2      | Main results  | 53        |
| 4.2.1    | Observed historical hydrological trends   | 53        |
| 4.2.2    | Streamflow composition  | 53        |
| 4.2.3    | Long-term projections   | 54        |
| 4.2.4    | Intra-annual changes in flow  | 56        |
| 4.2.5    | Extreme events  | 58        |
| 4.3      | Summary remarks   | 58        |

|          |  |           |
|----------|--|-----------|
| <b>5</b> | <b>Glacial Lakes and GLOF</b>                            | <b>60</b> |
| 5.1      | Glacier lakes in HKH basins                              | 60        |
| 5.2      | Trends in glacial lakes                                  | 62        |
|          | 5.2.1 Glacial lake trends in the Bhutan Himalaya         | 63        |
|          | 5.2.2 Glacial lake trends in the Nepal Himalaya          | 63        |
| 5.3      | Critical lakes   | 65        |
| 5.4      | Case studies   | 66        |
|          | 5.4.1 Vulnerability assessment                           | 66        |
|          | 5.4.2 Mitigation and Early Warning Systems in the region | 68        |
| 5.5      | Summary remarks  | 71        |
| <b>6</b> | <b>Conclusions</b>                                       | <b>72</b> |
| 6.1      | Summary of results                                       | 72        |
| 6.2      | Impacts on hydropower                                    | 73        |
| 6.3      | Limitations in our understanding                         | 74        |
| 6.4      | Research proposal  | 74        |
| <b>8</b> | <b>References</b>  | <b>76</b> |

## Tables

|   |    |
|---|----|
| Table 1: Constraints on the development of small hydropower projects in the HKH region.<br>Source: [Vaidya, 2012] .....                                       | 13 |
| Table 2: Overview of gridded meteorological products. ....  | 17 |
| Table 3: Description and visualization of the four representative concentration pathways<br>(RCPs).....   | 21 |
| Table 4: Glacier cover and volume estimates from different studies in the Indus, Ganges and<br>Brahmaputra basins. ....                                       | 34 |
| Table 5: Glacier volume estimates for the whole HK region following different studies (km <sup>3</sup> )....  | 35 |
| Table 6: List of glaciers for which in-situ mass balance measurements were conducted in the<br>Indus, Ganges and Brahmaputra river basins (source: WGMS)..... | 44 |
| Table 7: Observed mass balance by remote sensing methods from various studies in the HKH<br>region during recent years.....                                   | 46 |
| Table 8: Results from various regional modeling studies of future glacier changes in the HKH<br>region.....   | 47 |
| Table 9: Overview of some of the available sub-basin scale studies on snow cover in the HKH<br>and methods used. ....   | 49 |
| Table 10: Contribution to total runoff by different components averaged over the upstream<br>basins [Lutz et al., 2014]. ....                                 | 54 |
| Table 11: Results of studies estimating streamflow composition at selected locations. ....  | 55 |
| Table 12: summary of glacial lakes and potentially dangerous glacial lakes in selected parts of<br>the HKH region. ....                                       | 61 |
| Table 13: Number and area of glacial lakes in the Third Pole (Source: [Zhang et al., 2015]) ....  | 62 |
| Table 14: Populations that could be affected within 100 km downstream (Source: [Mool et al.,<br>2011]) .....  | 67 |
| Table 15: summary of livelihoods and property exposed to a potential GLOF risk (Source: [Mool<br>et al., 2011]).....  | 67 |
| Table 16: summary of monetary value of elements exposed to a potential GLOF risk (USD '000)<br>(Source: [Mool et al., 2011]) .....                            | 68 |

# Figures

Figure 1: Infographic showing the links between changes in climate and changes in hydrology and impacts on different sectors. .... 15

Figure 2: Map of the HKH region, Tibetan Plateau and surroundings, showing the Indus, Ganges and Brahmaputra basins and the dominant precipitation sources. .... 16

Figure 3: Percentage of the mean annual precipitation distributed over the periods December to February (DJF), March to May (MAM), June to August (JJA) and September to November (SON) [Maussion *et al.*, 2014]. .... 17

Figure 4: Multi-annual mean (1998-2007) of monsoon (JJAS) and winter (DJFMA) precipitation over the HKH region as represented by different datasets [Palazzi *et al.*, 2013]. .... 19

Figure 5: Spatial maps of summer (JJAS) precipitation trends for different products [Palazzi *et al.*, 2013]. .... 20

Figure 6: RCPs. blue: RCP8.5, black: RCP6, red: RCP4.5, green: RCP2.6 ..... 21

Figure 7: Schematic representation of RCM nesting approach (source: World Meteorological Organization website). .... 22

Figure 8: Scheme of different downscaling approaches. Traditional empirical-statistical downscaling (right pathway) calibrates the statistical transfer function between large-scale observation/reanalysis data and local-scale observations. These empirical-statistical relationships can be used for downscaling of any GCM. Empirical-statistical downscaling and error correction methods (DECMs) (left pathway) are calibrated on RCM (or GCM) data and local observations, account for downscaling as well as model errors, but can only be applied to the model they are calibrated for. Source: [Thiemeßl *et al.*, 2011a]. .... 23

Figure 9: Projected ranges of changes in mean air temperature and total precipitation between 1961-1990 and 2021-2050 [Lutz *et al.*, 2014] ..... 27

Figure 10: Projected percentage precipitation change in 2071–2100 (RCP 8.5 scenario) relative to 1971–2100 in summer (top left) and winter (top right) for the multi-model-mean of the CMIP5 ensemble. Number of models (out of 32) showing, in each 2°x2° pixel, a positive precipitation change [Palazzi *et al.*, 2014]. .... 28

Figure 11: Scatterplot of the pattern correlation with observations of the simulated pentad of monsoon onset versus a) the pattern correlation with observations of the simulated pentad of monsoon peak, b) the pattern correlation with observations of the simulated pentad of monsoon withdrawal, and c) the pattern correlation with observations of the simulated number of pentads of monsoon duration. d) Scatterplot of the Monsoon Domain Hit Rate versus the Monsoon Domain Threat Score. In a–d the simulation ability is with respect to GPCP for the region 50°E–180°E, 0°–50°N. Source: [Sperber *et al.*, 2013]. .... 31

Figure 12: Left: Distribution of historical (1951–2005) simulations of seasonal and annual rainfall over continental India with CMIP5 (red, uppercase) and CMIP3 (blue, lower case) as difference between simulation and composite of observations (green). The scatter in the observations (green) is shown as a percentage deviation (simulation – observed composite) from the observed composite. The acceptable uncertainty is defined by the difference ( $\Delta$ ) between the maximum and the minimum in the observed values, centered at the observed composite; the inner shaded box (pink) is defined by  $1\Delta$ , while the outer square (green) is defined by  $2\Delta$ . The inset table shows the number of simulations that fall in each category. Right: Inter-annual variability in Continental Indian Monsoon (CIM) rainfall from the composite observations and ensemble of simulations (normalized to the respective 1951–2005 mean). The linear trend for the respective case is given in the bracket. .... 31

Figure 13: Distribution of glaciers in the HKH, as obtained from ICIMOD's inventory [Bajracharya & Shrestha, 2011], by Bhambri *et al.* [2013], and the Chinese Glacier Inventory

|   |    |
|---|----|
| (Sia: Siachen, Bal: Baltoro, Bia: Biafo, Yin: Yinsugaiti, His: Hispar, BaS: Bara Shigri, Miy: Miyar, Gan: Gangotri, Ngo: Ngozumpa, Zem: Zemu) (Source: [Frey et al., 2014]).....  | 33 |
| Figure 14: Permafrost zonation index map of the Tibetan plateau [Gruber, 2012]......  | 36 |
| Figure 15: Regional distribution of debris-covered and stagnating glaciers. a) Location of glaciers (circles) grouped by region. Histograms give relative frequencies (y-axis, 0–40%) of debris cover (x-axis, 0–100% in 5% bins). Number of studied glaciers is given in upper-right corner, measured frontal changes in parentheses. Globe depicts location of subset and atmospheric transport directions. b) Regional distribution of mean annual frontal changes. Boxes give lower and upper quartiles and median (notches indicate 95%-confidence intervals). Whiskers extend 2.5 times the interquartile data range, crosses lie outside this range. Numbers left of boxes indicate percentage of advancing/stable (top) and retreating (bottom) glaciers. Source: [Scherler et al., 2011b]..... | 43 |
| Figure 16: Projected future changes in snowfall in sub-basins of the Indus, Ganges and Brahmaputra basins. (a) Absolute change (km <sup>3</sup> ) with reference to MERRA reference snowfall. (b) Absolute change (km <sup>3</sup> ) with reference to APHRODITE snowfall. (c, d) Corresponding relative changes (%) with reference to MERRA and APHRODITE. Multi-model means for 2071-2100 with respect to 1979–2008 are shown. Source: [Viste and Sorteberg, 2015].....   | 50 |
| Figure 17: Projected future changes in water balance components for the Baltoro and Langtang catchments. All changes are relative to 1961–1990. Runoff is the sum of base flow, rain runoff, direct snow runoff and direct glacier runoff. All values are expressed as a catchment average in mm yr <sup>-1</sup> . Changes are shown for RCP4.5 for the period 2021–2050 (a) and 2071–2100 (b) and for RCP8.5 for 2021–2050 (c) and 2071–2100 (d). The error bars show the standard deviation of four selected GCM runs [Immerzeel et al., 2013].....  | 55 |
| Figure 18: Projected discharges for three GCMs in the RCP2.6 (a), RCP4.5 (b) and RCP8.5 (c) scenarios [Soncini et al., 2015]. .....   | 57 |
| Figure 19: Average annual hydrographs for the period 2041-2050, RCP8.5 at major river's outlets. Plots show the mean projected discharge when forced with a 4 GCM ensemble (red line) and the discharge for a reference period (1998-2007, blue line). For the future period four streamflow components are shown: baseflow (red), glacier melt (blue), snow melt (orange), rainfall-runoff (green). The error bars indicate the variability in projections for the future period when forced with the ensemble of 4 GCMs [Lutz et al., 2014].....  | 58 |
| Figure 20: Decadal lake development in the Lunana region from 1980 to 2010. ....  | 63 |
| Figure 21: Development trend of glacial lakes in the Lunana region .....  | 63 |
| Figure 22: Decadal lake development of Imja Tsho from 1979 to 2009. ....  | 64 |
| Figure 23: Development trend of Imja Tsho.....  | 64 |
| Figure 24: Aerial view of Tsho Rolpa (Photo: Sharad Joshi, 2000) .....  | 65 |
| Figure 25: Development trend of Tsho Rolpa from 1959 to 2000.....   | 65 |
| Figure 26: Development of Lumu Chimi and Ganxi Co. ....   | 65 |
| Figure 27: Trend analysis of Lumu Chimi and Ganxi Co lakes from 1977 to 2003. ....  | 65 |

# 1 Introduction

## 1.1 Background and regional context

Warming of the climate system is unequivocal. The atmosphere and ocean have warmed, the amounts of snow and ice have diminished, sea level has risen, and the concentrations of greenhouse gases have increased. The Himalayan region (after Antarctica and the Arctic) has the third largest amount of ice and snow in the world, and is exceptionally vulnerable. The various Global Climate Models (GCM) predict very similar future temperature trends for the region, but projections of future precipitation patterns differ widely. As a consequence, the need for increased knowledge about future climate change remains high. The main focus of GCMs thus far was on temperature increases and potential changes to the hydrological cycle. The overall tendency that has emerged is that wetter regions are likely to become wetter and drier regions drier. Increased scientific knowledge, coupled with recent weather events, show that changes in hydrological extreme events can be substantial and the geographical and temporal resolution of predicted changes remains low in many areas.

For Statkraft, as the largest generator of renewable energy in Europe and a leading company in hydropower internationally, an understanding of future changes to the hydrological cycle and its uncertainty is crucial for effective business planning. Investment decisions regarding the business strategy for the next 50 years depend on accurate predictions of climate change impacts on inflow over that period. In addition, changing probabilities and magnitudes of extreme events can put additional risk on infrastructure (dams and hydropower plants) or on other crucial infrastructure (roads and transmission lines). Statkraft's intention to grow in the region makes it necessary to assess short, medium and long-term impacts, risks and opportunities resulting from climate change, to ensure sustainable management of the water resources for all stakeholders. Currently, Statkraft's main business focus lies with northern India (mainly the state of Himachal Pradesh) and Nepal, while Bhutan and Myanmar might be areas of future business development as well.

The International Centre for Integrated Mountain Development (ICIMOD) is a regional inter-governmental learning and knowledge sharing Centre serving the eight regional member countries of the Hindu Kush Himalayas (HKH) – Afghanistan, Bangladesh, Bhutan, China, India, Myanmar, Nepal, and Pakistan – and is based in Kathmandu, Nepal. ICIMOD's mission is to enable sustainable and resilient mountain development for improved and equitable livelihoods through knowledge and regional cooperation. ICIMOD's regional transboundary approach enables them to serve as a regional knowledge hub. ICIMOD has a rich experience in climate and water related issues in the HKH region and in developing climate and water availability scenarios for the future. Through its Regional Program on River Basins and Water and Air Theme, ICIMOD is working towards improving the understanding of climate change on cryosphere and water resources and providing knowledge and information to relevant stakeholders.

## 1.2 Hydropower issues in the HKH

Water and energy are interrelated: water for energy, and energy for water. Every drop of water that has to be pumped, moved, or treated to meet domestic, industrial, or agricultural needs, requires energy. However, water is also a source of energy and hydropower has been used for centuries as an energy source. Although hydropower is a typical example of water for energy,

the water is not actually consumed, because water leaving the generator can be used for other purposes. Therefore hydropower can be regarded as a form of renewable energy, and it is amongst the most mature and developed forms of renewable energy, representing a significant share of the global energy supply. Hydropower accounts for about 16% of global electricity generation, and some countries, notably Norway and Brazil, rely almost 100% on hydropower for their energy requirements.

However, the hydropower sector is sensitive to changes in seasonal weather patterns and weather extremes that can adversely affect the supply of energy and also adversely impact the integrity of transmission pipelines and power distribution. In addition, most infra-structure has been built to design codes based on historic climate data and could therefore require extensive maintenance, upgrading, or replacement in the coming years. Expected climate impacts range from increasing temperatures (across the region), changes in precipitation and snow, as well as an increase in the incidence and magnitude of extreme weather events. The hydrological regimes of the Brahmaputra, Ganges and Indus basins are complex and vulnerable to climate change. The situation is further complicated by the fact that most basins are transboundary, which causes political sensitivities.

Because of the rapid pace of industrialization, urbanization and an increase in demand for food for ever-growing populations, the power demand will increase. Ensuring the availability of an uninterrupted supply of power is a major challenge to sustainable development in the region. Energy is needed not only to sustain the region's growth, but also to improve socio-economic conditions and human development. At present, cross-border energy trade in the region is minimal and exists only at the bilateral level. Hydropower trade between India and Bhutan and between India and Nepal is taking place on a small scale. There is vast potential for joint development of the hydropower sector to support accelerating economic growth, reduce poverty, and enhance human development. Harnessing the huge untapped hydropower resources in Nepal, Bhutan, and north-east India could not only help meet the growing demand for power, but also help transform this region from poor to prosperous. The principal impediments to unlocking the potential of hydropower in this region include a lack of financial resources necessary to develop the required infrastructure and technical capability, as well as the risks associated with single buyers. Regional cooperation can help overcome these impediments by obtaining the necessary financial resources, utilizing suitable technologies, establishing guaranteed markets, and creating institutional mechanisms for sharing the costs and benefits of joint efforts [Rasul, 2014]. Regional trade can contribute to environmental and financial sustainability of hydropower in the region.

### **1.3 Hydropower potential in the Himalayan region**

The total theoretical hydropower generating, and economic consumption potentials in Nepal are 83,290 MW and 42,133 MW respectively. Over an overall distance of just 100 km, the Nepali rivers provide a total drop (or potential height) of 4 km. This represents a very significant hydropower generating potential. Unfortunately, Nepal has not been able to utilize this vast potential effectively and to date, excluding privately owned micro-hydropower plants, Nepal has only installed 689.3 MW generating capacity (which represents only 1.6% of the available potential). In addition, electricity is only available to 40% of the population and in rural areas electrification coverage is only about 29%. The majority of the population has to rely on traditional sources for their energy needs [Surendra et al., 2011]. Because of the steep terrain and the scattered settlements in a mountainous country like Nepal, electrification is very costly. The country lacks basic infrastructures like roads and transmission lines and therefore, the cost

of mega hydro-electricity generating projects will also demand inclusion of significant investments in infrastructure. The situation is further exacerbated by the high transport cost in Nepal of construction materials, as well as by the high inflation rate of the Nepalese currency. As a result it is inevitable that the cost to establish hydro-electricity generating plants in Nepal will be higher than in countries where infrastructure is more advanced. Other factors that contribute to the poor development of hydro-electricity development in Nepal are: (i) lack of capital investment; (ii) lack of long-term planning due to political instability in the country; (iii) an inefficient bureaucracy; and (iv) lack of effective treaties among co-riparian countries for sharing both the costs and benefits of large scale hydro-electricity projects [Surendra et al., 2011].

Bhutan has a high hydropower potential of 30,000 MW, of which 23,000 MW can readily be exploited. The total installed capacity is about 1,490 MW or 6.5% of the exploitable potential. The electricity demand is 105 MW or 0.4% of the exploitable potential [Uddin et al., 2007].

Pakistan has an estimated energy shortage of 4,500 MW. Here too the potential for hydropower is large; it is estimated to be 42,000 MW out of which only 6,500 MW (15.5%) is being utilized. Hydropower is one of the main sources of energy for Pakistan and as of 2007 hydropower contributes to nearly 33% of the total electricity supply mix. A considerable part of the northern areas of Pakistan do not have access to the supply grid mainly due to their remoteness and difficult terrain. Most of these areas have a high potential for small-scale facilities and already nearly 300 micro and mini hydropower plants are in operation. These hydropower plants are making a valuable contribution to the livelihoods of people in small villages and clusters of homes. Unfortunately, despite these developments, increased hydropower generation capacity in the country has not been given sufficient attention with the result that the contribution of hydropower to the total electricity generation mix decreased from 70% in 1960 to 33% in 2006. The capacities of the existing three reservoir based hydropower facilities in the country (Tarbela, Mangla and Chashma) are declining due to sedimentation. The usable storage capacity of the three reservoirs has been reportedly reduced by about 20% [Asif, 2009].

In India's energy policy large dams are of strategic importance. Because of its low recurring costs, its lower carbon emissions compared to coal-based thermal power and because of its ability to supply peak demand power, large-scale hydropower is now a preferred power generation technology. Realizing the importance of hydropower for the national energy scenario, the Government of India, in collaboration with the Central Electrical Authority, initiated the preparation of preliminary feasibility studies for 162 new hydro-electric schemes totaling over 50,000 MW. At national level, the total hydropower potential is 148,000 MW, of which only 31% (42,780 MW) has been developed or is under construction. Arunachal Pradesh in the north-east of the country has the highest hydropower potential. Such states as Arunachal Pradesh and Sikkim in the north-east, and Himachal Pradesh and Uttaranchal in the north are rapidly developing hydropower [Choudhury, 2010].

China also has a tremendous hydropower potential estimated at 694,000 MW, which is largely located in the HKH region, and China needs to develop hydropower to alleviate the energy crisis and environmental pollution resulting from the rapid Chinese economic growth in the 21st century. China's hydropower has developed quickly and the installed capacity of hydropower is 145,260 GW (20.9%). Some large hydropower plants have been in operation and many are still under construction, including the Three Gorges Project (TGP) and pumped-storage power stations. Small hydropower development is accelerating rural electrification.

Although there is great variation in the potential of hydropower between the different countries which share Himalayan water resources, it is clear that overall there is a huge untapped potential for hydropower development in the region.

#### **1.4 Criteria and constraints for hydropower development**

Proper assessment of the cost-effectiveness and risks of hydropower projects is usually done beforehand for each specific project. The general rule of thumb is that a project must be profitable with manageable risks in all areas, such as:

- Health, Safety and Security;
- Environmental and Social;
- Integrity;
- Reputation;
- Financial.

Risks are strongly dependent on policies, renewable resources and hydrology. Security risks can be imposed by political conflicts or high numbers of criminal activities in an area. Models are used to make thorough forecasts of the markets and energy prices, to determine financial risks. The initial amount to be invested for construction of the project, availability of infrastructure to access the project site, and operating costs are also to be taken into account. Hydrological risks can be assessed by establishing and using a comprehensive and reliable database of hydrological processes as a reference for changes. A year-round uniform streamflow regime over all seasons is required for effective energy production. In most parts of the HKH region, the streamflow regime is characterized by high flows during monsoon and/or melting season and low flows in other seasons. Other environmental risks are direct impacts on flora and fauna, including endangered species, and natural hazards like glacial lake outburst floods (GLOFs), earthquakes and landslides. Reservoir sedimentation also forms a risk imposed by the environment, and sedimentation rates should be assessed. From a social point of view, projects which require physical and economical displacements are avoided or minimized.

The constraints on the development of the hydroelectric power industry in the HKH region can be categorized as technological, environmental, economic, financial, and institutional [Vaidya, 2012] (Table 1). The major technological constraints are the transmission and distribution networks to deliver the electricity to the users and for connecting grids. Hydropower projects are located far away from the consumers and require a vast infrastructure to get the energy there from the production sites. Furthermore cross-border grid connections are needed to trade power between industrialized and less industrialized countries in the region [Vaidya, 2012; Molden *et al.*, 2014]. Possible consequences of climate change form environmental constraints. These include possible changes in river flow variability, sedimentation and potential GLOFs. Changes can be expected extreme events such as floods and droughts which will significantly affect the operation of hydropower stations [Molden *et al.*, 2014]. More intense rainfall events in the future may lead to increased floods and sedimentation, leading to increased siltation for hydropower infrastructure to contend with. It has been reported that several projects have stranded at different stages because plans have been revisited in view of ecological concerns [Molden *et al.*, 2014]. The major economic barrier is the low load factor, being the ratio of average energy demand over peak energy demand. This lead to high energy tariffs in countries with a low industrial base. The difficulty in raising funds at reasonable prices is the main financial constraint. The major risks for investment in hydropower are production risks, country risks,

market risks and currency risks. The major institutional constraint at the development stage is the lack of a domestic construction industry able to undertake hydropower projects [Vaidya, 2012]. At the operational stage the main constraint is the lack of mechanisms for transmission and distribution and a lack of mechanisms to prevent the theft of power during distribution. Another institutional constraint is the development of methodologies to mitigate negative social and environmental costs and ensuring equal distribution of the benefits of hydropower. For example, people living in the mountains and hills commonly complain that the benefits of hydropower go to the people downstream while the people in the mountains bear the bulk of social and environmental costs [Molden et al., 2014].

**Table 1: Constraints on the development of small hydropower projects in the HKH region. Source: [Vaidya, 2012]**

| Country  | CONSTRAINTS     |   |  |  |  |
|----------|-----------------|---|--|--|--|
|          | Economic        | Environmental   | Technological  | Financial  | Institutional  |
| Bhutan   |                 | Glacial Lake<br>Outburst Floods;<br>river flow<br>variability |  |  |  |
| China    |                 |   | Hydropower resources<br>far from consumption<br>centres  | Long pay-back<br>period; difficult to<br>raise funds |  |
| India    | Low load factor |   | Scaled down technology<br>not appropriate for small<br>plants  |  | High<br>construction<br>costs; lack of<br>technical<br>expertise and<br>experienced<br>local contractors                             |
| Nepal    | Low load factor |   | High cost of<br>development; lack of<br>domestic electro-<br>mechanical equipment<br>manufacturing<br>capability; access to<br>potential sites | Difficult to raise<br>funds                          | Domestic<br>construction<br>industry<br>capacity;<br>wheeling<br>facilities;<br>community<br>participation;<br>high system<br>losses |
| Pakistan |                 | Sedimentation   |  |  |  |

## 1.5 About this review

This project is a joint initiative between ICIMOD and Statkraft to establish mutual collaboration in assessing impacts of climate change on the hydrological regimes in the Himalayas. The overarching objective of this project is to jointly improve understanding of the impacts of climate change on the cryosphere and water resources in the Himalayan region with a focus on changes relevant to hydropower production. We review the state-of-understanding related to climate change, cryosphere dynamics, changes in the hydrological regime, and glacial lake outburst flood hazard in the Indus, Ganges and Brahmaputra basins specifically. Based on the

outcomes of this review we then provide a detailed analysis of the potential impact of climate change on the cryosphere, glacial hazard and the hydrological regime in catchments of mutual interest to Statkraft and ICIMOD.

## **1.6 Geographic scope**

The region for which this review will be conducted is confined to the river basins of the Indus, Ganges and Brahmaputra rivers and in particular the upstream parts where the largest hydropower potential is. Statkraft is currently interested in almost the whole HKH region. The firm owns and operates hydropower plants in East Nepal and Himachal Pradesh. In addition they are developing or have developed advanced projects in Nepal, Myanmar, Uttar Pradesh, Arunchal Pradesh and Bhutan.

Predominantly peer reviewed literature in journals registered at the Thomson Institute for Scientific Information after the year 2000 is included in this review, except for the chapter on glacial lake outburst floods, for which topic available peer-reviewed literature is very limited.

## **1.7 Thematic scope**

This comprehensive review focuses on four topics.

1. The climate variability (both spatial and seasonally) is assessed and future projections by climate models are summarized and reviewed.
2. Observed changes in the cryosphere are reviewed and include an inventory of the snow and ice reserves using different monitoring methods as well as a review of future projections.
3. The impact of those projected climate changes on cryosphere dynamics and hydrological regimes is analyzed. A distinction is made between long term changes in water availability, seasonal variability, the occurrence of extreme events and changes in the contributing components to the total river flow.
4. Climate change impacts on glacier lakes, with a particular focus on the potential for glacier lake outbursts are analyzed. This may directly impact the selection of planned hydropower sites.

All of these topics are closely interlinked and changes in one component has influences the other components as highlighted in Figure 1.

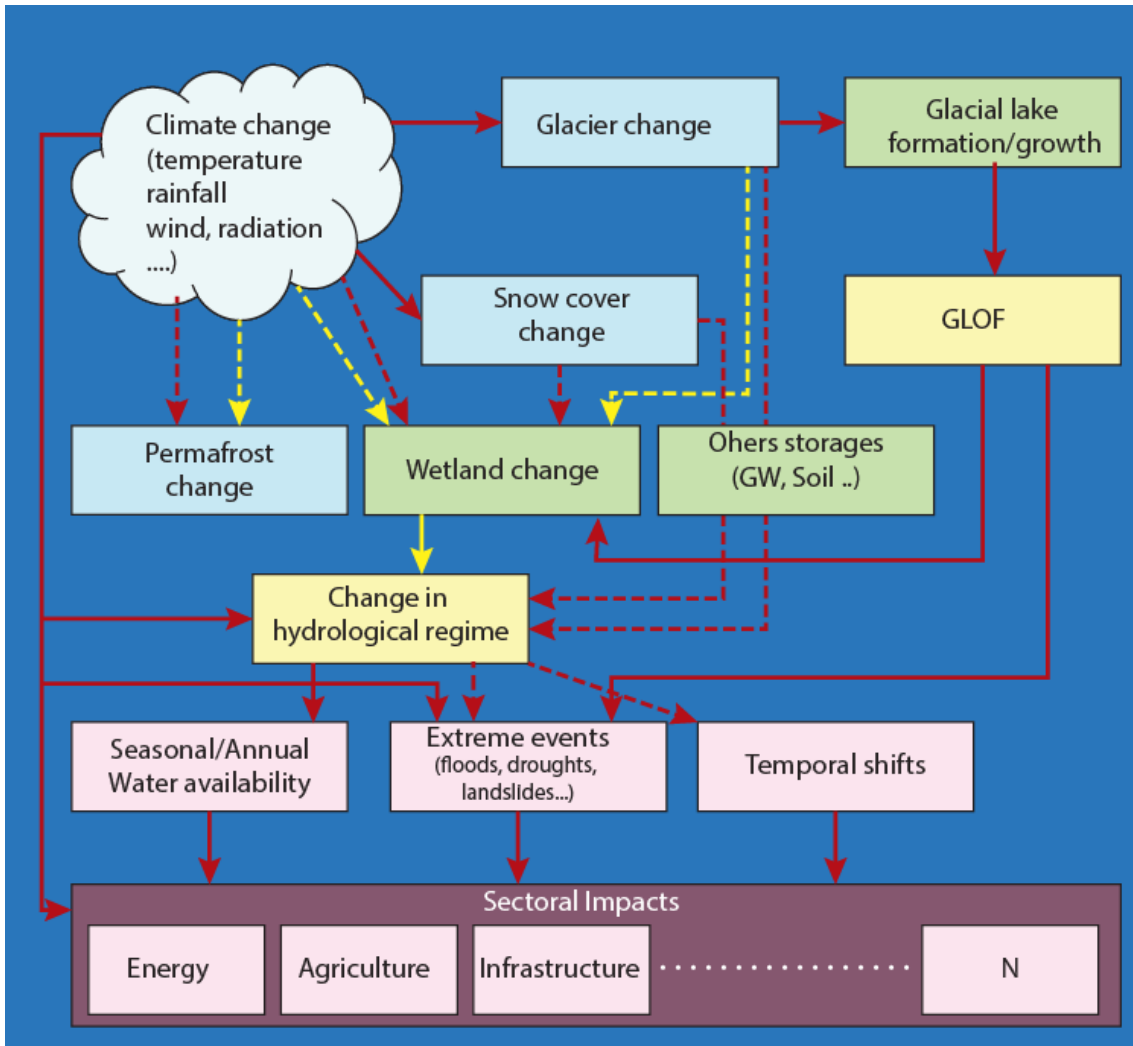


**Figure 1: Infographic showing the links between changes in climate and changes in hydrology and impacts on different sectors.**

## 2 Climate Change and its Variability

### 2.1 Historical trends and variability

In general, the climate in the eastern part of the Himalayas is characterized by the East-Asian and Indian monsoon systems (Figure 1), causing the bulk of precipitation to occur during June to September. The precipitation intensity shows a strong north-south gradient caused by orographic effects [Galewsky, 2009]. Precipitation patterns in the Hindu Kush and Karakoram ranges in the west are characterized by westerly and southwesterly flows, causing the precipitation to be more evenly distributed over the year compared to the eastern parts [Bookhagen and Burbank, 2010] (Figure 2). In the Karakoram, up to two-thirds of the annual high-altitude precipitation occurs during the winter months [Winiger et al., 2005; Hewitt, 2011]. About half of this winter precipitation is brought by Western Disturbances, being westerly-driven eastward propagating cyclones bringing sudden winter precipitation to the north-western parts of the Indian subcontinent [Barlow et al., 2005].

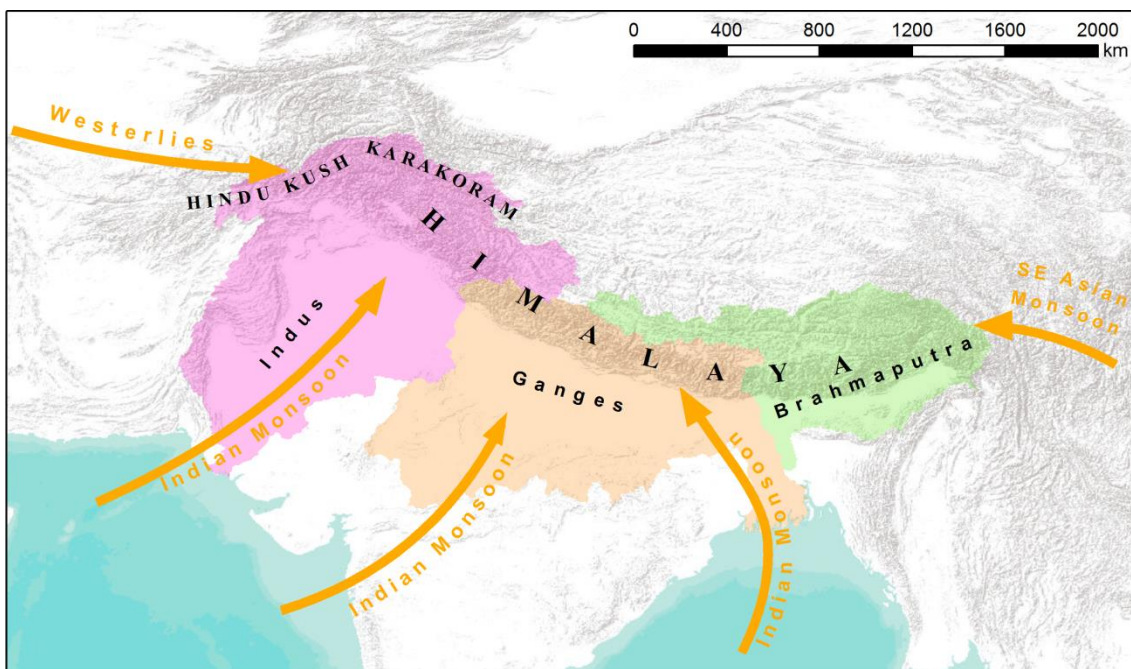


**Figure 2: Map of the HKH region, Tibetan Plateau and surroundings, showing the Indus, Ganges and Brahmaputra basins and the dominant precipitation sources.**

Meteorological ground stations are relatively sparse in the Hindu Kush Himalayas because of the complexity of the terrain. Precipitation specifically has a high spatial variability in the mountainous regions, where precipitation gauge networks are virtually non-existent. If there are gauges, they are mostly located in the valley bottoms where precipitation amounts are smaller compared to higher altitudes. Besides, most gauges have difficulties capturing snowfall accurately. Precipitation can also vary enormously over short distances due to orographic effects. Snow-accumulation measurements, using snow pillows, snow courses, pits, and cores from accumulation zones are also scarce and usually confined to short observation periods. Precipitation predictions for the HKH region based on ground observations, which are not able to capture all the variations spatially, are therefore not very accurate. Other approaches such as the use of remote sensing and re-analysis techniques to generate gridded climate products, are necessary for more accurate predictions (see Table 2).

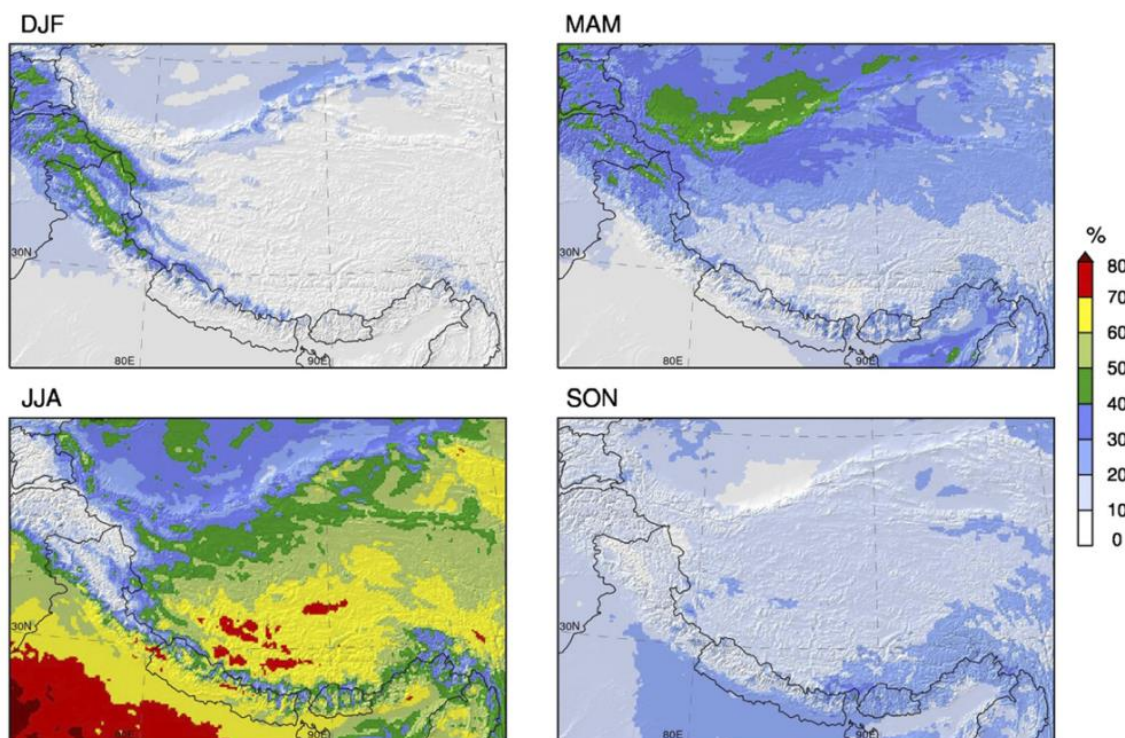


**Figure 3: Percentage of the mean annual precipitation distributed over the periods December to February (DJF), March to May (MAM), June to August (JJA) and September to November (SON) [Maussion et al., 2014].**

A thorough comparison of the performance of existing gridded climate products for the HKH region [Palazzi et al., 2013] highlights the striking differences between them (Figure 4). All currently available products are subject to limited spatial resolution. They are mostly suitable for large-scale continental studies, but do not accurately depict climate variations at smaller scales and in orographically complex regions. The differences in precipitation estimates between the products are large for the monsoon-dominated Himalayan arc as well as for the westerly-influenced Hindu-Kush and Karakoram. Another approach, using the observed glacier mass balance as a proxy to reconstruct the total precipitation for the upper Hunza basin of the Indus basin, indicated that total annual precipitation is likely to be more than double the precipitation derived from interpolated gauge data [Immerzeel et al., 2012].

**Table 2: Overview of gridded meteorological products.**

| Dataset                          | Type        | Coverage | Resolution                    | Frequency                   | Period         | Parameters                           | Institute |
|----------------------------------|-------------|----------|-------------------------------|-----------------------------|----------------|--------------------------------------|-----------|
| <b>NCEP/NCAR reanalysis data</b> | Re-analysis | Global   | ~209 km (T62 grid)            | 6 hourly                    | 1948 - present | Prec, Tmax, Tmin, Tavg (+ many more) | NCEP/NCAR |
| <b>CFSR</b>                      | Re-analysis | Global   | ~ 50 km (0.5 degree)          | 1 hourly, 6 hourly, monthly | 1979-2010      | Prec, Tmax, Tmin, Tavg (+ many more) | NCEP      |
| <b>ERA 15 basic</b>              | Re-analysis | Global   | basic: ~ 250 km (2.5 degrees) | monthly                     | 1979 - 1994    | Prec, Tmax, Tmin, Tavg (+ many more) | ECMWF     |
| <b>ERA 15 advanced</b>           | Re-analysis | Global   | ~ 120 km (N80 grid)           | monthly                     | 1979 - 1994    |                                      | ECMWF     |

|  |                            |           |                               |          |                    |                                      |  |
|--|----------------------------|-----------|-------------------------------|----------|--------------------|--------------------------------------|--|
| <b>ERA 40 basic</b>  | Re-analysis                | Global    | ~ 250 km (2.5 degrees)        | 6 hourly | 1957 - 2002        | Prec, Tmax, Tmin, Tavg (+ many more) | ECMWF  |
| <b>ERA 40 advanced</b>   | Re-analysis                | Global    | ~ 120 km (N80 grid)           | 6 hourly | 1957 - 2002        | Prec, Tmax, Tmin, Tavg (+ many more) | ECMWF  |
| <b>ERA Interim</b>   | Re-analysis                | Global    | ~ 70 km (N128 grid)           | 6 hourly | 1979 - present     | Prec, Tmax, Tmin, Tavg (+ many more) | ECMWF  |
| <b>ERA 20 CM</b>   | Climate model ensemble     | Global    | ~ 120 km (N80 grid)           | 3 hourly | 1900-2009          | Prec, Tavg                           | ECMWF  |
| <b>NASA MERRA</b>  | Re-analysis                | Global    | ~ 70 km (0.5 x 0.67 degrees)) | 3 hourly | 1979 - present     | Prec, Tmax, Tmin, Tavg (+ many more) | NASA   |
| <b>Global Meteorological Forcing Dataset for land surface modeling</b> | Re-analysis + observations | Global    | ~ 50 km (0.5 degree)          | 3 hourly | 1948 - 2008        | Prec, Tmax, Tmin, Tavg (+ many more) | Princeton University                                   |
| <b>APHRODITE</b>   | Observations               | Asia      | ~ 25 km (0.25 degree)         | Daily    | 1961 - 2007        | Prec, Tavg                           | Meteorological Research Institute of Japan             |
| <b>CRU TS 3.10.01</b>  | Observations               | Global    | ~ 50 km (0.5 degree)          | Monthly  | 1901-2009          | Prec, Tmax, Tmin, Tavg (+ many more) | Climate Research Unit at the University of East Anglia |
| <b>GPCC</b>  | Observations               | Global    | ~ 50 km (0.5 degree)          | Monthly  | 1901-2007          | Precipitation                        | Global Precipitation Climatology Centre                |
| <b>GPCP</b>  | Observations               | Global    | ~ 250 km (2.5 degrees)        | Monthly  | 1979 - present     | Precipitation                        | GEWEX  |
| <b>CPC-UGBAGDP</b>   | Observations               | Global    | ~ 50 km (0.5 degree)          | Daily    | 1979-present       | Prec                                 | CPC  |
| <b>DEL</b>   | Observations               | Global    | ~ 50 km (0.5 degree)          | monthly  | 1900-2008          | Prec, Tair                           | CCR Univ of Delaware                                   |
| <b>WATCH (based on ERA-40)</b>   | Reanalysis                 | Global    | ~ 50 km (0.5 degree)          | 3-hourly | 1901-2001          | Prec, Tair + many more               | Met Office Hadley Centre                               |
| <b>WFDEI (based on ERA-Interim)</b>                                    | Reanalysis                 | Global    | ~ 50 km (0.5 degree)          | 3-hourly | 1979-2012          | Prec, Tair + many more               | Met Office   |
| <b>High Asia Reanalysis (HAR)</b>                                      | Downscaled WRF             | High Asia | 30 km, 10 km                  | 3-hourly | Oct 2000-Sept 2010 | Prec, Tair, many more                | TU Berlin  |

The quality of the gridded datasets varies strongly over the HKH region, and quality within datasets differs strongly in space. It is recommended that a number of products are compared to station data for a particular region of interest, to select the best performing dataset.

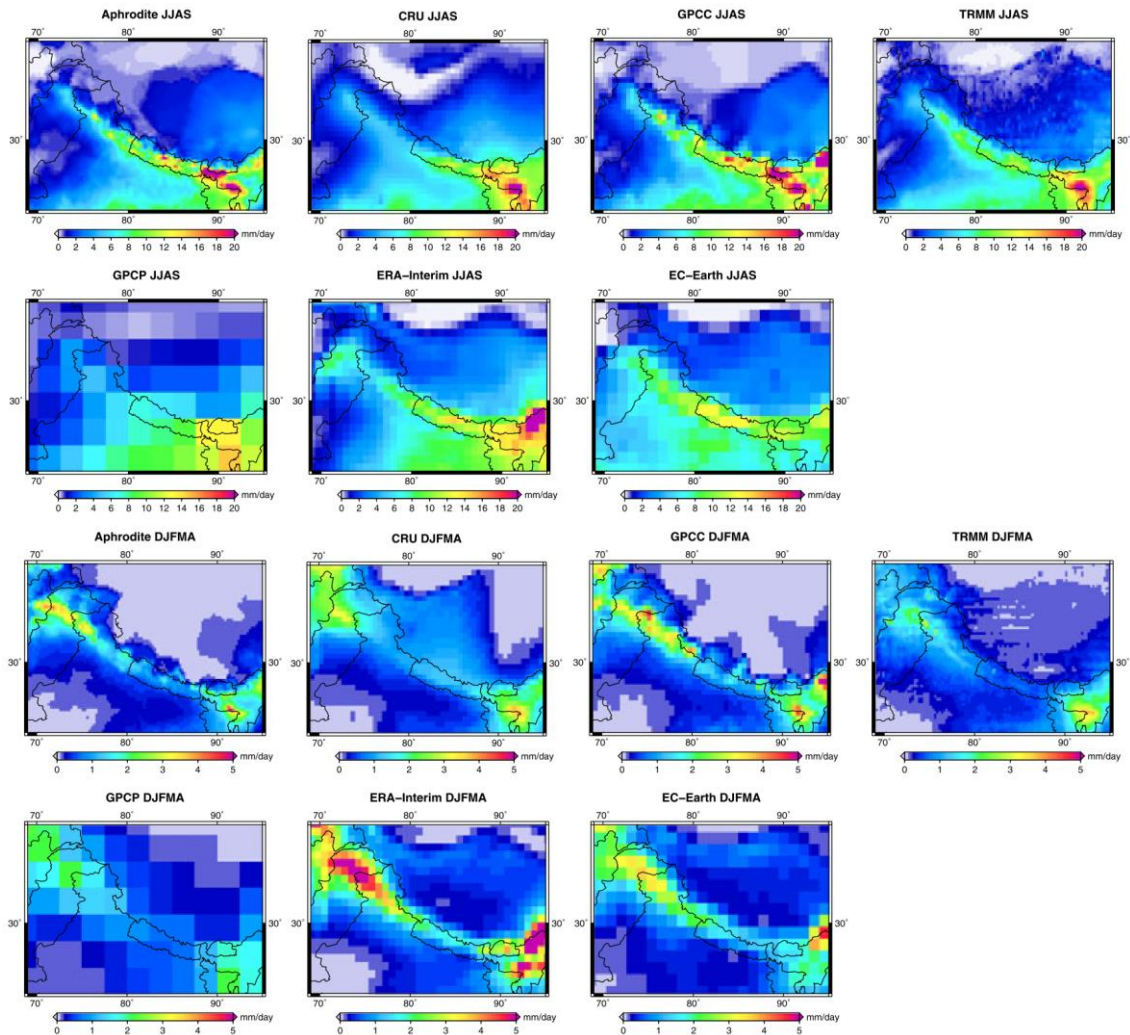


**Figure 4: Multi-annual mean (1998-2007) of monsoon (JJAS) and winter (DJFMA) precipitation over the HKH region as represented by different datasets [Palazzi et al., 2013].**

Past trends in climate in the upstream Indus, Ganges and Brahmaputra basins have been analyzed in many studies. Palazzi et al. [2013] analyzed trends in precipitation for different products, with records varying in length from 30 to 60 years, and ending around 2010. They found no statistically significant long-term trends for winter precipitation averaged over the area. Slightly increasing, though significant, trends in precipitation during the monsoon season were found for 2 out of 9 products, whereas no significant trends were found in the 7 other products. The trends show a very large spatial variability (Figure 5).

Trends in meteorological variables measured at ground stations were analyzed in a number of studies. Fowler and Archer [2006] analyzed temperature records in the upper Indus basin for the period 1961-2000. They showed that winter mean and maximum temperatures increased significantly while mean and minimum summer temperatures declined consistently. The diurnal temperature range increased in all seasons. An analysis of precipitation records for the upper Indus basin by the same authors, showed significant increases in winter, summer and annual precipitation for several stations over the period 1961-1999 [Archer and Fowler, 2004]. Khattak et al. [2011] found stronger increasing trends in winter maximum temperature at higher elevations but no significant precipitation trends.

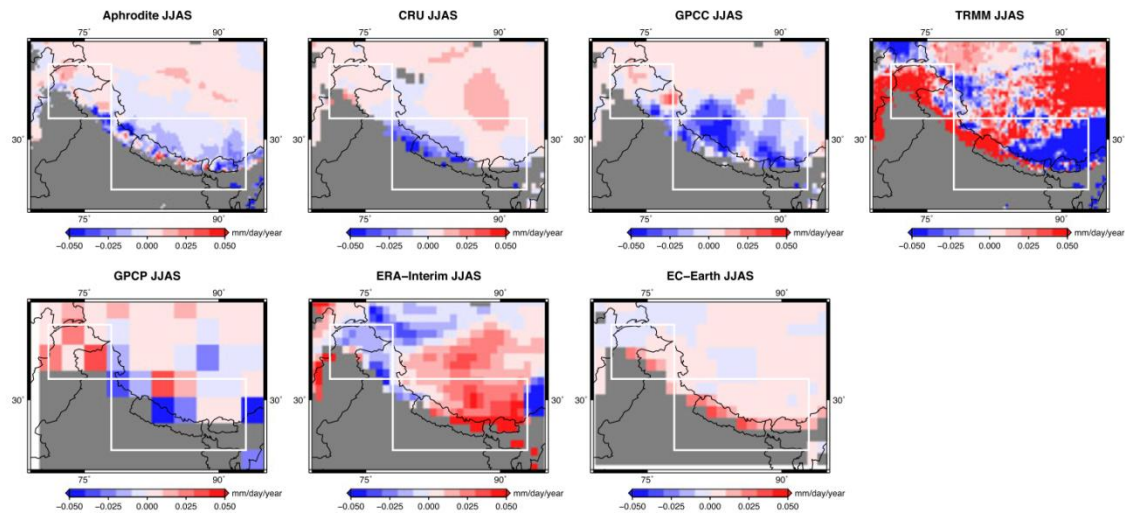


**Figure 5: Spatial maps of summer (JJAS) precipitation trends for different products [Palazzi et al., 2013].**

Studies worldwide show that recent increasing temperature trends are stronger for mountainous regions than for other land surfaces [Rangwala and Miller, 2012; Pepin et al., 2015]. Such trends have been observed for the Himalayan region as well [Bhutiyani et al., 2007; Lu et al., 2010].

An analysis of the multi-annual variations in winter westerly disturbance (WWD) activity over the period 1971 to 2010 indicated enhanced strength and frequency of WWD and associated heavy precipitation events in the Karakoram and western Himalaya [Cannon et al., 2014]. The central Himalaya, in contrast, experienced weakening influence of these disturbances and decreases in heavy winter precipitation.

## 2.2 Climate change studies

### 2.2.1 Climate modeling and climate change scenarios

Climate is modeled at different spatial scales. General Circulation Models (GCMs) are used to simulate global climate and operate at spatial resolutions ranging from ~100 km to ~250 km. Regional Climate Models (RCMs) can be used to simulate regional climate at a typical resolution of ~50 km. Climate change information is usually required at a higher spatial resolution. Different downscaling techniques are used to bridge these scale differences.

The current state-of-the-art GCMs are organized in the CMIP5 archive [Taylor et al., 2012], which is used as a basis by the Inter-governmental Panel on Climate Change (IPCC) for the generation of its Assessment Reports. A similar effort to organize the output from RCMs is the CORDEX framework [Giorgi et al., 2009]. The earlier CMIP3 [Meehl et al., 2007] archive is the main archive used for studies prior to the release of the CMIP5 archive.

Since the release of IPCC's fifth Assessment Report, four representative concentration pathways (RCPs) are used as a basis for long-term and near-term climate modeling experiments in the climate modelling community [van Vuuren et al., 2011a]. The four RCPs together span the range of radiative forcing values for the year 2100 as found in literature, from 2.6 to 8.5  $\text{Wm}^{-2}$  (Table 3, Figure 6). Climate modelers use the time series of future radiative forcing from the four RCPs for their climate modeling experiments to produce climate scenarios. The development of the RCPs allowed climate modelers to proceed with experiments in parallel

to the development of emission and socio-economic scenarios [Moss *et al.*, 2010]. The four selected RCPs were considered to be representative of the literature, and included one mitigation scenario (RCP2.6), two medium stabilization scenarios (RCP4.5/RCP6) and one very high baseline emission scenario (RCP8.5) [van Vuuren *et al.*, 2011b].

**Table 3: Description and visualization of the four representative concentration pathways (RCPs).**

| RCP    | Description  |
|--------|--|
| RCP8.5 | Rising radiative forcing pathway leading to $8.5 \text{ Wm}^2$ ( $\sim 1370 \text{ ppm CO}_2\text{eq}$ ) by 2100   |
| RCP6   | Stabilization without overshoot pathway to $6 \text{ Wm}^2$ ( $\sim 850 \text{ ppm CO}_2\text{eq}$ ) at stabilization after 2100   |
| RCP4.5 | Stabilization without overshoot pathway to $4.5 \text{ Wm}^2$ ( $\sim 650 \text{ ppm CO}_2\text{eq}$ ) at stabilization after 2100   |
| RCP2.6 | Peak in radiative forcing at $\sim 3 \text{ Wm}^2$ ( $\sim 490 \text{ ppm CO}_2\text{eq}$ ) before 2100 and then decline (the selected pathway declines to $2.6 \text{ Wm}^2$ by 2100) |

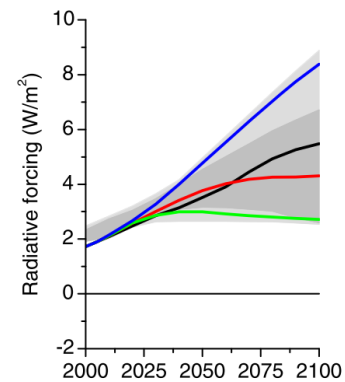


**Figure 6: RCPs. blue: RCP8.5, black: RCP6, red: RCP4.5, green: RCP2.6**

Since the four RCPs are considered (according to the literature) to be representative of radiative forcing that can be expected by 2100, each of them should theoretically be considered to be included in climate change impact studies with equal probability. However, in climate change impact studies there is usually a tradeoff in how many RCPs and how many climate models can be included within the available time and resources, whilst at the same time having the ability of producing robust and reliable results.

Between 1996 and the release of the IPCC's fifth assessment report in 2013, the IPCC used a different set of future scenarios, combining main demographic, economic and technological driving forces with future greenhouse gas emissions. Because these scenarios were used in some of the cited literature in this report, they are summarized here:

- A1: The A1 storyline and scenario family describes a future world of very rapid economic growth, global population that peaks in mid-century and declines thereafter, and the rapid introduction of new and more efficient technologies. Three groups within the A1 storyline are defined based on different pathways of technological change in the energy system:
  - A1F1: fossil energy intensive
  - A1T: non-fossil energy sources
  - A1B balance across energy sources
- A2: The A2 storyline and scenario family describes a very heterogeneous world. The underlying theme is self-reliance and preservation of local identities. Fertility patterns across regions converge very slowly, which results in continuously increasing population. Economic development is primarily regionally oriented and per capita economic growth and technological change more fragmented and slower than other storylines.
- B1: The B1 storyline and scenario family describes a convergent world with the same global population, that peaks in mid-century and declines thereafter, as in the A1 storyline, but with rapid change in economic structures toward a service and information

economy, with reductions in material intensity and the introduction of clean and resource-efficient technologies.

- The B2 storyline and scenario family describes a world in which the emphasis is on local solutions to economic, social and environmental sustainability. It is a world with continuously increasing global population, at a rate lower than A2, intermediate levels of economic development, and less rapid and more diverse technological change than in the A1 and B1 storylines.

### 2.2.2 Downscaling techniques

Because of the discrepancy in spatial resolution between climate models, different downscaling techniques can be applied to overcome difference in resolution when such models are used to force other models such as hydrological models.

#### 2.2.2.1 Dynamic downscaling

Dynamic downscaling is generally the nesting of climate models of different spatial resolutions. A GCM usually provides the boundary conditions for a RCM that has a nested domain within the GCM domain. Higher resolutions can be reached when a finer resolution RCM or weather model is nested within the RCM domain. The RCM then in turn provides the boundary conditions for the finer resolution RCM. On finer scales, Large Eddy Simulation (LES) models can be deployed, which can include atmospheric turbulence in its simulations. Because of the high spatial resolution of RCMs, computation resources are a limiting factor for the simulation of the length of the temporal period and its size (spatial dimension).

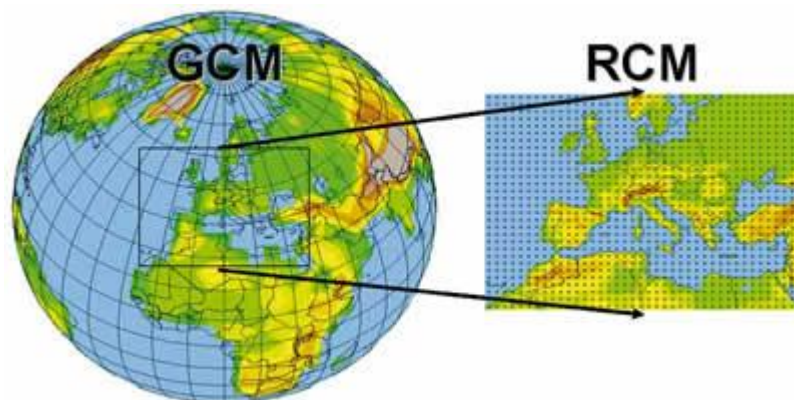


**Figure 7: Schematic representation of RCM nesting approach (source: World Meteorological Organization website).**

In climates with large spatial variation, such as occurring in mountainous regions, the RCM resolution is generally not sufficient to satisfactorily simulate the climate. Therefore, additional empirical statistical downscaling and error correction is usually required, which is also required when directly downscaling GCM data (Figure 8).

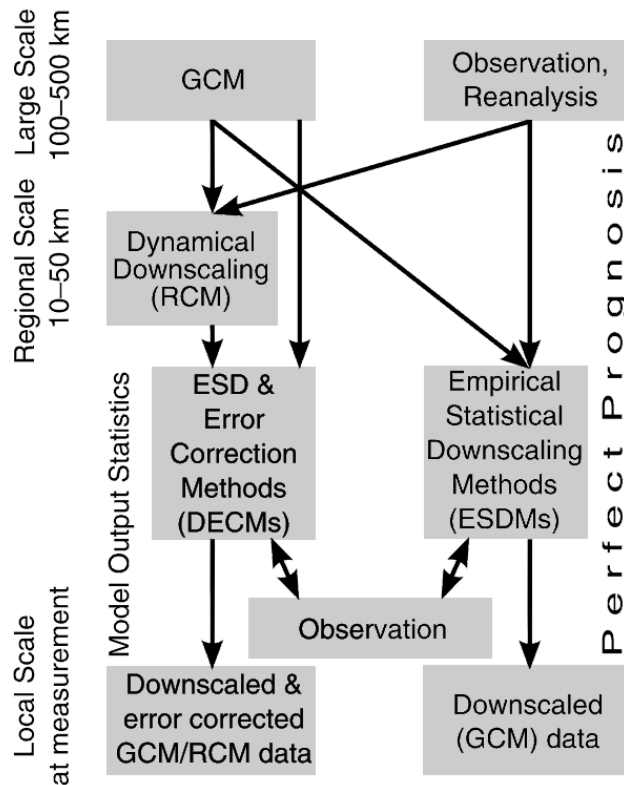


**Figure 8: Scheme of different downscaling approaches. Traditional empirical-statistical downscaling (right pathway) calibrates the statistical transfer function between large-scale observation/reanalysis data and local-scale observations. These empirical-statistical relationships can be used for downscaling of any GCM. Empirical-statistical downscaling and error correction methods (DECMs) (left pathway) are calibrated on RCM (or GCM) data and local observations, account for downscaling as well as model errors, but can only be applied to the model they are calibrated for. Source: [Thiemeßl et al., 2011a].**

#### 2.2.2.2 Empirical-statistical downscaling

Since the venture of GCMs, statistical downscaling techniques have been developed to account for the scale differences between GCMs and hydrological models, and to interpolate regional scale atmospheric predictor variables to station-scale meteorological series. GCMs typically operate at  $\sim 1^\circ$ -  $3^\circ$  spatial resolution, but applications like hydrological models, forced by the data from GCMs, operate at higher resolutions, down to several meters. Many processes, such as local circulation patterns leading to hydrological extreme events cannot be resolved by GCMs [Christensen and Christensen, 2002].

Fowler et al. [2007] distinguish four approaches for downscaling. They identify the ‘delta change’ or ‘perturbation method’ as the simplest statistical downscaling technique. They regard regression models, weather typing schemes and weather generators as more sophisticated statistical downscaling methods. Maraun et al. [2010] categorize statistical downscaling methods into ‘weather generators (WG)’, ‘perfect prognosis (PP)’, and ‘model output statistics (MOS)’. We followed the categorization by Maraun et al. [2010] to summarize different approaches for statistical downscaling, including an overview of their pro’s and con’s as described in the scientific literature. Because little applications of empirical-statistical downscaling methods are published for the HKH region, the focus of this section is on application of empirical-statistical downscaling methods in mountainous terrain in general.

Perfect Prognosis Statistical Downscaling approaches (or traditional empirical-statistical downscaling methods [Thiemeßl *et al.*, 2011c]) establish links between observed large-scale (synoptic scale) predictors and observed local-scale predictions. These include the classical statistical downscaling approaches including regression models and weather-pattern based approaches [Maraun *et al.*, 2010]. Regression methods were among the earliest downscaling approaches. In a standard linear regression model, the unexplained variability is assumed to be Gaussian distributed [Maraun *et al.*, 2010]; such models can be used for downscaling of mean precipitation and mean air temperature, but they are not suitable for shorter timescales, because daily precipitation is commonly modeled using a gamma distribution. An extension of the linear model is the generalized linear model, where the predicted variable may follow different distributions, or the general additive model, where the linear dependency is replaced by nonparametric smooth functions. Vector generalized linear models don't solely predict the mean of a distribution, but a vector of parameters of a distribution, including for example the mean and the variance of a distribution. These models are useful when studying the behavior of extreme events, and to estimate the dependence of the variance or the extreme tail on a set of predictors [Maraun *et al.*, 2010]. In weather type-based downscaling, a set of categorical weather types are used to predict the mean of local precipitation and temperature. This is a special type of linear downscaling model. Other perfect prognosis approaches are non-linear regressions like for example the use of an artificial neural network [Maraun *et al.*, 2010]. The analogue method is based on selecting the most similar large-scale weather situation in the past and selecting observations from corresponding local-scale situations. This method is thus limited to past events. The analogue method can be extended by randomly choosing the analogue from a number of most similar historical conditions [e.g. Moron *et al.*, 2008]. Physical processes on intermediate scales, like mesoscale weather patterns, are usually ignored in perfect prognosis statistical downscaling approaches.

The most basic linear regression model is the simple delta change or perturbation method [Prudhomme *et al.*, 2002; Kay *et al.*, 2008], which downscales GCMs to local scale using change factors. Differences between a future and control GCM run are superimposed on a local-scale baseline observation dataset. Because of the simplicity of this method, a large number of GCMs can be downscaled, facilitating the possibility to use a large ensemble of possible future climates in climate change impact studies. Shortcomings of this method are the assumption that the bias between the GCM and the local-scale data remains constant in time, and also the fact that only changes in the mean, minima and maxima of climatic variables are considered [Fowler *et al.*, 2007], making this less suitable for hydropower related assessments.

The Advanced Delta Change (ADC) approach [van Pelt *et al.*, 2012], built on work by Leander and Buishand [2007], has the advantage over the classical delta change method that not only changes in the mean are considered, but also the changes in extremes, thus making a non-linear transformation of climate signals in GCMs. Besides, changes in multi-day precipitation events are also modeled. The approach has been successfully applied in the Rhine basin in Europe [van Pelt *et al.*, 2012]; it was also applied in the upper Indus basin (unpublished), where some difficulties were experienced with the downscaling of precipitation, which probably stem from the high spatial variability of meteorological variables in the high mountainous terrain. Additional corrections had to be applied to correct unrealistic changes in extreme precipitation events. To test the usefulness of the initial nonlinear bias-correction approach developed by Leander and Buishand [2007] in complex, orographically influenced climate systems, it was used to bias-correct RCM temperature and precipitation for the upper Rhone basin in Switzerland [Bordoy and Burlando, 2013]. They concluded that the method is able to dramatically reduce the RCM errors for both air temperature and precipitation and further

concluded that the method could successfully be used for correcting future projections. However, they also observed that an undesired effect of the technique developed by *Leander and Buishand* [2007] was that it generated extreme precipitation values which considerably exceeded the range of the observations.

In Model Output Statistics (MOS) approaches, the statistical relationship between predictors and predicted values is established by using simulated predictor values instead of observed values to make predictions. In most applications local-scale climate is predicted, and a correction and a downscaling step are combined in MOS. The predictors can be either simulated time series or properties of the simulated intensity distribution. The predicted (simulated) values can either be local-scale precipitation time series or local-scale intensity distributions. MOS is mostly used for RCM downscaling, while MOS application for GCM downscaling is still limited [*Eden et al.*, 2012; *Eden and Widmann*, 2014].

Multiple post-processing methods, termed empirical-statistical downscaling and error correction methods (DECMs), are based on the MOS approach. *Thiemeßl et al.* [2011a] tested seven DECMs for RCM-downscaling of climate in the mountainous terrain of Austria, and found that point-wise methods like quantile mapping, and local intensity scaling as well as indirect spatial methods as non-linear analogue methods improve the original RCM signals. Quantile mapping can in principle be used to downscale and bias-correct multiple climatic variables. Successful applications for air temperature and precipitation have been reported. Since these are the main drivers for most hydrological models, also improvement in other variables, that are derived from temperature and precipitation (e.g. snow accumulation, melt water generation) can be expected.

Multiple linear regression methods however, show significant shortcomings in modelling daily climate due to their linear nature. At the same time, satisfactory downscaling of precipitation is of utmost importance for mountainous terrain such as the upstream sections of the Indus, Ganges and Brahmaputra. Local intensity scaling applies a spatially varying scaling to climate model precipitation accounting for its long-term bias at the location of the observation [e.g. *Schmidli et al.*, 2006]. Quantile mapping [e.g. *Boé et al.*, 2007] corrects for errors in the shape of the distribution and is therefore capable to correct errors in variability as well as the mean. According to *Thiemeßl et al.* (2011a), quantile mapping performed the best of seven DECMs that they compared for mountainous terrain in Austria. Adaptations in the quantile mapping method also allow for good simulation of future extremes, which do not occur in the calibration period [*Thiemeßl et al.*, 2011c]. *Immerzeel et al.* [2013] successfully applied the Quantile Mapping method developed by *Thiemeßl et al.* [2011b] to downscale GCM data using observed data from two ground stations in the HKH region.

Weather generators are statistical models generating random sequences of weather variables, with statistical properties resembling observed weather. They are most commonly used to simulate weather at point locations. The weather generator based approaches that generate spatial fields are grouped in three categories [*Ferraris et al.*, 2003]: multifractal cascades, nonlinearly filtered autoregressive processes, and point processes based on the random positioning of a given number of rainfall cells. Attempts to generate continuous spatial precipitation fields have only recently been extended for downscaling [*Maraun et al.*, 2010].

*Forsythe et al.* [2014] combined a stochastic rainfall model and a rainfall conditioned weather generator to assess climate change signals for three ground stations in a section of the Upper Indus basin. Validation against a time-series of observations at these three locations showed that the model simulated means of climatological variables well, despite the complex climate of

the mountainous region at the boundary of monsoonal and westerly climate systems. Future climate was assessed using change factors derived from comparison of a future and control time slice of an RCM.

*Bordoy and Burlando* [2014] used a stochastic approach to downscale climate model outputs, from several locations in the Swiss Alps, to a sub-daily temporal resolution. Their methodology is based on re-parameterizing the Spatiotemporal Neyman-Scott Rectangular Pulses model (ST-NSRP) for climate predictions. Their approach showed to be robust and effective in addressing the internal variability of precipitation, compared to other downscaling techniques which are hindered by computational and resolution problems [*Bordoy and Burlando, 2014*]. *Ragetti et al.* [2013] successfully applied the same methodology to downscale GCM monthly data to a daily temporal resolution at three stations in the Hunza basin, which is located in the upper Indus basin.

### **2.3 Future climate change and variability in the Indus, Ganges and Brahmaputra basins**

Climate change in the upstream Indus, Ganges, Brahmaputra, Salween and Mekong has been simulated for up to 2050 in a study by ICIMOD's HICAP Program, using the simple delta change method [*Lutz et al., 2014*]. For both RCP4.5 and RCP8.5 four GCM runs were selected covering the entire range of area-averaged projected changes in mean air temperature and total precipitation for the entire upstream parts of the Indus, Ganges, Brahmaputra, Salween and Mekong basins. The analysis showed that mean air temperature is expected to increase between ~1.7 and 2.9 °C (RCP4.5) and ~2.0 to 3.5 °C (RCP8.5) for the upstream Indus, Ganges and Brahmaputra between 1961-1990 and 2021-2050 (Figure 8). The projections for precipitation are more uncertain, indicating potential changes ranging from -10% to +10% for the upper Indus and +5% to +15% for the upper Ganges and Brahmaputra (RCP4.5). For RCP8.5 the numbers are -15% to +10% for the upper Indus +5% to +35% for the upper Ganges and +5% to +15% for the upper Brahmaputra. The large differences in the projections for the winter season and monsoon season are striking, indicating that GCM outputs for climate change impact studies, including hydropower related studies, should be analysed at least at seasonal level, but preferably at monthly or even narrower level.

An analysis of PRECIS RCM data for the A1B scenario in the Indus basin, until the end of the century, indicated a potential increase in winter precipitation in the upper Indus basin, whereas decreasing winter precipitation is projected for the lower Indus basin [*Rajbhandari et al., 2014*]. The projected change in monsoon precipitation is highly variable. Greater warming is projected for the upper basin than for the lower basin, indicating that the observed elevation-dependent warming is likely to continue in the future. Furthermore a slightly greater increase in minimum air temperature than maximum air temperature is projected. A stronger warming of winter temperatures is projected, compared to other seasons. Three simulations indicated that changes in precipitation are more uncertain than temperature change.

Projections of 32 GCMs, from the CMIP5 model ensemble, were analysed for the Hindu-Kush-Karakoram and the Himalaya [Palazzi *et al.*, 2014] (Figure 10). RCP4.5 and RCP8.5 were considered. The CMIP5 models predicted wetter future conditions in the Himalaya during the monsoon season, with precipitation gradually increasing until the end of the century. For the Hindu-Kush-Karakoram, wetter summer conditions were also projected for RCP8.5, whereas in both regions no significant change in winter precipitation was observable. The authors emphasize that no single model performs significantly better than the others, and the projections vary to a large degree.

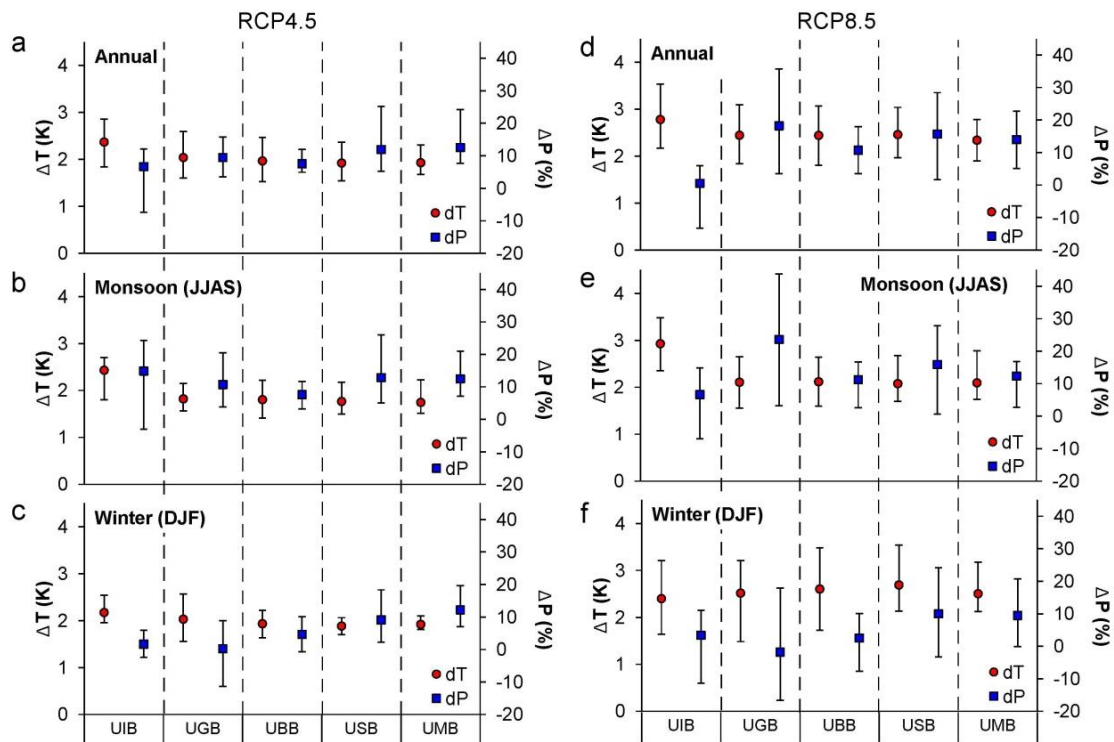


**Figure 9: Projected ranges of changes in mean air temperature and total precipitation between 1961-1990 and 2021-2050 [Lutz *et al.*, 2014]**

Six statistically downscaled GCMs predicted accelerated seasonal increases in temperature and precipitation in the Brahmaputra basin for the period 2000 to 2100, with largest changes on the Tibetan Plateau and smallest changes on the Brahmaputra floodplain [Immerzeel, 2008].

For India, RCM based climate change projections were generated for the 21<sup>st</sup> century [Rupa Kumar *et al.*, 2006]. Projections were made for the IPCC SRES scenarios. The projections indicated uniform widespread warming over the country. Extremes in minimum and maximum temperatures are projected to increase. Substantial spatial variation in precipitation change is projected. Maximum increase in precipitation is projected for west-central India. Precipitation extremes are projected to increase over a large area, with strongest increases projected for the Indian west coast and west-central India.

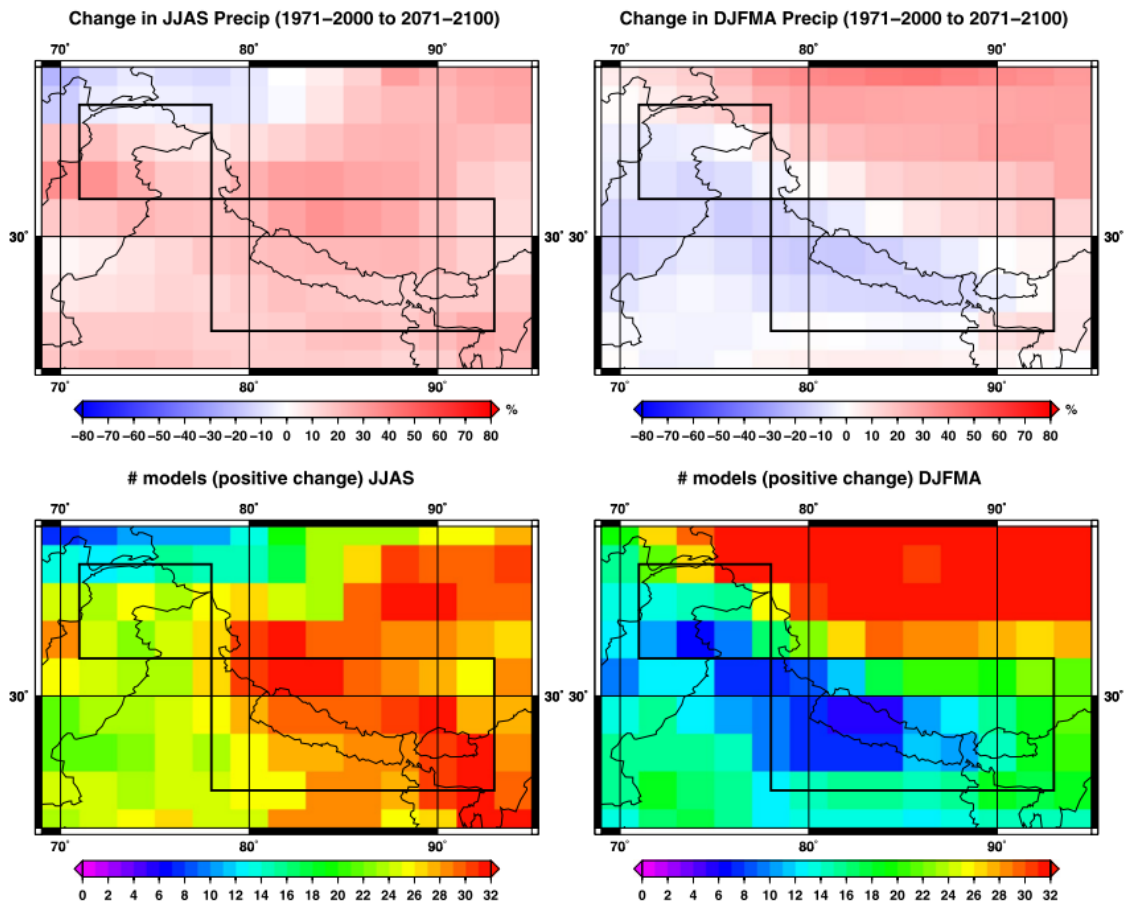


**Figure 10: Projected percentage precipitation change in 2071–2100 (RCP 8.5 scenario) relative to 1971–2000 in summer (top left) and winter (top right) for the multi-model-mean of the CMIP5 ensemble. Number of models (out of 32) showing, in each 2°x2° pixel, a positive precipitation change [Palazzi et al., 2014].**

Multiple studies on climate changes in smaller areas within the basins have been conducted. A study using downscaled RCM output for the northern part of the upper Indus basin projected year-round increases in precipitation between 1961-1990 and 2071-2100 (+18% annual mean change) with increased intensity in the wettest months February, March and April (+27% seasonal mean) [Forsythe et al., 2014]. In addition, year-round increases in mean temperature around +4.8 °C were projected. The authors emphasize that the year-round uniformity in temperature increase is in contrast to the asymmetrical recent trend in observations. Furthermore the authors emphasize that this study can be seen as exploratory because only one RCM was used, whereas the use of an ensemble of RCMs to force the model would provide more information about possible future “trajectories” of the climate in the upper Indus basin.

Downscaled climate change scenarios for the Langtang and Baltoro catchments, using the Quantile Mapping downscaling approach [Themeßl et al., 2011c], showed that a consistent temperature increase is expected in both catchments until the end of the 21<sup>st</sup> century [Immerzeel et al., 2013]. A stronger increase in precipitation is projected for the Langtang catchment (upper Ganges) than for the Baltoro catchment (upper Indus), with a larger uncertainty of precipitation projections in Baltoro due to the large variability in GCM results over the Indus basin. For the Hunza basin, Ragetti et al. [2013] also found a consistent temperature increase until 2050, based on three downscaled GCMs. Two GCMs indicated an increase in precipitation whereas the third indicated a decrease.

*Sharmila et al.* [2015] analyzed future projections of Indian summer monsoon variability in CMIP5 GCMs for RCP8.5. The authors first filtered the CMIP5 ensemble for models simulating the monsoon satisfactory over a historical period. Subsequently changes in future monsoon dynamics were assessed for the five remaining models. The projections of these five models are consistent and are summarized as follows:

- The Indian summer monsoon is very sensitive to global warming.
- Summer monsoon mean rainfall is likely to increase moderately.
- Higher rainfall intensity is likely over the core monsoon zone.
- A decreasing number of wet days is likely.
- The monsoon season lengthens due to later withdrawal.
- Larger inter-annual variability in monsoon intensity is likely.

Earlier projections for summer monsoon climate over India using a RCM and IPCC SRES scenarios already indicated an expected increase in summer monsoon precipitation by 9-16% in the 2080s compared to the 1970s. Besides the number of rainy days was projected to decrease accompanied by increasing rainfall intensity on wet days [*Krishna Kumar et al.*, 2011].

## 2.4 Performance of climate models

*Mishra* [2015] showed that in the CORDEX framework all RCM ensemble members fail to reproduce observed climatic trends in the Indus, Ganges and Brahmaputra basins, and that the GCMs which provide the boundary conditions for the RCMs in general simulate winter climate in the region better than the CORDEX RCMs. The authors conclude that reliability of future climate projections and their impacts on water resources in the region will depend on improvements in the models and observations in coming years.

From their analysis of 32 CMIP5 GCMs in the region, *Palazzi et al.* [2014] concluded that there is no particular model that is “best” in simulating the climate in the HKH region. From their pool of models only three were able to satisfactorily simulate the annual cycle of precipitation in the region. However, even these three models failed to reproduce observed trends in precipitation. The authors conclude that since no single model can be chosen as best performing, it is important to use results from the whole range of models in climate change impact assessments.

### 2.4.1 Monsoon dynamics

Since the monsoon is a crucial climatic feature in the HKH region it is important to know how well the regional monsoon dynamics are represented in climate models. A study focusing only on representation of the Asian summer monsoon compared performance of CMIP3 and CMIP5 GCMs, by pattern correlation of spatial grids of models and observations [*Sperber et al.*, 2013]. The authors conclude that GCMs in CMIP5 are better able to simulate monsoon dynamics than CMIP3 models. The pattern correlation of the timing of monsoon peak and withdrawal is better simulated than that of monsoon onset. The simulated onset of the monsoon over India is typically too late in both the CMIP3 and CMIP5 models. Furthermore the simulation of intra-seasonal variability remains problematic, but several models show improved skill between CMIP3 and CMIP5 at representing the northward propagation of convection and the development of the tilted band of convection that extends from India to the equatorial west Pacific.

Figure 11 shows the performance of the models in simulating the pattern correlation relative to the observations-based GPCP [Schneider et al., 2013] of the onset versus the peak, withdrawal, and duration of the monsoon, respectively. The purpose is to evaluate which aspects of the annual cycle are best represented, and to test whether the ability to simulate the onset also translates into the ability to represent the other stages in the annual cycle of the monsoon. Panels a and b indicate that the ability to simulate the pattern of monsoon peak and monsoon withdrawal is typically better than simulating the onset, but there is no statistical relationship in the ability to simulate peak or withdrawal relative to onset. The panels c and d indicate that the pattern of the monsoon duration is better represented in models that simulate the onset pattern better. In summary the authors state that the pattern correlation skill metrics indicate that the models are very diverse in their ability to simulate the monsoon annual cycle, with the CMIP5 multi-model-mean outperforming the CMIP3 multi-model mean.

Using a different technique to assess monsoon representation in CMIP5 climate models Sperber and Annamalai [2014] concluded that most model simulations show delayed onset of summer rainfall over India. They also observed that most models simulate the inter-annual variability in the date of monsoon onset quite well; the exceptions being models with the most pronounced dry biases.

In another study the conclusion was drawn that no significant progress has been achieved by comparing the CMIP3 ensemble to the CMIP5 ensemble in representing the continental Indian monsoon [Ramesh and Goswami, 2014]. The authors observed a larger bias in CMIP5 models' predictions than in CMIP3 models', and that inter-annual variability of the CMIP3 multi-model mean was better than the CMIP5 multi-model mean (Figure 12).

Sharmila et al. (2015) assessed the performance of 20 CMIP5 GCMs in simulating: precipitation during the monsoon season; inter-annual variability; latitudinal migration of daily precipitation; and intra-seasonal variance of precipitation within the monsoon season, for the Indian summer monsoon. Based on these criteria the authors conclude that only 5 out of 20 models represented the monsoon satisfactorily.

From these studies it is clear that satisfactory representation of monsoon dynamics in climate models remains problematic, which also makes projections of future climate more uncertain in the HKH region, compared to most other regions. The spread in model outcomes also implies that it is preferable to use an ensemble of climate models over a single or a few climate models.

Applying empirical-statistical downscaling and bias-correction techniques to the raw GCM data can overcome this poor representation to large extent. These techniques introduce historical climatic information from observations that have higher quality and higher resolution than the raw GCM data. This additional information is used to correct for biases between the GCM historical run and observations for the same period at the spatial resolution of the observations-based dataset. The corrections can then be applied to a GCM run in the future, assuming that the error characteristics stay constant in time. The improvement of raw GCM data by empirical-statistical downscaling and bias-correction techniques has been demonstrated in multiple studies [e.g. Piani et al., 2010; Terink et al., 2010; Themeßl et al., 2011b, 2011c; Wilcke et al., 2013; Maurer and Pierce, 2014]. Very recent research suggests that some empirical-statistical downscaling and bias-correct techniques even improve the climate change signal from the raw GCM data [Maurer and Pierce, 2014; Gobiet et al., 2015]. Despite that part of the errors stemming from poor representation of monsoon dynamics in GCMs can be corrected using

these techniques, uncertainty remains as the projected changes by a GCM with poor representation of the actual climate may be more uncertain.

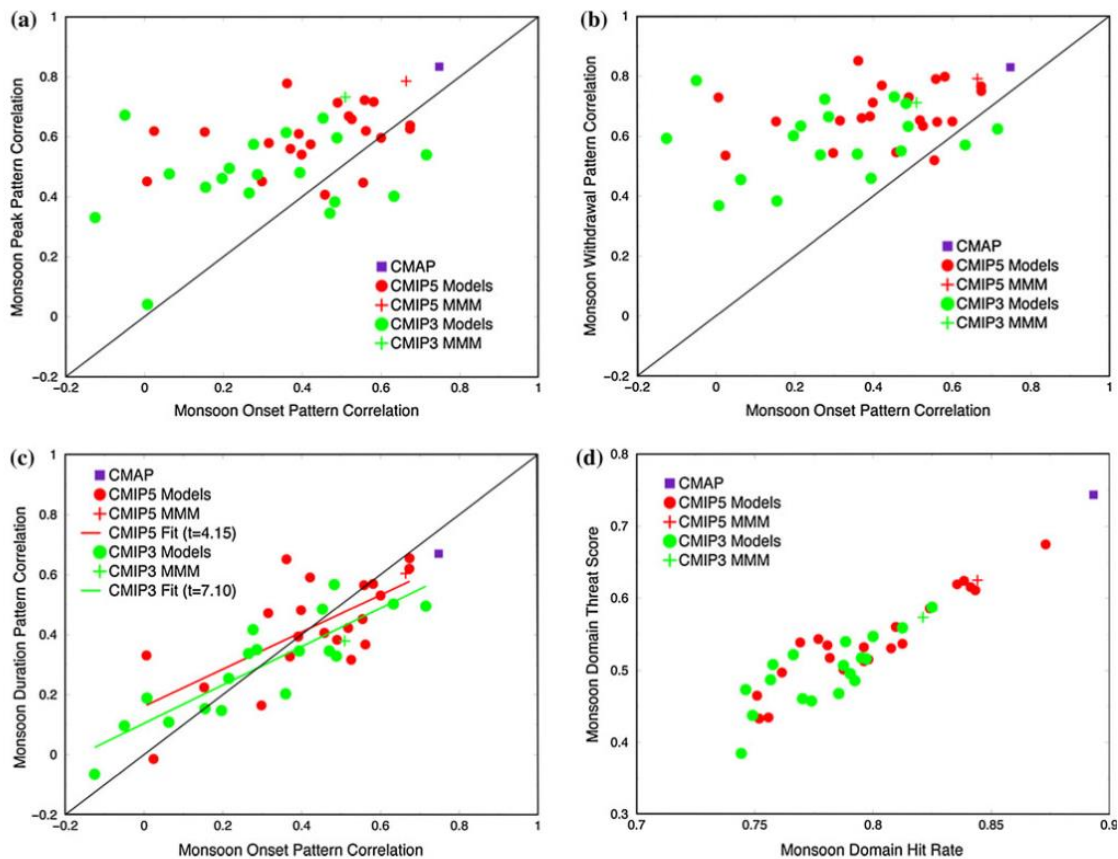
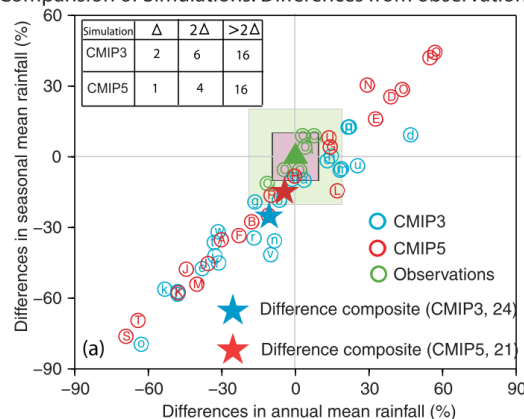


**Figure 11: Scatterplot of the pattern correlation with observations of the simulated pentad of monsoon onset versus a) the pattern correlation with observations of the simulated pentad of monsoon peak, b) the pattern correlation with observations of the simulated pentad of monsoon withdrawal, and c) the pattern correlation with observations of the simulated number of pentads of monsoon duration. d) Scatterplot of the Monsoon Domain Hit Rate versus the Monsoon Domain Threat Score. In a–d the simulation ability is with respect to GPCP for the region 50°E–180°E, 0°–50°N. Source: [Sperber et al., 2013].**

Comparison of Simulations: Differences from observations



Comparison of Simulations: Interannual variability

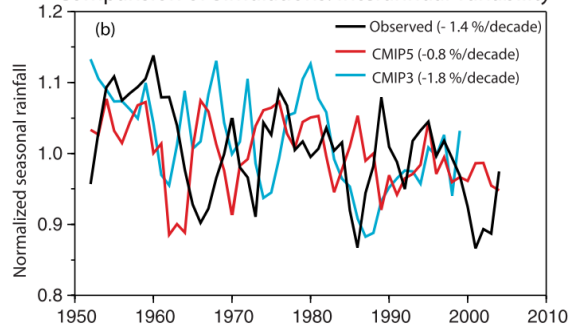


**Figure 12: Left: Distribution of historical (1951–2005) simulations of seasonal and annual rainfall over continental India with CMIP5 (red, uppercase) and CMIP3 (blue, lower case) as difference between simulation and composite of observations (green). The scatter in the observations (green) is shown as a percentage deviation (simulation – observed composite) from the observed**

**composite** The acceptable uncertainty is defined by the difference ( $\Delta$ ) between the maximum and the minimum in the observed values, centered at the observed composite; the inner shaded box (pink) is defined by  $1\Delta$ , while the outer square (green) is defined by  $2\Delta$ . The inset table shows the number of simulations that fall in each category. Right: Inter-annual variability in Continental Indian Monsoon (CIM) rainfall from the composite observations and ensemble of simulations (normalized to the respective 1951–2005 mean). The linear trend for the respective case is given in the bracket.

## 2.5 Summary remarks

Findings from analyses of historical climatic trends in the HKH region are summarized below.

- Air temperature has been increasing in the HKH region over the past decades. Rates of increase are different for daily mean air temperature, maximum air temperature and minimum air temperature. Temperature increase is elevation dependent; increase is stronger for higher elevations
- Precipitation shows no significant increasing or decreasing trends generally, but this varies locally.

Future projections of climate change are analyzed with dynamically or statistically downscaled global and regional climate models. The major findings from analyses of future climate are summarized below.

- Climate warming is likely to continue during the 21<sup>st</sup> century
- For precipitation change, the climate models project a wide range of possible futures, including strong precipitation increases and precipitation decreases. For the upstream Ganges and Brahmaputra precipitation increase is most likely, but the magnitude is highly uncertain. For the upstream Indus precipitation projections point to increases and decreases, but with large variability (uncertainty).
- For the Indian summer monsoon increases in precipitation totals, precipitation intensity, inter-annual variability in monsoon strength, and inter-daily variability are likely to increase.

The important remark has to be made that the current state-of-the art GCMs and RCMs have significant difficulties in simulating the complex climate in the HKH region. Only a limited number of models can satisfactorily simulate the monsoon dynamics and no model is able to simulate all important features in the HKH precipitation regimes.

# 3 Cryosphere Dynamics

## 3.1 Cryosphere components distribution

### 3.1.1 Glaciers

According to the ICIMOD glacier inventory [Bajracharya and Shrestha, 2011], there are 37,955 glaciers in the Indus, Ganges and Brahmaputra basins, covering 44,224 km<sup>2</sup>. The same study evaluated the total volume of ice to be about 4,793 km<sup>3</sup>. Characteristics such as surface cover, volume or climatic response have been shown to differ significantly in the different basins (Table 4, Figure 13).

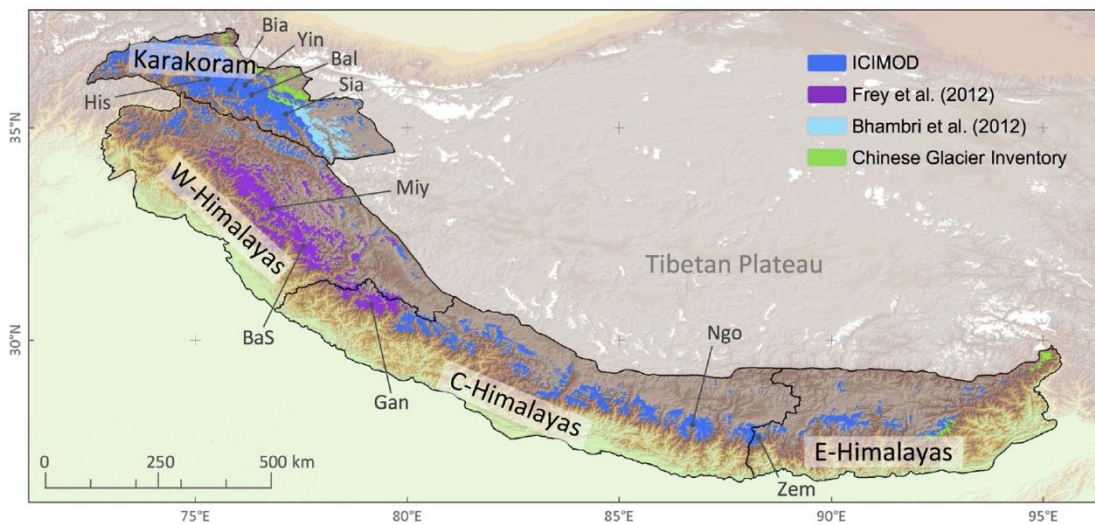


**Figure 13: Distribution of glaciers in the HKH, as obtained from ICIMOD's inventory [Bajracharya & Shrestha, 2011], by Bhambri et al. [2013], and the Chinese Glacier Inventory (Sia: Siachen, Bal: Baltoro, Bia: Biafo, Yin: Yinsugaiti, His: Hispar, BaS: Bara Shigri, Miy: Miyar, Gan: Gangotri, Ngo: Ngozumpa, Zem: Zemu) (Source: [Frey et al., 2014])**

The Indus basin includes large glaciers from northern Pakistan, and north western India. The Ganges basin includes glaciers from western India (Uttarakhand State), and Nepal. Brahmaputra basin includes glaciers located at the China border with Nepal on the southern part of the Tibetan Plateau; as well as glaciers at the north-east of Lhasa, in the Nyaingentanglha mountain range; and glaciers at the south-east of the same plateau in the ParlangZangbo Mountains near the China's border with Arunachal Pradesh Indian state. Part of the glaciers of this basin is also located in the Sikkim state of India, in Bhutan, and in Arunachal Pradesh state of India. The Indus basin probably has the largest volume of ice of all the three basins. Finally, the Ganges has the least glacier cover and volume [Bajracharya & Shrestha, 2011; Frey et al., 2014]; see also Table 4 and Table 5.

**Table 4: Glacier cover and volume estimates from different studies in the Indus, Ganges and Brahmaputra basins.**

|                                | Study  | Indus                         | Ganges                       | Brahmaputra                    |
|--------------------------------|--|-------------------------------|------------------------------|--------------------------------|
| <b>Basin area</b>              |  | 1,116,086 km <sup>2</sup>     | 1,001,019 km <sup>2</sup>    | 528,079 km <sup>2</sup>        |
| <b>Number glaciers</b>         | ICIMOD [ <i>Bajracharya and Shrestha, 2011</i> ] | 18,495                        | 7,963                        | 11,497                         |
| <b>Glacier Surface</b>         | ICIMOD   | 21,192 km <sup>2</sup> (1.8%) | 9,012 km <sup>2</sup> (0.9%) | 14,020 km <sup>2</sup> (2.6%)  |
|                                | Nuimura et al., 2015                             | 23,668 km <sup>2</sup>        | 7,537 km <sup>2</sup>        | 9,803 km <sup>2</sup>          |
|                                | RGI [ <i>Pfeffer et al., 2014</i> ]              | 26,018 ± 1750 km <sup>2</sup> | 10,621 ± 824 km <sup>2</sup> | 17,419 ± 1,373 km <sup>2</sup> |
| <b>Debris covered fraction</b> | ICIMOD [ <i>Bajracharya and Shrestha, 2011</i> ] | 9.6%                          | 12.6%                        | 11.1%                          |
| <b>Volume</b>                  | ICIMOD [ <i>Bajracharya and Shrestha, 2011</i> ] | 2,696 km <sup>3</sup>         | 794 km <sup>3</sup>          | 1,303km <sup>3</sup>           |

The Indus basin in the western part of the HKH (junction of Hindu Kush, Karakoram and Himalaya) is influenced by the westerlies and most of the yearly precipitation comes from winter snowfall. In this basin glaciers accumulate snow during the winter. In the central and eastern parts of the HKH, where the Brahmaputra and the Ganges basins lie, most of the yearly precipitation occurs during the monsoon, and glaciers tend to accumulate snow during the summer and the accumulation and melt seasons tend to overlap.

A significant proportion of the glaciers in the region are covered by a layer of rock debris in their frontal part. Melting of glacier surfaces below a layer of debris can be either accelerated compared to debris-free surfaces if the debris layer is thin (a few centimeters), or dampened if the thickness is more than a threshold of 5 cm [*Mihalcea et al., 2006; Brock et al., 2010; Nicholson & Benn, 2006*]. Assessment of the distribution and percentage of debris-covered glacier is thus crucial when studying changes in the cryosphere of the region. Debris-covered glaciers should thus be identified and taken into account when selecting benchmark glaciers for mass balance studies [*Scherler et al., 2011a*].

In 2011, ICIMOD developed a glacier inventory of the entire HKH region from satellite images [*Bajracharya and Shrestha, 2011*]. ICIMOD has mapped the debris-covered part of the HKH glaciers for their inventory, but unfortunately the Chinese section of the catchment was treated separately and the calculations did not include a differentiation of the clean and debris-covered ice. *Nuimura et al. [2015]* also propose a High Asian glacier inventory, and data can also be obtained from the Randolph Glacier Inventory [*Pfeffer et al., 2014*]. We compared herein the results from these three inventories, to emphasize that large differences can arise resulting from the method chosen to define glacier boundaries, as well as different interpretations of debris-covered glaciers (Table 4). Glacier volumes are difficult to determine. They are generally inferred from the knowledge of the area of a glacier and its slope, using parameterizations [*Frey et al., 2014*]. Table 5 shows example estimates of glacier volumes in the HKH from various studies implying volume-area relationships (The studies presented do not propose a basin-related analysis).

**Table 5: Glacier volume estimates for the whole HK region following different studies (km<sup>3</sup>).**

|                               | Karakoram   | Western-Himalaya | Central-Himalaya | East-Himalaya | Total       |
|-------------------------------|-------------|------------------|------------------|---------------|-------------|
| <b>Frey et al, 2014</b>       | 2,965-1,537 | 759-394          | 723-345          | 283-147       | 4,731-2,453 |
| <b>Marzeion et al. (2012)</b> | 2,748       | 611              | 771              | 279           | 4,409       |
| <b>Grinsted (2013)</b>        | 1,896       | 584              | 714              | 265           | 3,459       |
| <b>Radic et al. (2013)</b>    | 2,953       | 657              | 828              | 300           | 4,738       |

### 3.1.2 Snow cover

For higher altitude river basins in the HKH, annual snow melt is an important contributor to river runoff [Bookhagen and Burbank, 2010]. Furthermore, recent studies have shown that snow cover extent in the Himalayas and on the Tibetan-Qinghai plateau could influence the strength of the monsoon: an extensive winter snow cover on the Tibetan plateau generally leads to weaker monsoon intensity [Pu and Xu, 2009]. The variations of the snow-rain altitude transition line impacts the reflectivity of glaciers (albedo) and plays a crucial role in the melt dynamics of the glaciers. Studying the spatial and temporal variations of snow-cover extent, snow accumulation and melt dynamics is thus crucial.

Snow cover varies greatly seasonally and as such is much more dynamic than glacier cover. Understanding of its spatial distribution as well as its seasonal variation is important. One of the most extensive studies on snow-cover extent in the HKH is the ICIMOD study based on MODIS products [Gurung et al., 2011]. This study investigated the snow cover area (SCA) in time steps of 8 days, covering all the Hindu-Kush Himalaya from 2000 to 2010. A study by Immerzeel et al. [2009] covered all the HKH with stronger emphasis on the Indus basin.

ICIMOD's study showed that in the Indus basin the mean SCA between 2000 and 2010 was 167,992 km<sup>2</sup>, thus covering 16.7% of the total area. But focusing only on the upper Indus basin, Immerzeel et al. (2009) found a mean SCA of 33%. The SCA in the Ganges is 47,742 km<sup>2</sup> (5% of the total area). In the Brahmaputra river basin, this area was found to be 107,121 km<sup>2</sup> (20.4% of total area). The study didn't find significant trends in the SCA for any of the three river basins between 2000 and 2010.

In the Himalaya, the maximum of SCA occurs at the beginning of spring [Bookhagen and Burbank, 2010]. The large SCA in the Indus and Brahmaputra basin builds up during the winter, whereas the Ganges basin's SCA only slightly increases during this time. During the other seasons SCAs in the basins are comparable. In the Indus basin the snow line varies from 2,336 m.a.s.l in winter to 4,109 m.a.s.l in summer. In the Ganges the snow line is highest in winter at 3,330 m.a.s.l, which is nearly 1,000 m higher than in the Indus basin [Immerzeel et al., 2009].

### 3.1.3 Permafrost

Studying and understanding of permafrost in the HKH region is very limited compared to for example the European Alps or the Canadian tundra. Permafrost is defined as sub-surface material (excluding glaciers) having a temperature of less or equal to 0 °C during at least two consecutive years. Mean annual ground temperature (MAGT) as well as permafrost occurrence and properties exhibit strong lateral variation over ranges of only few meters to few kilometers. This is mostly due to the effects of topography, vegetation cover, ground material, water bodies and/or snow distribution.

A global permafrost zonation map [Gruber, 2012] is probably the best available indication of the occurrence of permafrost in the HKH region at the moment. This map was generated with a global model of permafrost extent including established links between air temperature and permafrost occurrence and uses parameterizations based on published estimates. It is available at 1 km<sup>2</sup> resolution.

The maps show that it is likely that the river basin with the most permafrost is the Brahmaputra, since a large portion of this basin lies on the Tibetan plateau, where large areas are likely to be permafrost areas (Figure 14).

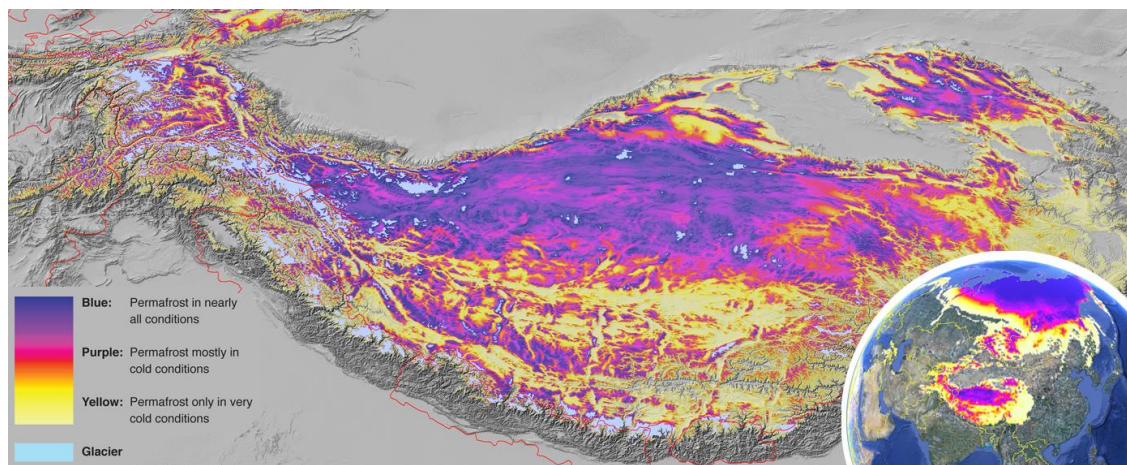


**Figure 14: Permafrost zonation index map of the Tibetan plateau [Gruber, 2012].**

It is clear that the knowledgebase on permafrost in the HKH region is rather limited. Although much more is known about permafrost and changes in permafrost in well monitored regions like the European Alps, it is not recommended to transfer findings from there to the HKH region because the regions differ strongly in climate, bedrock, elevation differences and steepness of the terrain.

## 3.2 Approaches to measure cryosphere components

### 3.2.1 *In-situ*

#### 3.2.1.1 Glaciers

The variation in the front position of glaciers is the variable most easily measured in-situ. These variations could be linked to the mass balance of glaciers and, therefore, provide information on climate variations [Oerlemans, 2005]. Because of this many studies in the HKH, especially in western India, have focused on the variations in front positions (Geological Survey of India, 1998, Annual General Report, Part 8, Vol. 132). However, significant areas of Himalayan glaciers are covered with debris, and the presence of debris on the surface of glaciers can provide varying degrees of insulation [Mihalcea *et al.*, 2006]. Therefore, it can be expected that the melt processes on debris-covered glaciers could vary significantly from those of debris-free glaciers. As a result, variations in the front positions of debris-covered glaciers would not be suitable indicators of recent climate change [Scherler *et al.*, 2011a]. Furthermore, glaciers with extensive stagnant tongues (i.e., motionless fronts) may still present negative mass balances [Scherler *et al.*, 2011a]. More recent studies have determined that thinning rates of debris-covered glaciers were similar to those of clean glaciers [e.g., Kääb *et al.*, 2012]. Our conclusion

is that we do not expect the variations in the front positions of glaciers in the HKH to be relevant indicators for hydrological change assessments.

In-situ glacier mass balance (iMB hereafter) estimates are obtained by determining variations in the height of glaciers (by manually measuring the emergence and position of stakes inserted into the glaciers during field campaigns), combined with determining snow accumulation in the upper sections of the glaciers (using stakes)). Geodetic mass-balances are obtained from differential GPS (DGPS) measurements of the variation in the surface altitude of the glacier, combined, ideally, with snow and ice density measurements [Zemp *et al.*, 2013]. The spatial density and distribution of stakes (or DGPS) measurements can significantly influence the accuracy of the iMB evaluation. Because the various monitoring programs are not using a standardized methodology there are large variations in the spatial coverage between sites and therefore also in overall iMB accuracy [Zemp *et al.*, 2013]. iMB measurements require thorough field work and this is hampered by the remoteness of most areas, as well as by the high altitudes of many accumulation zones frequently found in the HKH. Glacier accumulation monitoring is nearly impossible above 6,500 m.a.s.l. Therefore, the few sites that can be monitored regularly must be carefully selected to ensure that they represent as closely as possible the different climatic regions in the geographical areas involved. In-situ iMB measurements contribute data crucial for validating the large scale mass balance assessments obtained by using remote sensing techniques.

Glacier surface velocity provides information pertaining to the dynamics of the redistribution of mass from the upper parts of the glacier to its lower parts. This, in turn, provides insight into the glacier's response to climate change [Azam *et al.*, 2012; Gardelle *et al.*, 2012]. The velocity of the ice can be inferred by measurement of either stake positions, or of the positions of boulders on the glacier surface using differential GPS.

The volume of glaciers is a variable of high interest with regards water storage. Glacier volume is usually inferred by combining knowledge of glacier area and slope using parameterized relationships linking observed glacier surface to glacier volume [Frey *et al.*, 2014]. However, parameterizations can only be validated by in-situ measurements of ice depth. On site ground penetrating radar provides information about the depth at which abrupt changes in the dielectric constant occurs. This technique can therefore be used to monitor the thickness (depth) of glaciers. However, the technique has only been used sporadically in the HKH [e.g. Azam *et al.*, 2012].

The World Glacier Monitoring Service (WGMS) collects and provides information on glaciers that are monitored during field measurement campaigns, including stake measurement, geodetic mass balances and front variations. Over the Indus, Ganges and Brahmaputra basins, iMBs were measured on several glaciers in most of the climatically representative regions. Unfortunately, time coverage of these monitoring programs is poor and geographically inhomogeneous. The main in-situ glaciological mass balance measurement programs existing over the region and their characteristics are presented in the results section in Table 6.

In India many glaciological studies were done by the Geological survey of India (GIS) in the Indus basin, mainly in the Indian part of the catchment. The front variations of a tenth of the glaciers in the Himachal Pradesh and Jammu and Kashmir were monitored by the GIS monitored in the seventies and eighties. Mass balance measurements were also done mostly in the seventies and eighties, but less frequently and for fewer glaciers. Since programs were periodically interrupted, the registered time series remain short (a few years). New

measurement programs were started in this region at the beginning of this century, they are still on-going, and focus on glaciers that were not monitored previously.

In Nepal only single measurements of yearly mass balance were recorded sporadically between 1978 and 1979, and new glaciological programs were started from 2007, some including previously measured glaciers. Whereas on the Tibetan plateau, new mass balance programs started in 2005 on glaciers that contribute to the Brahmaputra outflow, but no measurements were recorded previously.

On the Tibetan plateau, new mass balance programs started in 2005, on glaciers that contribute to the Brahmaputra outflow, but no measurements were recorded before.

### 3.2.1.2 Snow

Seasonally, snow-melt can be an important contributor to the runoff of rivers in the HKH [Bookhagen and Burbank, 2010]. *In-situ* measurements of snow water-equivalent precipitation are needed in hydrological modeling to assess the maximum amount of melt that can be expected from snow cover. Characterizing the snow-rain transition altitude and its evolution with regard to time and meteorological factors is also essential in order to correctly model the future evolution of snow cover. The snow-rain transition altitude also plays a crucial role in the mass balance of glaciers by influencing the height at which the glacier albedo is increased by freshly fallen snow. Most snow-cover studies in the Himalayas have used satellite imagery to assess snow cover and snow depth, but *in situ* measurements remain essential to validate remote sensing measurements.

Snow water-equivalent can be calculated from the measured snow thickness and the known snow density. Snow depth can be measured either manually using stakes, or automatically with sensors on meteorological stations, such as sounding height rangiers or lasers. Snow density is measured by weighing known volumes of snow manually. Note that *in-situ* measurements on a snow-pack integrate snow deposition, melt, sublimation, as well as aeolian erosion.

Some sensors can also automatically monitor snow water-equivalent directly: if it is possible to distinguish between snow and rain events, a classical rain gauge could provide measurements of the snow equivalent [Lejeune *et al.*, 2003, 2007]. However, distinguishing between rain and snow remains a challenge and precipitation gauges often underestimate precipitation, especially during snow events [Lejeune *et al.*, 2003, 2007]. New generation, real-time, laser based precipitation sensors, allowing for counting hydro-meteors and assessing their magnitude (disdrometers), can help to distinguish snow and rain during precipitation events [Löffler-Mang and Joss, 2000]. When coupled with a properly calibrated and corrected pluviometer, they may enable the evaluation of the snow precipitation water-equivalent. Other sensors measure the change in natural occurring electromagnetic energy emanating from the ground as it passes through snow-cover [Ducharme *et al.*, 2015]. They provide an average snow cover on area extent of a few tenths of meters.

Very few studies focused on *in-situ* measurements of snow cover in the Indus, Ganges and Brahmaputra river basins. Brown [2000] used measurements obtained since 1800 from the Chinese measurement network on the Tibetan plateau to reconstruct trends in snow cover areas in the northern hemisphere. In two recent studies, automatic snow height sensors were installed on measurement sites in the HKH. Measurements on the Chhota Shigri glacier in India are briefly described by Azam *et al.* [2014], and data obtained in the Langtang catchment in

Nepal are described by *Immerzeel et al.* [2014]. Sonic height range measurements are also available from Pyramid station (EVK2CNR) in the Khumbu region, in Nepal [*Shrestha et al.*, 2012]. The Snow & Avalanche Study Establishment of India is running a few snow dedicated meteorological stations in Jammu & Kashmir and in Himachal Pradesh.

Ground penetrating radar can be used to determine the depth of the snow pack, in the same way as it is done for determining the thickness of glaciers. It is a non-invasive measurement (as opposed to traditional invasive measurements using stakes) and enables surveys of snow depth and snow water-equivalent to be conducted over larger areas. Such studies have been suggested and tested by *Singh et al.* [2011] in the Indian Himalayas. However, because GPR gives a signal for each layer where snow density changes abruptly, this method is dependent on knowledge of the stratigraphy of the snow.

Most snow-cover studies use remote sensing techniques in order to cover large areas, therefore calibration strategies, based on the comparison of field measurement data with remote sensing data are needed. Spectrometry measurements of snow on-field were made by *Negi et al.* [2010] to gain some understanding of the influence of snow grain size, contamination, moisture, aging, snow depth, slope and aspect on spectral reflectance, as well as to determine the wavelengths most appropriate for the mapping of snow. *In-situ* measurements of microwave penetration into snow were done and the data obtained could be useful for calibration of satellite-based microwave measurements of snow depth [*Singh et al.*, 2015].

### 3.2.2 Remote Sensing

#### 3.2.2.1 Glaciers

Remote sensing techniques are probably the most convenient methods for monitoring glacier changes in order to build up databases covering large and inaccessible areas and therefore most of the information about the state and evolution of glaciers in the HKH has been inferred from remote sensing. It is possible to derive geodetic mass balances of glaciers by remote sensed surface height variations of glaciers using Digital Elevation Model (DEM) differentiation [*Racoviteanu et al.*, 2008]. Remote sensing can also be used to infer glacier surface velocities and to determine their spatial cover. Unfortunately satellite data has been available only since the early seventies [*Racoviteanu et al.*, 2008].

Essentially there are two classes of sensors that are used to monitor elevation changes: active and inactive. Active sensors use the reflection of an emitted signal (by the sensor), whereas inactive sensors use natural signals emanating from the surface (reflection from the sun or emission). Within the active sensor class, LiDAR airborne measurements provide high-resolution elevation maps with accuracies up to 20 cm in the vertical axis and 30 cm in the horizontal axes [*Carter et al.*, 2012] thereby providing very accurate estimates of variations in height. Such measurements are very valuable for assessing glacier changes, but unfortunately they have not yet been used for this purpose in the HKH. This is probably due to the high cost involved because of the extensive flights required to cover such large areas. LiDAR measurements are more frequently obtained from satellite-borne altimeters. Data from satellites like the ICESat's GLAS sensor have been used [*Carter et al.*, 2012; *Bamber & Rivera*, 2007; *Kääb et al.*, 2012]. The vertical accuracy of space borne LiDAR remains about a few tens of centimeters but the spatial resolution is of the order of tenth of meters. Satellite synthetic aperture radar (SAR) data has been used outside the HKH region to estimate ice movement

velocities in Arctic glaciers [Strozzi *et al.*, 2008; Sund *et al.*, 2014], as well as glacier surface velocities in the Himalayas [Kumar *et al.*, 2011].

Photogrammetry is a passive elevation measurement in which several photographs of the same area, taken from different angles, are combined to obtain a DEM. Airborne photogrammetry provides high-resolution elevation maps but has rarely been used in the HKH. Space-borne photogrammetry has seen much wider use than airborne photogrammetry. Satellites like Corona, ASTER or SPOT5, [Hubbard *et al.*, 2000; Berthier *et al.*, 2007; Bolch, 2007; Gardelle *et al.*, 2012] cover large areas, but unfortunately horizontal resolution is coarse (~30 to 90 m). The vertical error of space-borne photogrammetry ranges from 10–20 m [Fujita *et al.*, 2008; Nuimura, 2012].

Data from the GRACE twin satellites, measuring gravity field changes (the so-called gravimetry technique), can be used for inferring glacier mass changes. Unfortunately, this method involves the use of numerous approximations. For example, gravity field changes account for variations not only of glacier mass, but also of snow mass; of gravity changes due to isostatic response; and of the continental crust and tectonic movements. The gravity field further includes the effects of underground water, as a result of which any melt water stored in the ground would not affect (change) the observed gravimetry data. This results in an underestimation of the mass balance of glaciers [Jacob *et al.*, 2012; Matsuo & Heki, 2010]. Nevertheless, results from gravimetry by Jacob *et al.* [2012] showed good agreement with results obtained from differentiating satellite-derived DEMs by Gardelle *et al.* [2013].

The presence of debris cover on glaciers presents the single greatest problem in mapping glaciers, using remote sensing. Delimitation of a debris covered ice surface cannot be achieved from spectral data alone [Racoviteanu *et al.*, 2008]. Manual inspection of satellite images is too time consuming and subject to error. Therefore, spectral ratios must be combined with DEM information. Thermal emission data could also be useful (debris on glaciers is usually colder due to the influence of the underlying ice), but its use is limited to thin debris-covering only. Manual input is still required to develop a standardized semi-automated mapping algorithm for debris-covered glaciers.

Recently, unmanned aerial vehicles (UAV) have been used above the debris-covered tongue of the Lirung glacier in the Langtang valley in Nepal [Immerzeel *et al.*, 2014] to picture the glacier front and reconstruct its surface velocities and volume change by stereo-photogrammetry. This technique permits a quick sampling and can be used over debris-covered glaciers which are difficult to access on foot. However, there is a limited range of a few kilometers for the flight paths of the UAV. This limits the use of this technique to small glaciers or only to parts of large glaciers. Furthermore, this technique cannot be used to map high-altitude accumulation areas.

Apart from these methods, some original approaches have been proposed in the literature. Brun *et al.*, [2015] proposed to monitor glacier albedo from MODIS imagery. Mass balance can be inferred by assimilating information of the snow-line altitude of the glacier into equilibrium line altitude information with the methodology developed by Rabatel *et al.* [2005].

Some recent studies outlined the possibility of characterizing the debris thickness on debris covered glaciers using remote sensing and could provide new insight on this difficult issue [Fujita & Sakai, 2014; Suzuki *et al.*, 2007]. However, although promising, this method relies on making demanding assumptions which still require further validation by on-field measurements.

### 3.2.2.2 Snow

The extent of snow cover can be monitored from differentiating spectral bands from satellite-based measurements. By combining the obtained snow cover maps with a digital elevation model, one can gain understanding of the links between elevation and snow line, or the persistence of snow, or links between snow cover and slope orientation. To gain understanding of the links with climate, meteorological data has to be incorporated. These methods rely on assumptions about emission or reflectivity from the snow surface, as well as radiative properties of clouds that can distort estimations of snow cover. Only few studies validate the remote-sensing with on-field measurements.

Numerous studies, done over different periods and utilizing remote sensing, have monitored the snow cover on a sub-basin scale in the HKH. These studies used different satellite products and methods. Some of these studies are summarized in Table 8.

Although local studies have been done, very few reports of large scale studies covering the entire Himalayan range are available. Long term studies are rare. A few recent studies have tentatively mapped snow cover all over the HKH for time periods of about ten years. These studies used MODIS products. ICIMOD did such a study between 2002 and 2010 [Gurung *et al.*, 2011], and a further study was also done between 2000 and 2008 [Immerzeel *et al.*, 2009].

Although monitoring the snow-cover area does not provide snow height or snow water-equivalent, it is crucial for hydrological modeling. A few studies have tried to establish methods to characterize this variable using data obtained from remote sensing. Data obtained from satellite based sensors using microwave technology can be used to infer snow depth. Shaman & Tziperman (2005) used the Nimbus-7 Scanning Multichannel Microwave Radiometer (SMMR) satellite estimates of snow depth between 1978 and 1987 over the Tibetan plateau. They compared these data with ENSO indices and NCEP/NCAR re-analysis.

Snow cover can also be characterized using information about snow precipitation. Products like TRMM, combining remote sensing techniques and field observation data, do infer that information about precipitation can be used [Bookhagen and Burbank, 2010], as do re-analysis products combined with field observations. However, it has been shown that these products provide significantly different results [e.g. Ménéguez *et al.*, 2013], and it is difficult to assess which is the more reliable. The use of a reanalysis product which is bias-corrected using local ground station data can be beneficial.

### 3.2.3 Modelling

#### 3.2.3.1 Glacier dynamics

A large number of numerical methods for modeling past or future glacier evolution are referenced in the literature. These methods range from very simple statistical relationships linking a few climatic parameters to glacial changes, to nearly-fully-physical based models that include complex processes such as ice rheology, fracturing, and complete assessment of the energy transfers at the boundaries of the ice mass. Statistical and empirical approaches have been used to predict future glacier wastage, linking the mass balance to simple parameters such as the temperature [e.g. Shi & Liu, 2000; Cogley, 2011].

However, in order to fully cover all the relevant processes governing glacier change in the Himalayas, modeling approaches should include 5 aspects: models of the accumulation (based

on knowledge of climate, or climate modeling); models of melting; models of glacial flow; models of glacier water storage (refreezing, groundwater, lakes); and models taking into account the effects of glacial lakes on melting. Models of growing complexity progressively incorporate all of these aspects.

Melting processes can be assessed using simple approaches utilizing information of measured mass balance gradients [Racoviteanu *et al.*, 2013]. More complex assessments could also use degree-day or improved degree-day approaches [Immerzeel *et al.*, 2012, 2013; Pellicciotti *et al.*, 2012; Shea *et al.*, 2015]. Improvements in the degree-day approaches to incorporate relevant melting processes will lead to full energy-balance models. Very few studies have been assessing full energy-balance models on Himalayan glaciers [e.g. Shrestha *et al.*, 2015], and application is limited to small areas due to high spatial resolution and calculation capacity requirements.

Glacial flow must be incorporated into the models before it will become possible to accurately predict or reconstruct glacial evolutions. Ice flow modeling can be done either with simplified parameterizations [Immerzeel *et al.*, 2012, 2013; Shea *et al.*, 2015], or with complex models; from one dimensional Stokes models [Zhang *et al.*, 2013] to fully resolved 3-dimensional Stokes models. None of these have thus far been applied at basin scale for Himalayan glaciers. In large scale studies, where spatial resolution does not allow for the simulation of glacial flow, parameterizations of future glacier change are used [Huss *et al.*, 2010; Lutz *et al.*, 2013].

#### 3.2.3.2 Snow and snow water equivalent

Because of the importance of snow melt in the hydrology of some basins in the HKH, modeling the future evolution of snow cover or its historical changes, is an important issue for assessing impacts of climate change on the hydrological regime in the region. For snow cover modeling to be accurate it would have to include two critical aspects: the modeling of snow precipitation and accumulation; and the modeling of snow depletion.

Modeling future snow accumulation must be done through precipitation estimates from climate models. However, it has been shown that large uncertainties pertain to predicted precipitation. Improvements might be obtained by downscaling global scale climate models with Regional Climate Models (RCM) which are able to provide precipitated snow water equivalent (e.g. MAR, WARF) [Collier and Immerzeel, 2015]. In this process, models shall be validated against precipitation measurements, from *in situ* or remote sensing methods, or from a combination of both (e.g. TRMM). Model results could also be compared to re-analyzes products like ECMWF or Aphrodite [e.g. Ménégoz *et al.*, 2013]. However, as stated previously, snowfall magnitude is hugely under-estimated – whether using remote sensing, or using surface rain gauges. Estimations of the future evolution of snow cover in the HKH were made in a few hydrological studies [Immerzeel *et al.*, 2012]. These provide estimates of snow precipitation by downscaling outputs from GCMs. Estimates of future melt are generally obtained with simplified degree-days approaches.

Snow pack evolution can be modeled by starting from the snow cover, or from snow water-equivalent accumulation (inferred from precipitation models, or from measurements). Snow undergoes numerous processes such as melt; sublimation; condensation; compaction; metamorphism or wind displacement. Whereas commonly used degree-days approaches infer the snow melt from observed statistical relationships between melt and temperature, snow models shall, in order to accurately predict snow pack evolution in changing climatic conditions,

include all the relevant processes among these. In order to identify which processes would be relevant, *in situ* measurements of the snow pack evolution must be compared with outputs from models including potentially relevant processes. Unfortunately, only few studies in the HKH have so far done that [e.g. *Shrestha et al.*, 2012; *Nepal et al.*, 2014].

### 3.3 Results

#### 3.4 Glacier observations

The evolution of glaciers in the Indus, Ganges and Brahmaputra basins is not homogeneous. The general tendency is that glaciers are retreating and losing mass in the three basins, as shown by *in situ* mass balance measurements (Table 4) and results from different remote sensing studies [*Bolch et al.*, 2012; *Jacob et al.*, 2012; *Kääb et al.*, 2012; *Yao et al.*, 2012; *Gardner et al.*, 2013]. *In situ* measurements show that glaciers in the Brahmaputra basin are strongly retreating in the eastern Himalaya (Parlang Zangbo mountains,  $\sim -1.1$  m w.e.  $\text{yr}^{-1}$  *in situ*) [*Yao et al.*, 2012] and weakly retreating on the Tibetan Plateau ( $\sim -0.4$  to  $-0.55$  m w.e.  $\text{yr}^{-1}$ ). The mass balances are moderately negative in the Ganges basin in Nepal ( $\sim -0.76$  m w.e.  $\text{yr}^{-1}$  *in situ*) [*Yao et al.*, 2012] and strongly negative in the Himachal Pradesh ( $\sim -0.91$  m w.e.  $\text{yr}^{-1}$  *in situ*) [*Yao et al.*, 2012], where part of the glaciers are in the Indus and part in the Ganges basin. In the Karakoram, located in the Upper Indus basin, glacier mass balances are less negative or even positive, as shown by remote sensing studies ( $+0.11 \pm 0.22$  m w.e.  $\text{yr}^{-1}$ ) [*Gardelle et al.*, 2012]. These anomalous observations are also known as the ‘Karakoram anomaly’. A review of debris-covered glacier changes in the HKH region shows a similar pattern, with mostly neutral mass balances in the Karakoram and negative mass balances in the other regions [*Scherler et al.*, 2011b] (Figure 15). According to this analysis glaciers in the northern part of the Central Himalaya are losing mass at the highest rate.

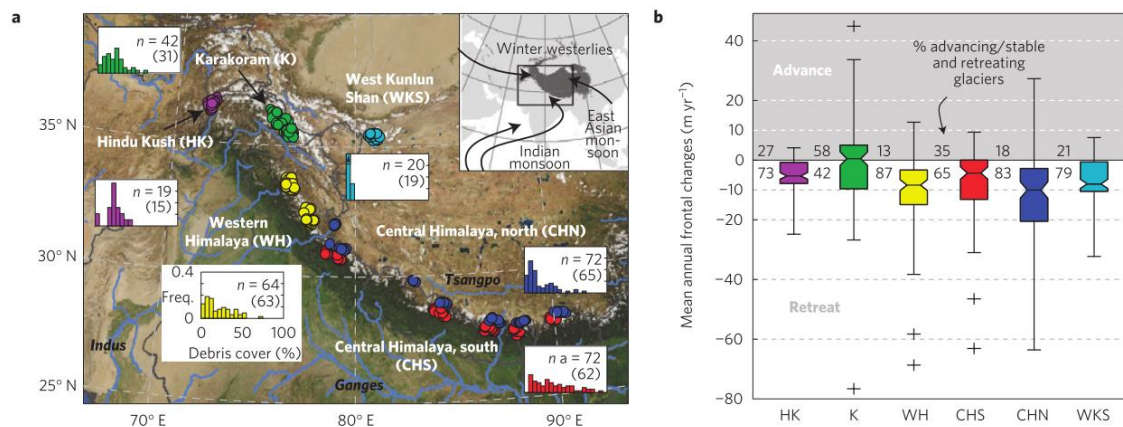


**Figure 15: Regional distribution of debris-covered and stagnating glaciers. a) Location of glaciers (circles) grouped by region. Histograms give relative frequencies (y-axis, 0–40%) of debris cover (x-axis, 0–100% in 5% bins). Number of studied glaciers is given in upper-right corner, measured frontal changes in parentheses. Globe depicts location of subset and atmospheric transport directions. b) Regional distribution of mean annual frontal changes. Boxes give lower and upper quartiles and median (notches indicate 95%-confidence intervals). Whiskers extend 2.5 times the interquartile data range, crosses lie outside this range. Numbers left of boxes indicate percentage of advancing/stable (top) and retreating (bottom) glaciers. Source: [*Scherler et al.*, 2011b]**

### 3.4.1 Indus

Most glaciers in the Indus region have been retreating from the 1980s to today (Table 4 and Table 5). Nonetheless, as previously mentioned, glaciers in the Karakoram range in the upper Indus basin have been at equilibrium or gaining mass over the last decades [*Gardelle et al.*, 2012, 2013; *Jacob et al.*, 2012] and Table 5. In terms of frontal changes, *Bolch et al.* [2012] stated that about 25% of glaciers in the Karakoram were advancing or stable between 1976 and 2007. This anomaly could be the result of increased winter accumulation in the region [*Tahir et al.*, 2011] and because these high altitude catchments remain less affected by climate change because temperatures are remaining below freezing point. Note that part of the glaciers in the Karakoram are surging or have been surging recently, which probably results from this increased accumulation and a slight increase in the ablation rate in the lower part of the glaciers.

**Table 6. List of glaciers for which in-situ mass balance measurements were conducted in the Indus, Ganges and Brahmaputra river basins (source: WGMS).**

| Indus (11 glaciers)                     | Stakes Survey years             | Geodetic survey years | References                                  | Mean mass loss rate m w.e. yr <sup>-1</sup> |
|---|---------------------------------|-----------------------|---|---|
| Siachen (Pakistan)                      | Hydrological method (1986-1991) |                       | Bhutiyani, (1999)                           | -0.51                                       |
| Shisram (India- Jammu and Kashmir)      | 1983-1984                       |                       | Dyurgerov & Meier, (2005)                   | -0.29                                       |
| Rulung (India- Jammu and Kashmir)       | 1980-1981                       |                       | Geological Survey of India                  | -0.11                                       |
| Kolahoi (India- Jammu and Kashmir)      | 1983-1984                       |                       | Dyurgerov & Meier, (2005)                   | -0.27                                       |
| Neh Nar (India - Jammu and Kashmir)     | 1975-1984                       |                       | Dyurgerov & Meier, (2005)                   | -0.54                                       |
| Hamtah (India – Himachal Pradesh)       | 2000-2009                       |                       | Geological Survey of India                  | -1.60                                       |
| ChhotaShigri (India – Himachal Pradesh) | 2002-2010                       | 1988<br>2002-2010     | Wagnon et al. (2007)Azam et al.(2012, 2014) | -0.67                                       |
| ShauneGarang (India – Himachal Pradesh) | 1981-1991                       |                       | Geological Survey of India                  | -0.36                                       |
| Gara (India – Himachal Pradesh)         | 1974-1983                       |                       | Raina(2009)                                 | -0.37                                       |
| Naradu (India – Himachal Pradesh)       | 2000-2003                       |                       | Koul & Ganjoo(2010)                         | -0.40                                       |
| GorGarang (India – Himachal Pradesh)    | 1976-1985                       |                       | Dyurgerov & Meier, (2005)                   | -0.43                                       |
| <b>Ganges (9 Glaciers)</b>              |                                 |                       |   |   |
| Tipra Bank (India - Uttarakhand)        | 1981-1988                       |                       | Dyurgerov & Meier, (2005)                   | -0.25                                       |
| Dokriani (India - Uttarakhand)          | 1992-1006<br>1997-2000          | 1962→1995             | Dobhal & Mehta, (2010)                      | -0.32                                       |
| Dunagiri (India - Uttarakhand)          | 1984-1990                       |                       | Geological Survey of India                  | -1.04                                       |
| Chorabari (India - Uttarakhand)         | 2003-2009                       |                       | Dobhal et al. (2013)                        | -0.74                                       |

|  |                        |   |                              |                                  |
|--|------------------------|---|------------------------------|----------------------------------|
| Rikha Samba<br>(Nepal - Daulaghiri)                    | 1998-1998              | 1994 →1974<br>1999 → 2000   | Fujita et al.(2001)          | -0.46                            |
| Yala<br>(Nepal – Langtang)                             | 1982-1984-1996         | 1982 → 1994<br>1982 → 1996<br>1996 → 2009                               | Fujita & Nuimura(2011)       | -0.58                            |
| AX010<br>(Nepal - Khumbu)                              | 1995-1999              | 1978 → 1991<br>1978 → 1999<br>1991 → 1996<br>1996 → 1999<br>1999 → 2008 | Fujita et al. (2001)         | -0.61                            |
| Mera<br>(Nepal - Khumbu)                               | 2007 - 2012            |   | Wagnon et al.(2013)          | -0.10                            |
| Pokalde<br>(Nepal – Khumbu)-                           | 2009-2012              |   | Wagnon et al.(2013)          | -0.72                            |
| Brahmaputra (11 glaciers)                              |                        |   |                              |                                  |
| Kangwure<br>(China - Tibet)                            | 1991-1993<br>2009-2010 | 1974 → 2008   | Yao et al.(2012)             | -0.66                            |
| Changmekhangpu<br>(India - Sikkim)                     | 1979-1986              |   | Dyurgerov & Meier,<br>(2005) | -0.26                            |
| 24K<br>(China-South east Tibet)                        | 2007-2008              |   | Yang et al.(2008)            | -1.22                            |
| Demula<br>(China-South east Tibet)                     | 2006-2010              |   | Yang et al.(2008)            | -1.02                            |
| ParlangZangbo<br>(China-South east Tibet)              | 2005-2010              | 4 Glaciers included   | Yao et al.(2012)             | -0.78<br>-1.70<br>-0.92<br>-1.02 |
| Zhadang<br>(China – Tibet Nyaingentanglha<br>range)    | 2005-2010              |   | Zhang et al.(2013)           | -0.57                            |
| Zhongxi<br>(China – Tibet Nyaingentanglha<br>range)    | 2007-2010              |   | Yao et al.(2012)             | -0.52                            |
| Gurenhekou<br>(China – Tibet Nyaingentanglha<br>range) | 2005-2010              |   | Yao et al., 2012             | -0.31                            |

### 3.4.2 Ganges

In situ measurements of annual glacier mass balance in the Ganges basin show an overall negative tendency (Table 4). See for example the Tipra Bank, Dokriani, Dunagiri, Chorabari, AX010, Rikha Samba, Mera and Pokalde glaciers. This is confirmed by the many remote-sensing studies conducted in the region (Table 5). In the Khumbu region, for instance, *Gardelle et al.*, [2013] measured an annual rate of mass loss of  $-0.26 \pm 0.13$  m w.e.  $\text{yr}^{-1}$  between 2000 and 2011. A slightly higher negative mass balance was measured by *Nuimura et al.* [2012] of  $-0.40 \pm 0.25$  m w.e.  $\text{yr}^{-1}$  over a longer time span (from 1992 to 2008). Glaciers thinning of  $-0.40$  m  $\text{yr}^{-1}$  were evidenced by remote sensing in the same region between 2003 and 2009 [*Gardner et al.*, 2013]. In the same region, a similar thinning rate of  $-0.33$  m  $\text{yr}^{-1}$  was measured by remote sensing by *Bolch et al.* [2008] for the years 1962 to 2002. Glaciers in the Ganges basin are expected to be more sensitive to climatic changes since they experience accumulation mostly at the same time as ablation, during the summer monsoon. It means the control of temperature on the snow line altitude is crucial, since the altitude of the snow cover

determines the percentage area of glaciers exposed to strong ablation induced by intense solar insulation. This could explain the retreat observed in these regions [Bolch *et al.*, 2012].

### 3.4.3 Brahmaputra

Similarly as for the other basins, in situ measurements in the Brahmaputra basin showed global glacier retreat (Table 4). Remote sensing estimates for the entire Tibetan Plateau are reported in many studies. The Brahmaputra basin encompasses glaciers pertaining to various climatic regions. Parlang Mountains' glaciers pertain to this basin, and in situ mass balance measurements in this region showed the biggest negative trend in recent years ( $-1.1 \text{ m w.e. yr}^{-1}$ ) [Yao *et al.*, 2012]. In the central Himalaya, even though the glacier are located on the leeward side of the chain, in situ mass balance measurements suggest a similar evolution than in the windward side of the Ganges basins (see Kangwure glacier and Yala glacier mass balance data in Table 4).

**Table 7: Observed mass balance by remote sensing methods from various studies in the HKH region during recent years.**

| Region   | Study                         | Time range                        | method              | Lowering (m yr <sup>-1</sup> )                   | Clean-ice    | Debris-covered | Mass balance                              |
|--|-------------------------------|-----------------------------------|---------------------|--|--------------|----------------|---|
| Hindu Kush and Karakoram (Indus)                                     | Kääb <i>et al.</i> (2012)     | 2003-2009<br>3 methods, 3 results | DEM differentiation | Oct-Nov<br>-0.26 ±0.06<br>Feb-Mar<br>-0.10 ±0.06 | -0.78 ±0.16  | -0.76 ±0.16    | -0.23 ±0.05<br>-0.19 ±0.04<br>-0.21 ±0.05 |
|  | Gardner <i>et al.</i> (2013)  | 2003-2008                         | DEM differentiation |  |              |                | -0.10 ±0.18                               |
| Karakoram  | Gardelle <i>et al.</i> (2012) | 1999-2008                         | DEM differentiation |  |              |                | +0.11±0.22                                |
| Himachal Pradesh, Uttarakhand and West Nepal (HP) (Indus and Ganges) | Kääb <i>et al.</i> (2012)     | 2003-2009<br>3 methods, 3 results | DEM differentiation | -0.38 ±0.06<br>-0.38 ±0.06                       | -1.20 ± 0.33 | -1.02 ± 0.29   | -0.34 ±0.05<br>-0.30 ±0.04<br>-0.32 ±0.06 |
|  | Gardner <i>et al.</i> (2013)  | 2003-2008                         | DEM differentiation |  |              |                | -0.48 ±0.17                               |
| East Nepal and Bhutan (NB) (Ganges and Bramaputra)                   | Kääb <i>et al.</i> (2012)     | 2003-2009<br>3 methods, 3 results | DEM differentiation | -0.38 ±0.06<br>-0.38 ±0.06                       | -2.30 ±0.53  | -1.53 ±0.43    | -0.34 ±0.08<br>-0.26 ±0.07<br>-0.30 ±0.09 |
|  | Gardner <i>et al.</i> (2013)  | 2003-2008                         | DEM differentiation |  |              |                | -0.40±0.23                                |
| East Himalaya  | Gardner <i>et al.</i> (2013)  | 2003-2008                         | DEM differentiation |  |              |                | -0.80 ±0.22                               |
| All Hindu Kush and Himalaya  | Jacob <i>et al.</i> (2012)    | 2003-2010                         | Gravimetric         |  |              |                | -5 ±6 Gt yr <sup>-1</sup>                 |

### 3.5 Glacier simulations

Numerical modeling efforts of glacier evolution have mainly focused on evaluating the mass balance and evolution of glaciers at regional scale. Such studies thus have to limit their degree of complexity in order to model on large scales. Table 8 provides results from various simulations of future trends in glacier mass balance for the HKH region. All studies project a clear decline of glacier ice throughout the 21st century. Nevertheless, complete disappearance of Himalayan glaciers is not expected within this time frame, but a large retreat towards new equilibrium states with high-altitude frontal lines. In most scenarios presented here, the rate of ice loss decreases towards the end of the simulation periods, which indicates a shift towards equilibrium mass balance conditions [Shea *et al.*, 2015]. Table 8 shows that the predictions are uncertain since there are large differences between results from different studies. This uncertainty mainly stems from different assumed scenarios of greenhouse gas emissions, different model parameterization approaches, and poor knowledge of initial glacial volumes (generally parameterized) due to the sparse network of in situ measurements. In the Himalayas, the evolution of the glaciers is also about to be influenced by the changes in the monsoon precipitation patterns. The climatic scenarios can't actually provide a clear estimate of the change in precipitation amounts. Especially in the Karakoram there are large uncertainties of future glacier change because current glacial behavior remains poorly understood [Marzeion *et al.*, 2012; Radić *et al.*, 2014; Zhao *et al.*, 2014].

**Table 8: Results from various regional modeling studies of future glacier changes in the HKH region.**

| Study                      | region           | Time range | remarks                              | method  | Mass balance results          | Volume change   |
|----------------------------|------------------|------------|--------------------------------------|---|-------------------------------|---|
| Radić <i>et al.</i> (2014) | South-west Asia  | 2003-2100  | Initial volume 4,475 km <sup>3</sup> | Degree-day and surface volume scaling                       | -0.68 m w.e. yr <sup>-1</sup> | +4 to -75 %<br>RCP4.5<br>-34 to -87 %<br>RCP8.5 (2006-2100)     |
|                            | South-east Asia  |            |                                      |   |                               | Initial Volume 1,852 km <sup>3</sup>                            |
| Zhao <i>et al.</i> (2014)  | HK and Karakoram | 2000-2050  | RegCM3 climatic projection scenario  | ELA temperature-precipitation dependence and volume scaling |                               | -0.47 to -0.26 % yr <sup>-1</sup><br>-23.5 to -13% (50 years)   |
|                            | Western Himalaya |            |                                      |   |                               | -0.79 to -0.47 % yr <sup>-1</sup><br>-39.5 to -23.5% (50 years) |
|                            | Central Himalaya |            |                                      |   |                               | -1.18 to -0.53% yr <sup>-1</sup><br>-59 to -26.5% (50 years)    |
|                            | Eastern himalaya |            |                                      |   |                               | -0.96 to -0.69 % yr <sup>-1</sup><br>-48 to -34.5 % (50 years)  |

|                        |                   |           |   |  |  |  |
|------------------------|-------------------|-----------|---|--|--|--|
|                        | Hengduan Shan     |           |   |  |  | -1.41 to -0.68 % yr <sup>-1</sup><br>-70% to -34 % (50 years)                      |
| Marzeion et al. (2012) | South-east asia   | 2100      |   |  |  | -60 to -70 %<br>RCP4.5 RCP8.5  |
| Lutz et al. (2014)     | upper Indus       | 2008-2050 | CMIP5 multi-model ensembles for RCP4.5 and RCP8.5 | Basin-scale parameterization for glacier cover evolution, based on degree-day modeling and volume-area scaling [Lutz et al., 2013] |  | Surface area remaining in 2050 compared to 2007:<br>80-76% RCP4.5<br>72-77% RCP8.5 |
|                        | upper Ganges      |           |   |  |  | Surface area remaining in 2050 compared to 2007:<br>55-64% RCP4.5<br>52-63% RCP8.5 |
|                        | upper Brahmaputra |           |   |  |  | Surface area remaining in 2050 compared to 2007:<br>58-69% RCP4.5<br>55-64% RCP8.5 |

We report on two detailed studies with projections of glacier evolution at sub-basin scale. *Immerzeel et al.* [2013] compared the evolution of Baltoro glaciers (Upper Indus basin, India) until 2100, and Langtang (Ganges basin, Nepal) glaciers under RCP4.5 and 8.5 emission scenarios from the CMIP 5 ensemble. Simulations show a strong retreat, declining, and disintegration of glacier tributaries in both cases. In the worst case RCP8.5 scenario, the much smaller Langtang glaciers show an area retreat of 54% in 2100 compared with 33% in the larger Baltoro glaciers. Volume changes are similar to the areal changes. Similar to the regional simulations listed above, the studies show a significant difference in projected glacier extent depending on the scenario (i.e. RCP4.5 or RCP8.5) and climate model used. In the Langtang Valley, for instance, the glacier area shrinks by 37% or 54% depending on the respective scenarios over a time period of 2071–2100.

*Shea et al.* [2015] simulated the evolution of Khumbu glaciers (Ganges basin, Nepal) using the CMIP5 ensemble scenarios RCP4.5 and RCP8.5 until 2100. In their simulation the projected mean total glacial volume loss, until 2100, is estimated at -83.7 % for RCP4.5 scenarios, and -94.7 % for RCP8.5, with a range between -70 and -99 %. Changes below 6,500 m are shown to be highly dependent on the chosen scenario, but no changes are expected in the glacier volumes above 7,000 m. In the best case scenarios, the glacierized area near the current ELA (5,500 m) will decline by as much as 80 %, and thinning will occur below 5,750 m. Debris-covered termini may see area reductions of 40 % by 2100. In RCP8.5, the most extreme scenario, glaciers below 6,500 m are essentially eliminated by 2100.

*Lutz et al.* [2014] projected basin-averaged glacier cover changes until 2050 by using a parameterization of future glacier changes. Decreases of -20 to -28% are projected for the Indus, whereas decreases of -36 to -48% and -31 to -45% are projected for the Ganges and Brahmaputra respectively.

### 3.6 Snow cover

Since snow-cover monitoring on a large regional scale has started only recently, with the availability of satellite data, long term trends cannot be established (Table 9). The studies reported herein cover at maximum ten years [Immerzeel *et al.*, 2009; Gurung *et al.*, 2011], starting from ~2000 and spanning to 2010. These studies are based on MODIS satellite products. They do not show clear general temporal changes in the SCA over the whole HKH region. A remote sensing study by Tahir *et al.* [2011] showed a slight increase in snow cover in the Hunza basin (upper Indus) between 2000 and 2009, which may be the result of an increase in winter precipitation caused by westerly circulation.

There is a possible negative feedback between the winter snow cover on the Tibetan Plateau and the monsoon intensity. Increased snowfall produces a larger Tibetan Plateau snowpack, which persists through the spring and summer, and weakens the intensity of the south Asian summer monsoons. However Immerzeel *et al.* [2009] showed this had recently changed into a positive relationship in the western Himalayas.

**Table 9: Overview of some of the available sub-basin scale studies on snow cover in the HKH and methods used.**

| Study                         | Region                                   | Mapping satellite               | DEM method       | Dates     | Slope/aspect | Climatic study   |
|-------------------------------|--|---------------------------------|------------------|-----------|--------------|--|
| Kaur <i>et al.</i> , (2009)   | Baspa (Upper Indus)                      | Resourcesat-I                   | SRTM             | 2004-2007 | No           | no   |
| Jain <i>et al.</i> (2009)     | Satluj, Chenab, Ravi, Beas (upper Indus) | MODIS                           | USGS             | 2003-2004 | Yes          | yes  |
| Kripalaniet <i>al.</i> (2003) | Western Himalaya                         | INSAT                           | ?                | 1986-2000 | No           | Yes (NCEP/NCAR) monsoon rainfall from the Institute of Tropical Meteorology. |
| Krishna (2005)                | Tista (Sikkim, Ganges basin)             | Indian Remote Sensing Satellite | ?                | 1992-1997 | ?            | No   |
| Negi <i>et al.</i> (2009)     | Kashmir                                  | AWiFS Resourcesat-I             | Topographic maps | 2004-2007 | ?            | no   |
| Pu & Xu (2009)                | Tibetan Plateau                          | MODIS                           | USGS             | 2000-2006 | no           | Pacific-East Asian Monsoon Index   |

Few studies focus on future snow cover trends. Snow cover evolution is linked to precipitation, and climate model predictions of future trends in precipitation are very uncertain. Furthermore, the presence of the negative feedback between monsoon and snow cover on the Tibetan plateau complicates the prediction of future trends in snow cover. Clearly, deeper insight into the precipitation patterns and processes in the Himalayas are needed. However, a study by [Viste and Sorteberg, 2015] using gridded products for historical precipitation and CMIP5 GCMs estimated changes in rainfall and snowfall for the Indus, Ganges and Brahmaputra basins. The GCM runs for RCP8.5 projected reductions in annual snowfall of 30-50% (Indus), 50-60% (Ganges) and 50-70% (Brahmaputra) by the end of the 21<sup>st</sup> century. The snowline increased in elevation by 400-900 meters, depending on the region.

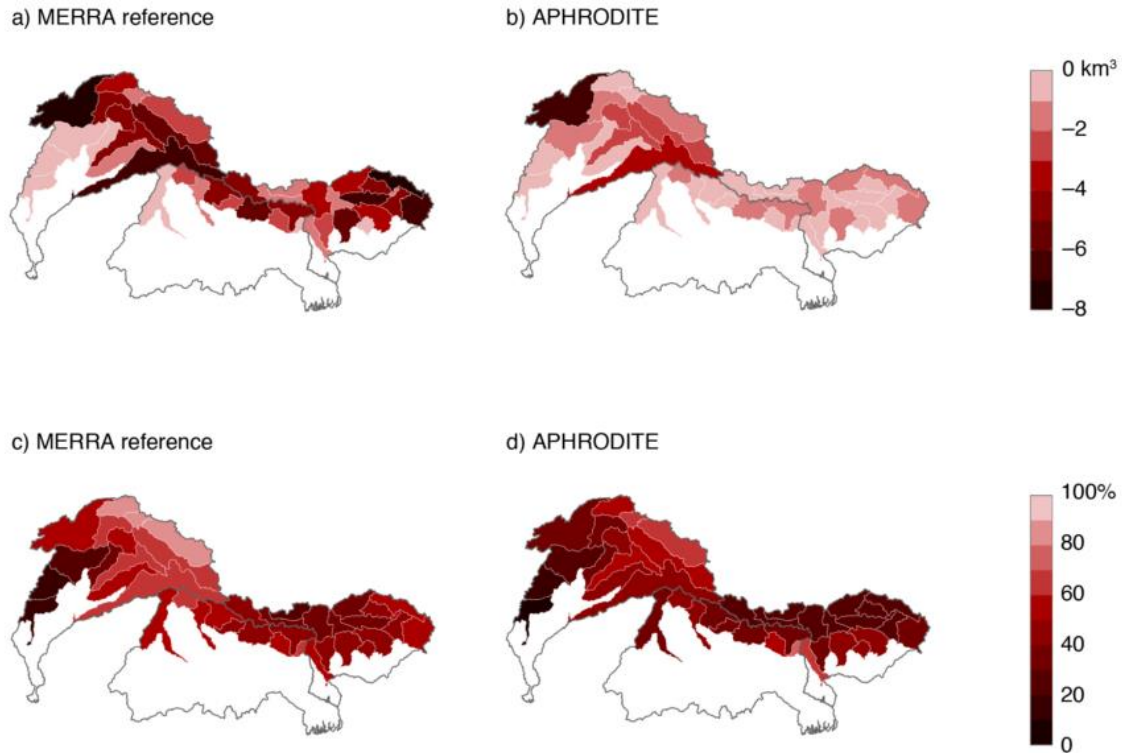


**Figure 16: Projected future changes in snowfall in sub-basins of the Indus, Ganges and Brahmaputra basins. (a) Absolute change ( $\text{km}^3$ ) with reference to MERRA reference snowfall. (b) Absolute change ( $\text{km}^3$ ) with reference to APHRODITE snowfall. (c, d) Corresponding relative changes (%) with reference to MERRA and APHRODITE. Multi-model means for 2071-2100 with respect to 1979–2008 are shown. Source: [Viste and Sorteberg, 2015]**

### 3.7 Key limitations

This section lists the key limitations in the understanding of cryosphere dynamics in the HKH region.

#### Glacier changes

##### In situ observations

- There are several studies doing observations all along the Himalaya but they are mostly short term. Long term observations and spatial coverage is insufficient.
- Studies are mostly not representative of relevant climatic conditions/type of glaciers.
- There is no consensus on measuring methods between different studies.
- There is a lack of in situ measurement of glacier volume to validate the widespread use of area-volume parameterizations.
- There is a shortage of energy balance measurements in the region.

##### Remote sensing observations

- IceSAT: uncertainty about penetration of radiation into the snow. This method also relies on an assumption of density to determine glacier losses.
- Airborne sensing is poorly used but efficient (LiDar, photogrammetry).

##### Glacier models

- There is a lack of relevant input information such as for example glacier thickness, climatic data.

- Precipitation gradients and snow/rain transitions are important phenomena in glacier dynamics and need more emphasis in studies.
- There are many difficulties with assessing debris-covered glacier processes.
- While many studies assessed glacier change in the past, few studies have focused on modelling glacier changes in the future. This is a global issue but more specifically in the HKH region.
- Spatial distributions in debris thickness and thermal conductivity are nearly impossible to measure.
- There are many simplifications that need to be applied due to a lack of data or knowledge. For example, degree-day modeling/volume-area scaling, simple parameterizations, poor knowledge of processes (energy balance to debris covering of glaciers, complex ice melting processes in debris covered glaciers)

#### **Changes in snow cover**

- Models are generally unable to simulate snow processes. The understanding of and prediction of precipitation processes is generally a shortcoming.
- There is poor coverage of in situ measurements in the HKH.
- Important snow phenomena such as the snow-rain transition line and precipitation gradients are poorly understood and monitored.
- There is no information on snow water equivalent.
- There are very sparse snow precipitation records at high altitudes.
- The role of ground sublimation and blowing snow sublimation in the HKH region is unknown.

### **3.8 Summary remarks**

Scientific literature regarding the state of the cryosphere in the HKH has increased rapidly and so did the state of knowledge on this subject, although it is still relatively weak. The current state of knowledge can be summarized as follows:

- Glaciers in most of the HKH region are losing mass in response to climate warming. Glaciers in the Karakoram region have been expanding in recent years, but the underlying reasons for this “Karakoram anomaly” is not yet fully understood.
- Total ice volume measurements vary considerably because of the difficulties in measuring ice volumes in situ or from remote sensing products and uncertainties in volume-area scaling relationships.
- No strong trends in snow cover changes have been observed. Minor increases or decreases have been reported for different areas.
- Little is known about the distribution of permafrost in the HKH region. Its importance for the regional hydrology thus remains unclear.
- Estimates of future glacier volume and area are uncertain and are hampered because thus far modelling of ice flow was restricted to catchment scale studies. However, strong decreases in glacier volume and area are projected for the entire HKH region.

## 4 Hydrological Regime

### 4.1 Approaches to quantifying the hydrological regime

#### 4.1.1 *Types of models*

The hydrological properties of single catchments or entire river basins are typically assessed with hydrological models. Hydrological models are simplified representations of components of the hydrological cycle. Many hydrological models are in use and depending on the model's purpose they are based on a variety of concepts and level of detail. The simplest hydrological models are black box or empirical models. These models are largely empirical (based on observed relationships) rather than deterministic (based on simulated physical processes). Their emphasis is mostly on correctly simulating the precipitation-discharge relationship. Parametric models are more physically based and simplify hydrological systems as a collection of storages and functions that transfer water between storages. They usually simulate the most important hydrological processes while keeping the number of model parameters limited. Physically-based models are more complex and have detailed, spatially distributed descriptions of physical parameters, and need a large number of input variables. They can include energy-balance modeling besides water balance modeling. Because the cryosphere processes are important in the Indus, Ganges and Brahmaputra basins, the quality of results generated with the models largely depends on the representation of the relevant processes in those basins.

#### 4.1.2 *Driving input data for hydrological models*

Climate is the major driving force of the hydrological cycle and climate data thus forms the most important input to simulation models. The type of climatic data that is used largely depends on the scale of the application. Catchment scale assessments often use station meteorological data [Bocchiola *et al.*, 2011; Ragetti and Pellicciotti, 2012; Ragetti *et al.*, 2013; Soncini *et al.*, 2015], whereas assessments on larger scales often use gridded regional or global climate datasets [Lutz *et al.*, 2014]. Due to the large horizontal and vertical variability in climatic variables in mountainous regions, challenges arise in extrapolating data from individual stations or downscaling to required spatial resolutions from coarser scale gridded datasets. The simplest models use air temperature and precipitation data from a single station, assuming the data measured there to be representative for the entire catchment. Distributed models use spatially interpolated data, corrected for elevation differences. Models that include simulation of the energy balance require data on more fluxes, including long-wave radiation, short-wave radiation, latent heat flux and albedo.

Most approaches use a digital elevation model (DEM) for elevation and hillslope data. Depending on the approach, digitized glacier outlines are often used, possibly with distinction of debris-covered and debris-free glaciers. Models that include evapotranspiration require data on soil properties and vegetation type or land use. Data on vegetation type, soils and land use is often not available and modelers rely on global datasets in that case. Modeling of future scenarios requires downscaled GCM or RCM projections to force the model.

#### 4.1.3 *Process representation*

A number of hydrological modeling exercises have been conducted in the Indus, Ganges and Brahmaputra basin, with varying ways of representing the hydrological processes. Cryosphere

processes play important roles in the regional hydrology, but can be simulated in different ways. A simple approach to estimate glacier melt is an ice ablation gradient model, such as applied in the Langtang catchment in the Ganges basin [Racoviteanu *et al.*, 2013b]. In ablation gradient models a gradient of increasing glacier melt with lowering altitude starting at zero melt at the equilibrium line altitude (ELA) is assumed, based on field measurements. Different ablation gradients can be adopted for clean ice glaciers and debris covered glaciers. Glacier- and snow melt is often simulated using a degree-day approach [Hock, 2003], based on the relation between air temperature and the amount of melt. A certain amount of melt water per positive degree is assumed. The advantage of this method is that it can be applied in most cases, because air temperature data is mostly available and relatively easy to interpolate to spatial fields. Enhanced degree-day models are also used to integrate more variables such as incoming radiation, aspect or albedo in the model [Pellicciotti *et al.*, 2005; Heynen *et al.*, 2013]. Glacier- and snow melt can be simulated more accurately using models that include the energy balance. Since the amount of snow transported downslope through avalanching can be substantial, it is also simulated in some models [Bernhardt and Schulz, 2010; Immerzeel *et al.*, 2013; Ragetti *et al.*, 2015]. A mostly disregarded component in the models applied in the HKH region is sublimation. This flux is difficult to measure and therefore no, or sparse observations are available. At the same time sublimation may constitute a significant component of the mountain water balance, especially in windy conditions [Wagnon *et al.*, 2013]. Similarly, the contribution of groundwater is difficult to observe and difficult to simulate. Yet, also this may be an important component of the water balance [Andermann *et al.*, 2012; Bookhagen, 2012].

## 4.2 Main results

### 4.2.1 Observed historical hydrological trends

A number of studies report analyses of observed discharge records and attempt to attribute the observed trends to observed meteorological trends. A study analyzing streamflow trends from nineteen stations in the upper Indus basin indicated that for highly glacierized catchments the discharge can be best correlated to temperature [Archer, 2003]. According to the analysis summer flow in middle latitude catchments are predominantly influenced by preceding winter precipitation whereas runoff in catchments further downstream is controlled mainly by rainfall in winter as well as during the monsoon. Khattak *et al.* (2011) found that increasing trends in streamflow could be related to increases in mean and maximum temperature, in particular in the winter and spring seasons. Sharif *et al.* (2013) concluded that highly glaciated catchments in the upper Indus basin show decreasing trends in streamflow, whereas for less glaciated catchments the streamflows have increased. They showed that flow occurring in early summer is decreasing but increasing in winter.

Others show that flows in the central Karakoram have been increasing during the melting season from 1985 to 2010 [Mukhopadhyay and Khan, 2014b]. The authors conclude that an increase in runoff is possible under neutral glacier mass balance conditions as a result of increasing temperature and precipitation, e.g. the mass turnover of the glacier is increasing, yet the mass balance remains neutral.

### 4.2.2 Streamflow composition

In a global study Schaner *et al.* (2012) showed that the contribution of glacier melt to rivers in the HKH region is substantial. One study estimated the contributions of glacier melt, snow melt, rainfall-runoff and baseflow to total runoff for the entire upstream basins of the Indus, Ganges

and Brahmaputra using a distributed cryosphere-hydrological model [Lutz *et al.*, 2014]. Their estimate indicates that total runoff in the Indus is most dependent on glacier- and snow melt, whereas the contribution of rainfall is much more prominent in the upper Ganges and upper Brahmaputra basins (Table 10).

**Table 10: Contribution to total runoff by different components averaged over the upstream basins [Lutz *et al.*, 2014].**

| Basin             | Contribution to total runoff (%) |           |                 |           |
|-------------------|----------------------------------|-----------|-----------------|-----------|
|                   | Glacier melt                     | Snow melt | Rainfall-runoff | Base flow |
| Upper Indus       | 40.6                             | 21.8      | 26.8            | 10.8      |
| Upper Ganges      | 11.5                             | 8.6       | 66.0            | 13.9      |
| Upper Brahmaputra | 15.9                             | 9.0       | 58.9            | 16.2      |

A limited number of published studies estimated the composition of streamflow in the Indus, Ganges, and Brahmaputra basins for different catchments or sub-basins (Table 11). Results are difficult to compare due to the difference in concepts and approaches used, and differences in application scales. *Mukhopadhyay and Khan* (2014, 2015) estimated the contributions by hydrograph separation methods at locations with available streamflow records. *Racoviteanu et al.* (2013b) estimated streamflow composition with a simple ice ablation model which was independently validated with stable water isotopes sampling. Their analysis showed that groundwater is an important component already close to the glacier outlets. The estimates by *Singh and Jain* (2002) were made by a basin-scale water balance analysis with the inputs from glacier melt and snow melt estimated from remotely sensed snow cover imagery. The estimates by *Immerzeel et al.* (2011, 2013) were made using a distributed model including a simple ice flow model, whereas the estimates by *Soncini et al.* (2015) were made using a semi-distributed cryospheric-hydrological model fed and validated with in situ measurements. *Ragetti et al.* (2015) used a high-resolution process-oriented, distributed model. *Prasch et al.* (2013) used a distributed process-oriented glacio-hydrological model in the Lhasa basin. The choice for model spatial resolution and amount of physical detail depends mostly on the scale of the applications, e.g. the size of the catchment or basin included in the simulation.

#### 4.2.3 Long-term projections

A projection up to the end of the century for the Baltoro and Langtang catchments with contrasting climates [Immerzeel *et al.*, 2013], indicated a consistent increase in total runoff for both catchments at least until 2100 for both RCP45 and RCP85 (Figure 17). These increases range from 172 mm yr<sup>-1</sup> (Langtang, 31%) to 278 mm yr<sup>-1</sup> (Baltoro, 46%) in 2021–2050 for RCP45 to 493 mm yr<sup>-1</sup> (Langtang, 88%) to 576 mm yr<sup>-1</sup> (Baltoro, 96%) in 2071–2100 for RCP85. In the Baltoro, glacier melt is a larger component of total runoff and the increased melt is the main cause of the strong increase in total runoff. In Langtang, the main cause of the increased total runoff is the increase in precipitation. Despite the contrasts in climate and hydrological regime, both catchments respond similarly to future climate change, especially for the first half of the 21<sup>st</sup> century.

**Table 11: Results of studies estimating streamflow composition at selected locations.**

| Site (river, location)     | Reference                   | Period    | Contribution per component (%) |           |             |           |
|----------------------------|-----------------------------|-----------|--------------------------------|-----------|-------------|-----------|
|                            |                             |           | Glacier melt                   | Snow melt | Rain runoff | Base flow |
| Satluj, Bhakra Dam         | Singh and Jain, 2002        | 1986-1996 | 59                             |           | 41          | -         |
|                            | Lutz et al., 2014           | 1998-2007 | 27.6                           | 20.8      | 38.6        | 13.0      |
| LangtangKholra, K yangjing | Immerzeel et al., 2011      | 2001-2010 | 47.0                           | 6.9       | 28.8        | 17.4      |
|                            | Immerzeel et al., 2013      | 1961-1990 | 13.0                           | 20.4      | 10.0        | 56.6      |
|                            | Racoviteanu et al., 2013    | 1988-2006 | 58.3                           | 41.7      |             |           |
|                            | Ragetli et al., 2015        | 2012-2013 | 26                             | 40        | 34          | -         |
|                            | Lutz et al., 2014           | 1998-2007 | 52.5                           | 12.8      | 25.0        | 9.7       |
| DudhKoshi, Rabuwa Bazar    | Racoviteanu et al., 2013    | 1988-2006 | 7.4                            | 92.6      |             |           |
|                            | Lutz et al., 2014           | 1998-2007 | 18.8                           | 4.8       | 64.8        | 11.6      |
| Lhasa basin                | Prasch et al., 2013         | 1971-2000 | 3                              | 41        | 56          | -         |
| Indus, BeshamQila          | Mukhopadhyay and Khan, 2014 | 1969-2010 | 70                             | 30        |             |           |
|                            | Lutz et al., 2014           | 1998-2007 | 67.3                           | 17.6      | 7.1         | 8.0       |
|                            | Mukhopadhyay and Khan, 2015 | 1969-2010 | 25.8                           | 44.1      | -           | 30.2      |
| Hunza, Dainyor bridge      | Mukhopadhyay and Khan, 2014 | 1966-2010 | 74                             | 26        |             |           |
|                            | Lutz et al., 2014           | 1998-2007 | 80.6                           | 9.6       | 1.3         | 8.5       |
|                            | Mukhopadhyay and Khan, 2015 | 1966-2010 | 42.8                           | 31.3      | -           | 25.9      |
| Baltoro watershed          | Immerzeel et al., 2013      | 1961-1990 | 38.7                           | 21.6      | 3.5         | 36.2      |
| Shigar, Shigar             | Soncini et al., 2015        | 1985-1997 | 32.9                           | 39.5      | 27.6        |           |

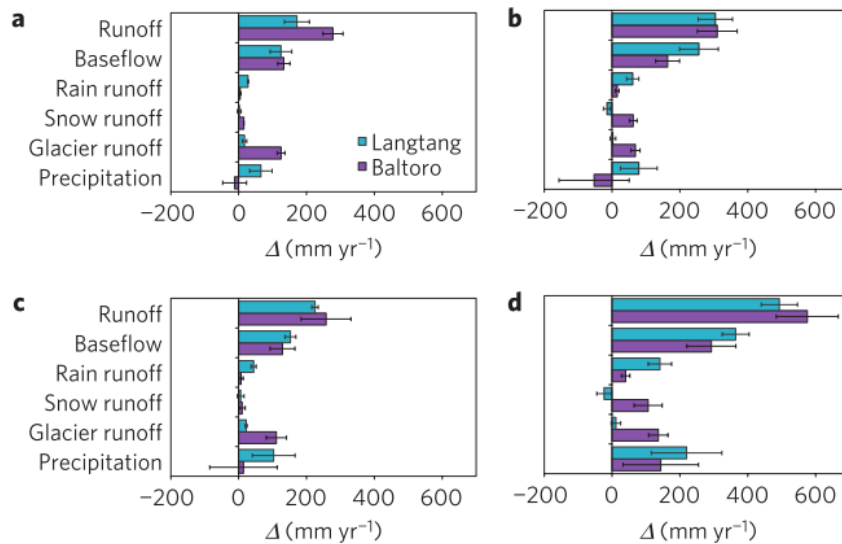


**Figure 17: Projected future changes in water balance components for the Baltoro and Langtang catchments. All changes are relative to 1961–1990. Runoff is the sum of base flow, rain runoff, direct snow runoff and direct glacier runoff. All values are expressed as a catchment average in  $\text{mm yr}^{-1}$ . Changes are shown for RCP4.5 for the period 2021–2050 (a) and 2071–2100 (b) and for RCP8.5 for 2021–2050 (c) and 2071–2100 (d). The error bars show the standard deviation of four selected GCM runs [Immerzeel et al., 2013].**

*Soncini et al.* (2015) found similar results for the Shigar watershed (which includes the Baltoro watershed) (Figure 18). The authors project mostly increases in flow until the end of the century and speculate on potential slight decrease thereafter when ice volumes continue to decrease. In this catchment changes in precipitation amount will hardly compensate for ice loss in the long run. It is striking that for the three different RCPs, the differences in streamflow changes are rather small.

*Lutz et al.* (2014) showed that a consistent increase in runoff is expected also at large scale for the upstream Indus, Ganges and Brahmaputra at least until 2050. For the upper Indus this is mainly due to increased glacier melt, whereas for the Ganges and Brahmaputra the projected increase in precipitation is the main driver. Especially for the upper Indus, the projections have a large uncertainty because the projections for precipitation show contradicting patterns.

Projections until 2050 for the Hunza basin *Ragetti et al.* [2013] showed that simulated decadal mean runoff is relatively constant but that strong contrasting changes occur in some of the sub-basins of the Hunza river, with some decreasing by up to 50% in flow volume due to decrease in ice melt, while others might increase due to increasing snow melt related to increasing precipitation and increasing temperatures.

In the Lhasa basin, *Prasch et al.* [2013] made hydrological projections until 2080 forcing a glacio-hydrological model with the IPCC SRES scenarios. They find that the contribution of ice melt to total runoff will almost remain stable until 2080, although there will be a slight increase during a short period in spring. Contrary, the contribution of snowmelt to river runoff will generally decrease in the Lhasa basin and result in changes in water availability. Additionally, the increase of evapotranspiration with increasing air temperatures will also reduce water availability.

#### 4.2.4 Intra-annual changes in flow

Most important intra-annual changes in flow are related to earlier onset of melting and changes in precipitation patterns. *Soncini et al.* [2015] showed that in the Shigar catchment the increasing temperature and increase in winter precipitation caused an increase in streamflow to begin earlier in the year due to onset of glacier melt and snow melt (Figure 18). This is most dramatic for RCP8.5, where for two out of three GCMs the flow starts to increase significantly in April instead of June. Other RCPs also show this shift, and the shift gets stronger towards the end of the century. One of the GCMs (CCSM4) shows a very different pattern, with decreasing flows in spring and a slight increase in flow for all other months.

In their basin-scale study *Lutz et al.* (2014) showed projected changes in the average annual hydrographs for main rivers with sources in the HKH during 2041-2050 that reveal how different the responses to climate change are between rivers with different streamflow patterns (Figure 19). For example, the flow in the Indus River is dominated by temperature-driven glacier melt during summer, and the uncertainty in future flow is therefore relatively small as a result of small uncertainty in future temperature changes. The Kabul River, on the other hand, has a much larger rainfall-runoff and snow component, leading to a larger uncertainty in future flow as a result of large uncertainties in future precipitation. For the rivers in the Ganges basin (Koshi and Ghaghara in Figure 19) and the Brahmaputra, the absolute amounts of glacier melt and snowmelt do not change much, but their relative contributions decrease owing to the increased

rainfall runoff. As a consequence, increased peak discharge is observed in the monsoon season, with large uncertainty in the magnitude of flow increase.

In the part of Hunza basin where flow will decrease, the months June to September are most affected by a decreases [Ragetti *et al.*, 2013]. The annual peak runoff will occur earlier in the year (in June/July) as compared to July/August during the control period.

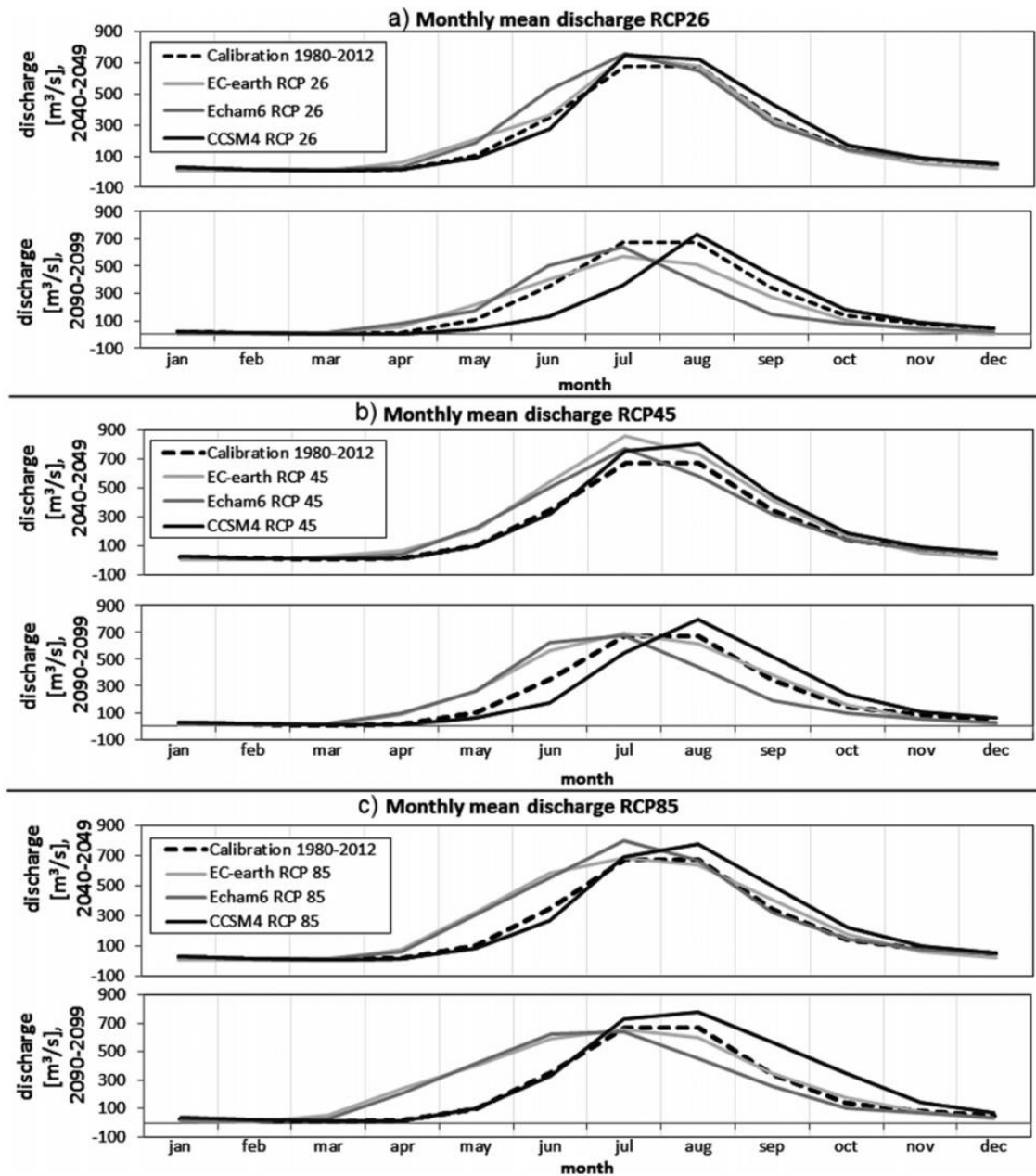
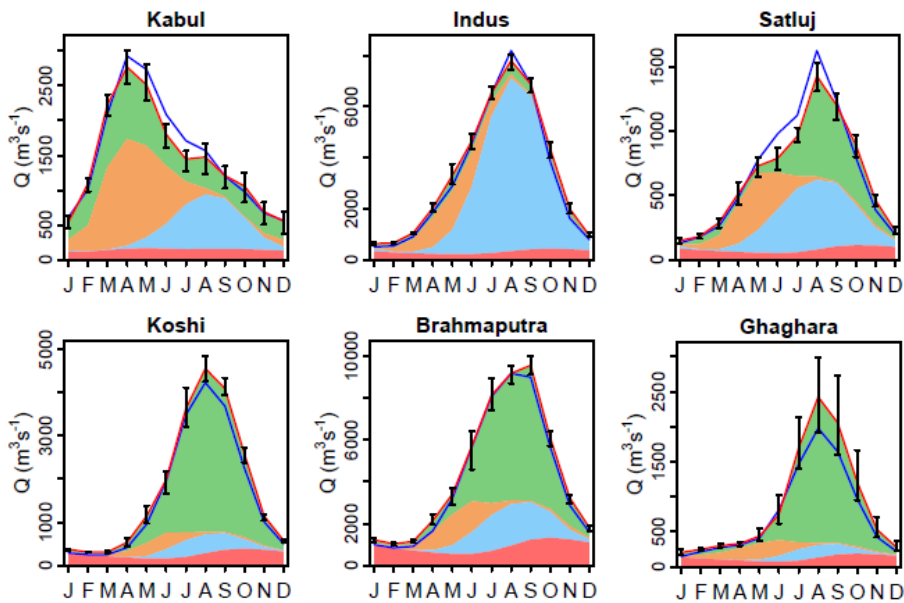


Figure 18: Projected discharges for three GCMs in the RCP2.6 (a), RCP4.5 (b) and RCP8.5 (c) scenarios [Soncini *et al.*, 2015].

As implications for hydropower production this means that more water is available for production during the low flow seasons. Besides, because the amount of water discharged during the high flow season (July, August), less water is lost due to spilling.



**Figure 19: Average annual hydrographs for the period 2041-2050, RCP8.5 at major river's outlets. Plots show the mean projected discharge when forced with a 4 GCM ensemble (red line) and the discharge for a reference period (1998-2007, blue line). For the future period four streamflow components are shown: baseflow (red), glacier melt (blue), snow melt (orange), rainfall-runoff (green). The error bars indicate the variability in projections for the future period when forced with the ensemble of 4 GCMs [Lutz *et al.*, 2014].**

#### 4.2.5 Extreme events

Changes in hydrological extreme events in the Indus, Ganges and Brahmaputra basins are poorly studied. Seeing that an increase in precipitation is generally projected, one may assume that precipitation extremes and associated extreme discharges may increase as well. *Soncini et al.* (2015) used downscaled GCM data to force a semi-distributed model to make a basic analysis of changes in extreme discharges in the Shigar catchment. Most models indicate increased discharge for the flow return periods they analyzed, indicating potential heavier floods during the flood season from June to October.

### 4.3 Summary remarks

The available hydrological knowledge in the HKH is based on historical streamflow measurements and hydrological modeling. Hydrological models are best suited to predict future changes in the hydrology, resulting from climate change. A variety of hydrological models are available that can use the range of available data on physical processes to model future changes at catchment scale to river basin scale. With climate warming a shift towards more precipitation falling as rain instead of snow is likely for the entire HKH region (except for the highest areas remaining below freezing point the entire year). For glacier- and snow melt dominated rivers it is likely that more water becomes available in winter and especially spring, due to earlier onset of melting. However, when rainfall is an important contributor this also largely depends on the changes in precipitation in winter, which are uncertain. The main published findings with regard to HKH hydrology are noted below.

- Main uncertainties in hydrological modeling of historical periods in the HKH region stem from uncertainties in model input data, and historical precipitation forcing in particular.
- The large differences in future precipitation projected by different climate models makes future predictions of hydrological changes very uncertain. The representation of the future extent in glacier cover is also a large source of uncertainty.
- Detailed modeling in the region is limited to catchment scale.
- Increasing trends in streamflow in the most upstream glaciated regions seem to be related to increasing temperatures, and at lower altitudes streamflow trends seem to be more controlled by precipitation trends.
- The Indus River receives the largest proportion of its water from glacier- and snow melt, whereas the Ganges receives most of its water from rainfall-runoff.
- It seems likely that a consistent increase in streamflow will occur in the HKH river basins during the first half of the 21<sup>st</sup> century. Streamflow increases in the Indus River are mainly a result of increasing glacier melt whereas increases in the other rivers are mainly a result of increasing precipitation.
- In the second half of the 21<sup>st</sup> century the contribution of glacier melt is likely to decrease, but the timing of the onset of the decrease is spatially highly variable. Changes in total water availability are uncertain due to uncertain precipitation projections.
- Increases in flows outside the monsoon and melting seasons are likely.
- Increases in extreme events (floods) are likely.

## 5 Glacial Lakes and GLOF

All lakes formed by present or past glacier activity are described as glacier (glacial) lakes. A glacial lake can form on the surface of the glacier itself (supra-glacial), within the glacier ice (englacial), below the glacier ice (subglacial), in front of a glacier (proglacial), inside/surrounding of glaciers (periglacial) or in relict cirques (cirque). The impact of climate change on the Himalayan glaciers is becoming apparent. As a result of glacial thinning and/or glacial retreat, glacial lakes are formed either between the frontal moraine and the retreating glacier, or on the surface of the lower section of glaciers. Studies show glacier-fed lakes have expanded significantly and that non glacier-fed lakes have remained stable [Wang *et al.*, 2015]. These (glacier-fed) lakes are dammed by moraines of varying instability and as a result some lakes could breach their dams. This phenomenon is known as a glacial lake outburst flood (GLOF) and has the potential of causing extensive destruction in the valley downstream. There is concern that the frequency of GLOFs could increase as a result of the formation and expansion of glacial-fed lakes. Under certain circumstances, a GLOF can instantaneously release a huge volume of water and debris, and when this happens it is highly probable that there will be extensive damage in the downstream areas that could include destruction of infrastructure and/or loss of human lives.

Thirty five GLOFs (5 in Bhutan including the Lemthang Tsho GLOF of June 2015; 16 in China; and 14 in Nepal) have been reported in the HKH region [Ives *et al.*, 2010]. In the Tibetan branch of the Kuri Chu, the Chamkhar Chu, the Pho Chu and Mo Chu rivers, 21 GLOF events were reported (17 before 1970 and 4 from the 1970s until 2010) [Komori *et al.*, 2012]. These GLOFs caused significant damages to people, crops, infrastructures and hydropower plants, as a result of which GLOF risk assessment has become an issue of considerable significance. Five GLOF events were reported during the first half of 2008 in the Gojal area of the Hunza valley, Pakistan. Substantial damage to infrastructure and arable land was also reported due to GLOF events associated with the Ghulkin and Passu glaciers [Ives *et al.*, 2010].

### 5.1 Glacier lakes in HKH basins

Although glacial lakes are significant natural resources they are potentially also sources of natural disasters. As a result of the remoteness and vast geographical area of the HKH region, as well as large number of lakes involved, only a very small percentage of those lakes has been studied in the field. With the exception of some isolated studies done prior to 2000, no glacial lake census exists for the Hindu Kush Himalayan region [Bajracharya *et al.*, 2007; Ives *et al.*, 2010].

The first glacial lake inventory of Nepal was prepared by the *Water and Energy Commission Secretariat (WECS)*, in 1987. This study included the mitigation of glacier hazards and the possibility of establishing early warning systems in susceptible areas (WECS 1987, Mool 1995). The joint expedition between WECS, the *Nepal Electricity Authority (NEA)* and the then *Lanzhou Institute of Glaciology and Geocryology (LIGG)* (and now *Cold and Arid Region Environmental and Engineering Research Institute (CAREERI)*), studied the GLOF phenomenon in the Pumqu (Arun river) and Poiqu (Bhote Koshi - Sun Koshi rivers) basins in 1987 [LIGG *et al.*, 1988].

A comprehensive inventory of glacier, glacial lakes and potentially dangerous glacial lakes of Nepal and Bhutan was published by ICIMOD [Mool *et al.*, 2001a, 2001b]. From 2003 to 2005 the study was subsequently extended (a) in India to the Teesta basin of Sikkim Himalaya, the

Ganges basin of Uttarakhand [Sah et al., 2005], and the Himachal Pradesh basin [Bhagat et al., 2004]; (b) in China to the Ganges basin and (c) in Pakistan to the Indus basin [Roohi et al., 2005] [Mool and Bajracharya, 2003; Mool, 2005] (Table 12).

Out of a total of 8,790 glacier lakes identified in Bhutan, India, Pakistan, Nepal and the Ganges basin in China, 203 are listed as potentially dangerous glacial lakes [Mool et al., 2001a, 2001b; Mool and Bajracharya, 2003; Bhagat et al., 2004; Roohi et al., 2005; Sah et al., 2005; Wu et al., 2005]. Those glacier lakes listed as potentially dangerous were derived from topographic maps published from 1963 to 1982 and based on aerial photographs of 1957 to 1958 verified with control checks done in the field. Following a detailed field study of lakes in Bhutan, Thorthormi Lake was subsequently added to the list [Karma et al., 2003]. Zhang et al. (2015) mapped 5,701 glacial lakes (areas > 0.0027km<sup>2</sup>) in the Pamir-Hindu Kush-Karakoram Himalayas and the Tibetan Plateau regions.

**Table 12: summary of glacial lakes and potentially dangerous glacial lakes in selected parts of the HKH region.**

| Countries | Glacial lakes |                         |                           | Remark                                   |
|-----------|---------------|-------------------------|---------------------------|--|
|           | Number        | Area (km <sup>2</sup> ) | Pot. dangerous (critical) |  |
| Bhutan    | 2,674         | 106.77                  | 25                        | Country                                  |
| China     | 824           | 85.19                   | 77                        | Ganges sub basin                         |
| India     | 549           | 407.91                  | 30                        | Himachal Pradesh, Uttarakhand and Sikkim |
| Nepal     | 2,323         | 75.64                   | 20                        | Country                                  |
| Pakistan  | 2,420         | 126.32                  | 52                        | Country                                  |
| Total     | 8,790         | 801.83                  | 204                       |  |

Some scattered and local studies have been completed throughout the HKH region. In Nepal, using satellite images of 2000-2001, ICIMOD updated the inventory of glacial lakes together with an assessment of glacial lake outburst flood (GLOF) risk. The updated number of glacial lakes in Nepal is 1,466 and covers an area of 64.75 km<sup>2</sup>. 21 potentially dangerous lakes were identified of which 6 were defined as high priority lakes requiring extensive field investigation and mapping [Mool et al., 2011].

Ukita et al. (2011) mapped 336 glacial lakes in four sub-basins of Bhutan: Mo Chu, Pho Chu, Mangde Chu and Dangme Chu, using high resolution satellite images of PRISM and AVNIR-2 and compared the results with ICIMOD data. The results show that the abundance of small glacial lakes (<0.05 km<sup>2</sup>) account for 55% of the total number of lakes and occupy 13% of the total lake area in Bhutan. These results indicate the importance of implementing high-resolution satellite remote-sensing data, such as those by ALOS, to study glacial lakes.

Some information on glacial lakes in the Indian Himalayas became available during the mapping of glaciers. Although no systematic mapping of glacial lakes was done, the Geological Survey of India (GSI) assessed the glacier cover of the Indian Himalayas [Puri et al., 1999]. Glacial lakes of Sikkim were mapped by applying a semi-automated method to Resourcesat-1 LISS III satellite data. 320 glacial lakes are shown to exist of which 85 are new when compared to a mapping of the study area done in 2003 [Govindha Raj et al., 2013]. The formation of new, and the expansion of supraglacial lakes are observed on many debris-covered glaciers in Sikkim [Basnett et al., 2013]. Glacial lakes were also mapped in Uttarakhand using high resolution multi-spectral and panchromatic satellite imageries from LISS IV and Cartosat 1 and 2A [Bhambri et al., 2015] and it was found that there are 1,266 glacier lakes (size > 500 m<sup>2</sup>) that cover a total area of 7.6 ±0.4 km<sup>2</sup>. 809 of these lakes are classified as supra-glacial lakes,

having a total area of  $2.0 \pm 0.1 \text{ km}^2$  (26.3% of the total glacier lake area). Most of the glacier lake area (52%) is represented by moraine-dammed lakes (329 lakes with a total area of  $3.9 \pm 0.2 \text{ km}^2$ ). During the mapping of glaciers, 50 moraine dammed lakes and 5 supraglacial lakes were mapped in the Chenab basin from satellite images [Randhawa *et al.*, 2005].

The variation of glacial lakes over time for ~1990, 2000, and 2010 was assessed using Landsat TM/ETM+ data and 5,701 glacial lakes larger than  $0.003 \text{ km}^2$ , covering areas of  $682.4 \pm 110 \text{ km}^2$ , were mapped in 2010 [Zhang *et al.*, 2015]. Thirty nine percent of these lakes are located in the Brahmaputra, 28% in the Indus, and 10% in the Amu Darya basins. The authors concluded that small lakes ( $\leq 0.2 \text{ km}^2$ ) are more sensitive to climate changes; lakes closer to glaciers and at higher altitudes, particularly those connected to glacier termini, have undergone larger area changes, and glacier-fed lakes are dominant in both number and area and exhibit faster expansion trends overall in comparison with non-glacier-fed lakes. However the number of mapped glacial lakes is smaller by comparison to those of other studies. For example, only 364 glacial lakes were mapped in the Ganges basin, whereas in the Nepal Himalaya and the Uttarakhand part of the Ganges basin alone there are 1,466 glacial lakes and ICIMOD mapped 1,266 glacial lakes.

**Table 13: Number and area of glacial lakes in the Third Pole (Source: [Zhang *et al.*, 2015])**

| Basin Name    | Number of lakes |             | Area of lakes (sq. km) |                  |
|---------------|-----------------|-------------|------------------------|------------------|
|               | Total           | Glacier Fed | Total                  | Glacier Fed      |
| Amu Darya     | 594             | 451         | $65.8 \pm 10.9$        | $50.3 \pm 8.3$   |
| Tarim         | 123             | 108         | $16.9 \pm 2.5$         | $13.9 \pm 2.1$   |
| Indus         | 1,607           | 868         | $141.6 \pm 26.4$       | $88.8 \pm 15.5$  |
| Inner Plateau | 352             | 266         | $38.3 \pm 6.1$         | $27.6 \pm 4.4$   |
| Qaidam        | 31              | 31          | $3.1 \pm 0.6$          | $3.1 \pm 0.6$    |
| Hexi Corridor | 11              | 11          | $2 \pm 0.3$            | $2 \pm 0.3$      |
| Yellow        | 15              | 13          | $3 \pm 0.4$            | $2.9 \pm 0.4$    |
| Yangtze       | 192             | 177         | $22.4 \pm 3.7$         | $20.7 \pm 3.4$   |
| Mekong        | 34              | 31          | $3.8 \pm 0.7$          | $2.3 \pm 0.5$    |
| Salween       | 131             | 114         | $22 \pm 3.1$           | $17.8 \pm 2.6$   |
| Brahmaputra   | 2,247           | 1,883       | $317.3 \pm 48.7$       | $285.6 \pm 42.8$ |
| Ganges        | 364             | 298         | $45.8 \pm 7.3$         | $41.4 \pm 6.3$   |
| Total         | <b>5,701</b>    | <b>4251</b> | <b>682</b>             | <b>556.4</b>     |

Formation and expansion of glacier lakes in the HKH region are increasing due to accelerated glacier melt in this region during the last century [Bajracharya *et al.*, 2007]. Moraine-dammed meltwater lakes near the termini of major glacier tongues are common and are potentially unstable [Ives *et al.*, 2010]. The end moraines may be underlain by masses of dead ice (remnants of earlier glacial extension) and permafrost may also be present. Buried dead ice and permafrost strengthen the end moraines and, to a great extent, reduce the risk of glacial lake outbursts. However, it should be noted that the current atmospheric warming also affects buried ice and permafrost. Furthermore, as these lakes increase in size and the depth and presence of open water in contact with the glacier terminus also increases, glacial retreat and thinning is accelerated and this may increase the instability [Bajracharya *et al.*, 2015].

## 5.2 Trends in glacial lakes

The glaciers of HKH region are shrinking and retreating as a result of climate change. The decrease in glacier area impacts the glacial lakes – they generally increase in size [Bajracharya

*et al.*, 2007], and melt water from glaciers plays a dominant role in this expansion. As a result the number of potentially hazardous moraine dammed lakes in the Himalaya has increased [Gardelle *et al.*, 2011; Govindha Raj *et al.*, 2013; Nie *et al.*, 2013], and this is giving rise to an increase in the number of unexpected breaches of moraine dammed lakes. In addition, increasing temperatures cause the disappearance of smaller lakes that are not glacier-fed. Merging of supraglacial ponds increases the areas of the remaining lakes but with a decrease in the number of lakes.

### 5.2.1 Glacial lake trends in the Bhutan Himalaya

ICIMOD mapped 2674 glacial lakes larger than 0.001 km<sup>2</sup> of the Indian surveyed topographic maps of the late 1960s [Mool *et al.*, 2001a]. In a case study repeated mappings of glacial lakes were carried out at Pho Chu basin based on the satellite images of 2000 and 2001 and topographic maps from the 1960s [Bajracharya *et al.*, 2007]. In the 1960s, 549 lakes in Pho Chu basin covered an area of 23.49 km<sup>2</sup>. By 2000-2001 the data shows that the number of lakes has decreased by 32% whereas the area had increased by 8%. Over a period of 40 years, a total of 175 lakes had either dried up or become too small to be mapped. Some 82 new lakes were formed. Most of the glacial lakes formed at glacier fronts increased in size and will probably continue to increase to the stage of becoming potentially dangerous lakes, putting their downstream areas at risk of GLOF events. Most of the lakes that disappeared were erosional lakes, whereas some supraglacial ponds merged to form single large lakes. Smaller lakes (< 2500 m<sup>2</sup> in area) could not be mapped in this study due to the low resolution of the satellite image used, whereas they were mapped in the previous study based on larger scale topographic maps [Mool *et al.*, 2001a, 2001b].

The major lakes Raphstreng, Thorthormi, and Luggye in the Lunana region increased in size from 1968 to 2001 (Figure 20) [Bajracharya *et al.*, 2007] and share a common feature: a sudden increase in area at one point of their evolution. The Luggye and Thorthormi lakes show similar expansion patterns and exhibit further expansion possibilities (Figure 21). Drukchung lake breached in the early 1990s [Leber *et al.*, 2002] and subsequent to this GLOF the lake area has remained constant.

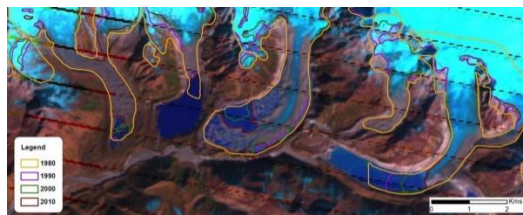


**Figure 20: Decadal lake development in the Lunana region from 1980 to 2010.**

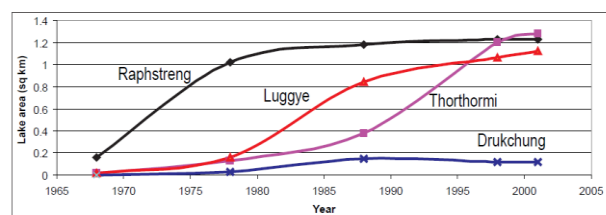


**Figure 21: Development trend of glacial lakes in the Lunana region**

A considerably high rate of increase in the area of glacial lakes were found in the Mo Chu (23 %), Pho Chu (21.5 %), Mangde Chu (16.5 %), and Chamkar Chu (22 %) basins [Veettill *et al.*, 2015].

### 5.2.2 Glacial lake trends in the Nepal Himalaya

Two detailed inventories composed by ICIMOD can be compared. Comparisons of the number as well as the areas of glacial lakes of the two inventories show decreases in glacial lake number, as well as area to the magnitude of -36.9% and -14.4% respectively. However, the

methodology and sources of base maps were not the same. The lakes mapped in 2001 were  $\geq 0.001 \text{ km}^2$ , whereas the lakes mapped from Landsat TM/ETM+ were  $> 0.003 \text{ km}^2$  due to the low resolution of the satellite image used [Bajracharya and Shrestha, 2011].

One of the studies in the Dudh Koshi sub-basin of Nepal shows that 37% of the number of lakes of the 1960s had disappeared by 2000-2001 [Bajracharya et al., 2007], the reason being the disappearance of erosional lakes and the merging of supraglacial ponds. However, although the number of lakes had decreased, the overall lake area increased by 21%. Most glacier associated lakes are expanding, and examples of rapidly growing lakes are described below.

### 5.2.2.1 Imja Tsho

Lake Imja Tsho is one of the fastest growing lakes in the Himalayas and has been identified as one of the potentially dangerous glacial lakes in the Nepal Himalaya. In the 1960s it consisted of a group of supraglacial ponds which developed into a moraine dammed lake by 1975. Subsequently, the lake has grown to a size of  $0.95 \text{ km}^2$  with a length of approximately 2 km and a growth rate of 74m/yr and an increase in area of  $0.02 \text{ km}^2/\text{yr}$  from 1962 to 2000 (Figure 22 and Figure 23) [Bajracharya et al., 2007].

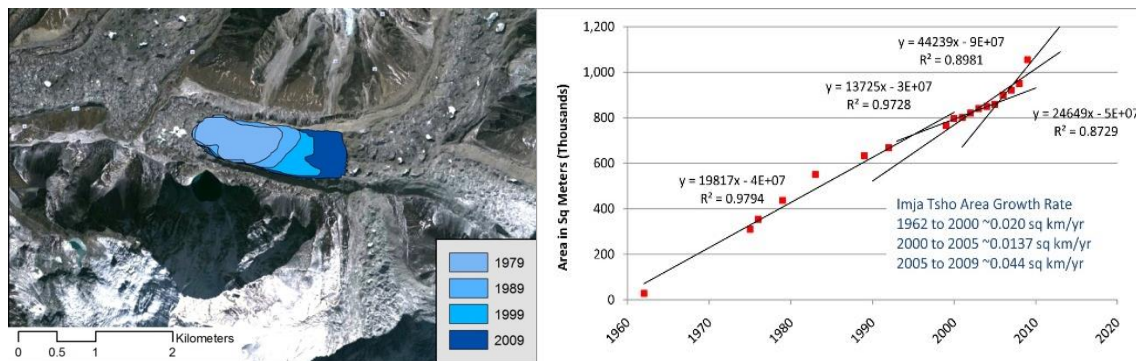


**Figure 22: Decadal lake development of Imja Tsho from 1979 to 2009. Figure 23: Development trend of Imja Tsho.**

### 5.2.2.2 Tsho Rolpa

Lake Tsho Rolpa is a moraine dammed lake first mapped in 1959 with an area  $0.23 \text{ km}^2$  and it was associated with many supraglacial lakes at the glacier front (Figure 24). The lake area expansion rate was  $0.03 \text{ km}^2/\text{yr}$  from 1959 to 2000 and the growth rate decreased to  $0.01 \text{ km}^2/\text{yr}$  after the mitigation work done in 2000 (Figure 25). The lake area progressively increased to  $0.61 \text{ km}^2$  by 1967,  $0.80 \text{ km}^2$  by 1976,  $1.37 \text{ km}^2$  by 1993 and  $1.55 \text{ km}^2$  by 1999. The maximum depth of the lake was 132 meters close to the glacier front and the stored water volume was estimated to be 76.6 million  $\text{m}^3$  [Kadota, 1994]. On average the lake is 52m deep, 3.2 km long and 0.5 km wide. The mitigation project succeeded to reduce the lake level by approximately 3 m, and the volume by approximately 4.5 million  $\text{m}^3$ . However, the water remaining still exceeds 72 million  $\text{m}^3$  and even a small glacial lake of  $0.02 \text{ km}^2$  can cause extensive damage in the downstream valleys as was the case with the Zhangzanbo GLOF.



**Figure 24: Aerial view of Tsho Rolpa (Photo: Sharad Joshi, 2000)**

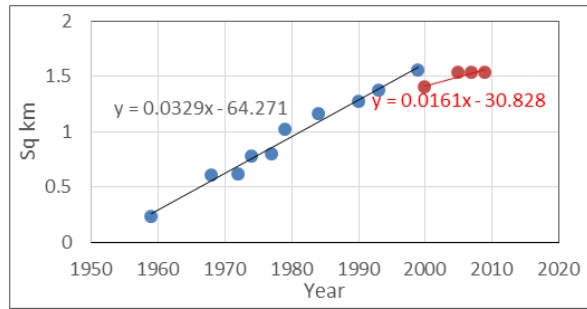


**Figure 25: Development trend of Tsho Rolpa from 1959 to 2000.**

### 5.2.2.3 Glacial lake trends in the Poiqu and Pumqu basins, China

The glacier area in the Poiqu basin decreased from 249.8 km<sup>2</sup> in 1975 to 203.4 km<sup>2</sup> in 2010 – a decrease of 18.6% over 35 years [Xiang *et al.*, 2014]. As a result of glacier retreat, the glacial lakes in the Poiqu basin increased from 119 to 139 in number from the 1970s to 2003 [Mool, 2005]. The Lumu Chimi and Gangxi Co lakes are two large growing lakes in the Poiqu basin (Figure 26) and are growing by 0.08 km<sup>2</sup>/yr and 0.07 km<sup>2</sup>/yr respectively (Figure 27). Both of these lakes formed at the glacier front. Similarly, the number of glacial lakes in the Pumqu basin has increased by almost 27% from the 1970s to 2013. The magnitude of the increase in the number of glacial lakes for the period of 2001–2013 is more significant than for the period of the 1970s–2001 [Che *et al.*, 2014].

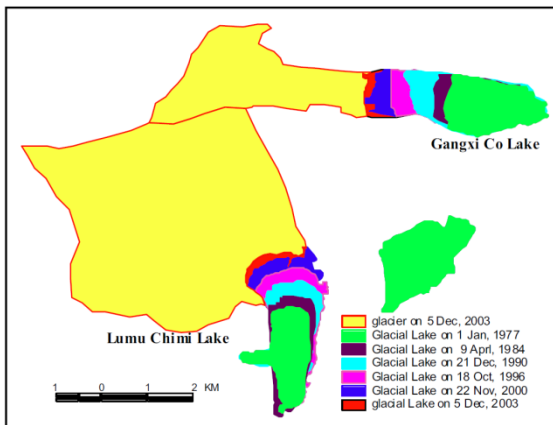


**Figure 26: Development of Lumu Chimi and Ganxi Co.**

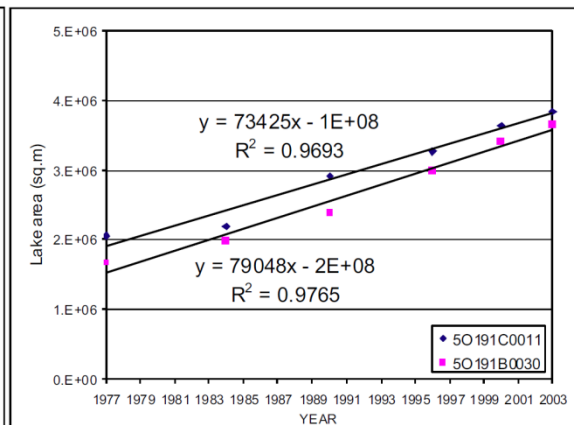


**Figure 27: Trend analysis of Lumu Chimi and Ganxi Co lakes from 1977 to 2003.**

## 5.3 Critical lakes

Accelerated glacier melt has resulted in the formation of new lakes, as well as the expansion of glacier fed lakes. Moraine dammed lakes near the termini of major glacier fronts are common and these meltwater lakes are potentially unstable [Ives *et al.*, 2010]. Increases in lake size and depth also increase the presence of open water in contact with the glacier terminus, and this further accelerates glacial retreat and thinning and could increase instability [Bajracharya *et al.*, 2015]. Glacial lakes that burst their banks can have catastrophic consequences for the economy and livelihoods of the people downstream. Development activities are mainly along

the terraces of river valleys of mountain regions and GLOF occurrences in the headwater could quite possibly damage, wash out or even completely destroy such development infrastructures. Thirty-five GLOF events have already been reported and 204 lakes (out of 8790) are listed as critical lakes – lakes that can cause downstream damage should they burst out (Table 12), these being lakes with an area > 0.02 km<sup>2</sup> in the mountain regions [Bajracharya *et al.*, 2007; Ives *et al.*, 2010; Mool *et al.*, 2011].

The geographic nature of the area, the extremely challenging inaccessibility of the mountains of the HKH region and the large number of lakes involved, limits the number of lakes that can be visited in the field to a very small percentage of the total. Detailed field investigations of all identified critical lakes are difficult, time consuming, and expensive. Most of the criteria were derived from remote sensed data. Geomorphic features and processes are very distinctive in the high spatial resolution satellite images and aerial photographs, and physical parameters of glaciers, glacial lakes, and associated moraines can be estimated easily using high resolution satellite images [Ives *et al.*, 2010]. The use of remote sensing has become a fundamental requirement for any assessment of the potential hazard posed by the rapid formation of new glacial lakes and the continuing enlargement of existing ones. Unfortunately, remote-sensing techniques are limited in their ability to see below the surface and ground-based surveys will be required for such investigations.

## 5.4 Case studies

### 5.4.1 Vulnerability assessment

Assessment of the vulnerability to, as well as the risk associated with GLOF is necessary in order to prepare suitable response strategies. GLOFs have two effects:

1. Primary - characterized by erosion, inundation, and sedimentation; and
2. Secondary - depending upon the slope and geology of the terrain there could be slope failure extending beyond the flood level.

A vulnerability assessment for Imja Tsho, Tsho Rolpa and Thulagi was done based on past records, flood modelling, and interaction with key local stakeholders in order to quantify the elements exposed to risk [Mool *et al.*, 2011]. In areas where slopes are steep and unstable the damage caused by previous GLOFs extended up to 35m above the river beds. If 35m is taken as a threshold value, the GLOF flood hazard zone can be divided into two distinct parts: (i) the 'modelled flood level', derived from a numerical analysis of the dam-break model, and (ii) the 'maximum affected level', which covers the area along the river bank up to a height of 35m above the river bed.

Populations in the areas downstream are 96,767 (for Imja), 141,911 (for Tsho Rolpa), and 165,068 (for Thulagi). These numbers are based on the results of the field validation done in 2010 for community levels, as well as on the demographic data of 2001 for VDC levels and number of households (Table 14 & Table 15). The number of people at risk to GLOF varied from 5,784 in the modelled scenario to 7,762 in a maximum scenario for Imja Tsho; 1,985 to 5,183 for Tsho Rolpa; and 953 to 3,808 for Thulagi. The maximum number of people who could be indirectly affected through infrastructural damage, loss of goods and services, are 501,773 for Imja, 524,323 for Tsho Rolpa, and 2,044,145 for Thulagi (Table 14).

**Table 14: Populations that could be affected within 100 km downstream (Source: [Mool et al., 2011])**

| Description   | Imja Tsho | Tsho Rolpa | Thulagi   |
|---|-----------|------------|-----------|
| Population potentially directly affected due to loss of resources | 96,767    | 14,1911    | 165,068   |
| Population potentially indirectly affected                        | 501,773   | 524,323    | 2,044,145 |
| Revenue earned in billion US\$                                    | 8.98      | 2.4        | 2.2       |

The potential impacts of GLOF in the three glacial lakes were compared with the documented impact of Zhangzangbo in 1981 on the Bhote Koshi - Sun Koshi. The potential impact for Imja was relatively higher than for Tsho Rolpa and Thulagi, and was found to be comparable to that of the Sun Koshi. This can be ascribed to the fact that whereas the Imja Tsho area lies within one of the top 10 tourist destinations in Nepal, Tsho Rolpa (Rolwaling Conservation Area) and Thulagi (Annapurna Circuit) receive fewer tourists.

**Table 15: summary of livelihoods and property exposed to a potential GLOF risk (Source: [Mool et al., 2011])**

| Flood scenario   | Imja Tsho      |              | Tsho Rolpa     |              | Thulagi Lake   |              | Bhote Koshi-Sun Koshi |               |
|--|----------------|--------------|----------------|--------------|----------------|--------------|-----------------------|---------------|
|  | Modelled flood | Maximum      | Modelled flood | Maximum      | Modelled flood | Maximum      | GLOF in 1981          | Maximum       |
| <b>Households</b>  |                |              |                |              |                |              |                       |               |
| No. of households living inside flood-prone area         | 360            | 710          | 142            | 331          | 132            | 298          | 731                   | 2,100         |
| No. of household having property inside flood-prone area | 715            | 801          | 280            | 835          | 41             | 339          | 135                   | 419           |
| <b>Total</b>   | <b>1,075</b>   | <b>1,511</b> | <b>422</b>     | <b>1,166</b> | <b>173</b>     | <b>637</b>   | <b>866</b>            | <b>2,519</b>  |
| <b>Population</b>  |                |              |                |              |                |              |                       |               |
| No. of people living inside flood-prone area             | 1,928          | 3,481        | 680            | 1,604        | 700            | 1,690        | 4,937                 | 13,873        |
| No. of people having property inside flood-prone area    | 3,856          | 4,281        | 1,305          | 3,579        | 253            | 2,118        | 845                   | 2,440         |
| <b>Total</b>   | <b>5,784</b>   | <b>7,762</b> | <b>1,985</b>   | <b>5,183</b> | <b>953</b>     | <b>3,808</b> | <b>5,782</b>          | <b>16,313</b> |

The monetary value of elements exposed to potential GLOFs in the lower downstream areas in all three basins is substantial (Table 16). According to the flood models, the area containing the monetary elements exposed represents 99% of the total areas of Tsho Rolpa and Thulagi, and 51% of Imja Tsho. This can be explained by the increased amount of infrastructure downstream. An increase in GLOF incidents, however, would lead to increased damage in the headwater regions. The revenue referred to in the table is derived primarily from hydroelectricity.

**Table 16: summary of monetary value of elements exposed to a potential GLOF risk (USD '000)**

(Source: [Mool et al., 2011])

| Glacial lakes         | Imja Tsho      |         | Tsho Rolpa     |         | Thulagi        |         | Bhote Koshi  | Koshi            | - |
|-----------------------|----------------|---------|----------------|---------|----------------|---------|--------------|------------------|---|
|                       | Modelled flood | Maximum | Modelled flood | Maximum | Modelled flood | Maximum | GLOF in 1981 | 1981 level + 10m |   |
| Real estate           | 8,917          | 31,729  | 1,411          | 6,524   | 2,036          | 6,685   | 15,889       | 40,606           |   |
| Agricultural sector   | 932            | 1,680   | 117            | 330     | 234            | 519     | 246          | 996              |   |
| Public infrastructure | 2,037          | 2,084   | 319            | 1,928   | 33,5784        | 33,9469 | 98,845       | 109,446          |   |
| Revenue               | 7              | 7       | 0              | 0       | 68,678         | 68,678  | 37,762       | 37,762           |   |
| <b>Total</b>          | 11,894         | 35,501  | 1,847          | 8,781   | 406,731        | 415,351 | 152,741      | 188,810          |   |

The vulnerability of people living downstream from these three lakes differs in relation to the livelihoods and infrastructure characteristics of the respective areas. In general, the risk (vulnerability) may change over time and could also increase when viewed in the context of the current trends in climate warming and the development of infrastructure.

#### 5.4.2 Mitigation and Early Warning Systems in the region

It has become a priority to identify critical glacial lakes together with their associated risks, and to rank them accordingly. As soon as the critical lakes have been identified, the planners, developers and scientists involved must develop and implement appropriate measures aimed at lowering the potential risks posed by these lakes. However, early warning systems that provides downstream residents and owners of infrastructure time to take some evasive action (thereby also reducing risk), should be installed prior to implementing mitigation measures.

##### 5.4.2.1 Early Warning System

In order to be effective, early warning systems must integrate four elements: (i) knowledge of the risk; (ii) a monitoring and warning service; (iii) dissemination and communication; and (iv) response capability. In addition, in order to be capable of providing accurate and timely warning, the warning systems should be technically sound, simple to operate, easy to maintain or replace, and reliable.

#### Early Warning System in Nepal

**Tsho Rolpa:** It was highlighted in 1993 that Lake Tsho Rolpa in the Tamakoshi sub-basin in eastern Nepal was potentially at serious risk [Mool et al., 1993; Kadota, 1994]. It was feared that a catastrophic Tsho Rolpa GLOF would cause widespread loss of life and severely damage local infrastructure (including potential damage to the 60 MW Khimti Hydroelectric Project) [Reynolds, 1999]. A manual early warning system was set up in 1997 in the Tsho Rolpa area as well as in the areas downstream. Following considerable efforts at raising the awareness levels of the inhabitants, the army and police in the area were also provided with communication sets. In 1998, before mitigation work commenced on Tsho Rolpa, a fully functional automatic early warning system was put in place [Reynolds, 1999; Bajracharya et al., 2007]. However, by 2002, only four years after being put in place, the system was no longer operational, this in spite of the fact that it was a robust system commissioned using the latest technology.

**Poiqu basin** (Sun Koshi - Bhote Koshi): An early warning system, aimed at protecting the Upper Bhote Koshi Hydroelectric Project was also installed in the upper Bhote Koshi valley near the Friendship Bridge on the Nepal-China border in eastern Nepal in 2001. Unfortunately, because the stations are all within the Nepal part of the catchment, this system has a lead time of only six minutes [Ives *et al.*, 2010]. To be truly effective the system should be extended further upstream into China. The system was still functional in 2009 - most probably because of the hydropower project involved.

#### **Early Warning System in the Sutlej river basin, India**

In order to provide forecasting, as well as early warning of flash floods and GLOF, a monitoring telemetry station was installed by the Snow and Hydrology Division of the Central Water Commission in Sumdo at the Spiti River and at the confluences of the Parechu and Sutlej rivers. This was done in response to a gap that was found to exist in early warning systems following the floods of 2000, as well as for the protection of hydropower projects. A wireless network at Reckong Peo, used by security personnel with connections to border outposts, and the Doordarshan Satellite Earth Station and All India Radio Relay Centre, have also been very useful in generating warnings and for communication during emergencies.

#### **Early Warning System in the Lunana region, Bhutan**

The Lunana area at the head of the Pho Chhu River in west-central Bhutan has been of considerable concern to the Bhutanese authorities. The Luggye Tsho GLOF of 7 October 1994 caused heavy damage to the Dzong at Punakha as well as 23 deaths [Richardson and Reynolds, 2000]. A manually operated early warning system has been put in place in the Lunana region by the Flood Warning Section (FWS) of the Department of Energy (DoE). Two staff members from the FWS, equipped with wireless sets and satellite telephones to report lake water levels on a regular basis and to issue warnings to downstream inhabitants, are stationed in the Lunana lake area. Several gauges have also been installed along the main river as well as at the lakes. The station is in regular contact with other wireless stations in the downstream areas along the Puna Tsang Chu, including the villages and towns of Punakha, Wangduephodrang, Sunkosh, Khalikhola, and Thimphu [Bajracharya *et al.*, 2007].

#### 5.4.2.2 Mitigation measures

Mitigation measures are developed to reduce the hazard and risk. The most common structural mitigation measures aim to reduce the volume of water in the lake, which in turn reduces both the potential peak surge discharge, as well as the hydrostatic pressure exerted on the moraine dam. This can be achieved in a number of ways that can either be used alone, or in combination:

1. Controlled breaching of the moraine dam.
2. Construction of an outlet control structure.
3. Pumping or siphoning the water from the lake.
4. Tunneling through the moraine barrier or under an ice dam.

In Bhutan (Raphstreng Tsho and Thorthormi Tsho) method one has already been implemented, whereas in Nepal (Tsho Rolpa) methods two and three were implemented. Some examples of mitigation measures that have been applied are described below.

## Nepal

Nepal has made considerable progress in GLOF risk knowledge, risk assessment, monitoring, and early warning and has also made some progress in mitigation measures. Structural mitigation measures were put in place to reduce the risk at Tsho Rolpa, but unfortunately such measures are very expensive. Therefore it is unlikely that this approach could be used at all 21 glacial lakes in Nepal that have been identified as potentially posing at risk of GLOF.

The Tsho Rolpa Mitigation and Early Warning Program was the first GLOF operation to include civil engineering structures in the entire HKH region. As an immediate measure, Wavin Overseas B.V., Holland, in cooperation with the Netherlands-Nepal Friendship Association, installed siphons over part of the terminal moraine in May 1995. This was primarily done to evaluate the use of siphons at high altitude. The siphon system consisted of three inlet pipes submerged in the lake and connected to a single pipe with a discharge outlet located at a stable part of the outer flank of the moraine. Although the installation was successful, the outflow achieved was far less than the flow required to reduce the lake level by the targeted three meters, and it also appeared as if the outflow may never exceed the inflow of additional glacier and snow melt.

In the second phase an open channel was cut through the moraine dam and the four-meter deep artificial spillway succeeded in lowering the lake level by three meters. This phase was supported by a contribution of \$2.9 million from the Dutch Government and the spillway was constructed in June 2000 by the Tsho Rolpa GLOF Risk Reduction Project of the Department of Hydrology and Meteorology.

Mitigation processes are proceeding on Lake Imja Tsho in the Khumbu region. Included in the studies designed to lower the level of Imja Lake and completed by December 2014 were: survey and design; Electrical Resistivity Tomography (ERT); Ground Penetrative Radar (GPR) and bathymetric assessments. The final design for lake lowering will be also be reviewed by the International Consultant and the Technical Advisory Group.

## Bhutan

The Indo-Bhutan team studied the GLOF risk in Lunana area during 1995 and recommended immediate mitigation measures for Raphstreng Tsho. Funding was provided by the Government of India with consulting by Water and Power Consultancy Services (India) Ltd (WAPCOS). Controlled opening of the moraine dam was done manually. The outlet channel was widened using crowbars, pickaxes, and spades and despite numerous constraints (having to work with manual tools; obstructions caused by huge boulders in the channel bed), as early as October 1995 the water level in the main lake was lowered by 0.95 m, and in the two subsidiary lakes by 0.94 m and 1.5 m respectively [Häusler and Leber, 1998; Mool et al., 2001a]. Lowering of the lake level continued until by 1998 the lake level was reduced by four meters.

Supported by Austro-Bhutanese Cooperation, Phase 2 of the Raphstreng Tsho Outburst Flood Mitigation Project began in 1999. The main aim was to assess the geo-risks of Raphstreng Tsho and Thorthormi Tsho in the Lunana area. The activities involved fieldwork with an integrated multi-disciplinary approach using remote sensing, geological, hydro-geological, and geophysical methods to interpret the subsurface characteristics of the moraine dam [Häusler et al., 2000; Mool et al., 2001a]. The results indicated that the risk of an outburst from Raphstreng Tsho was low, but the risk from Thorthormi Tsho high.

Therefore a project for 'Reducing climate change-induced risks and vulnerabilities from glacial lake outburst floods in the Punakha-Wangdue and Chamkhar valleys' was initiated by UNDP.

The project was to run from 2008 to 2012 and involved the Departments of Geology and Mines, Energy (Ministry of Economic Affairs), and the Disaster Management Division (Ministry of Home and Cultural Affairs). The Global Environment Fund (GEF) provided US\$ 3.5 million primarily for determining the effectiveness of structural risk reduction measures.

### **Pakistan**

The high altitude, fragile environment, and isolated nature of Pakistan's Northern Areas gives rise to special constraints and challenges for mitigating natural hazards such as glacial lake outburst floods. Ice-dammed lakes resulting from local glaciers that have thickened and advanced in recent decades predominate the glacial lakes in this area [Hewitt, 2005]. Risk reduction measures taken in Gojal include excavation, channeling, and spillway development. To reduce the threat posed by a potential outburst flood, a local village community used a siphoning technique to drain the lake associated with the Ghulkin glacier. A lateral moraine was excavated to set up the siphon [Roohi et al., 2005].

### **Awareness Raising**

In addition to monitoring lakes, it is essential to raise local awareness and to increase the knowledge of how to respond and minimize the risk. Community and local government bodies should focus on monitoring the lakes, mitigating their vulnerability to GLOF, and prepare to cope with such events should they occur. Early warning begins with preparedness for disaster. This involves raising awareness about glacial lakes, their characteristics, level of hazards, and the required responses during and after GLOF events.

## **5.5 Summary remarks**

The risk of GLOFs is real and should not be ignored. In the past years, knowledge on the distribution of glacial lakes and trends in lake numbers and lake dynamics has much increased. Still the assessment of actual risk for GLOF at particular glacial lakes remains difficult. It is recommendable to include an assessment of the glacial lakes present in a catchment in hydropower planning.

# 6 Conclusions

## 6.1 Summary of results

The climate, cryosphere and hydrology of the Hindu Kush Himalaya (HKH) region have been changing in the past and will change in the future. In this literature review, the state of knowledge regarding climate change and its connections to changes in the cryosphere and hydrology has been investigated.

From historical trends in climate it is clear that air temperature has been increasing in the HKH region over the past decades. Rates of increase are different for daily mean air temperature, maximum air temperature and minimum air temperature. Temperature in the higher elevations increased more over time than temperature in lower elevations. Historical precipitation trends on the other hand show no significant increasing or decreasing trends overall, but the trends vary locally.

Projections of future climate are made using dynamically or statistically downscaled General Circulation Models and Regional Climate Models. The current state of knowledge indicates that climate warming is likely to continue during the 21<sup>st</sup> century. The projections of precipitation change are uncertain as the climate models project a wide range of possible futures, including strong precipitation increases and precipitation decreases. An increase in precipitation is most likely for the upstream Ganges and Brahmaputra, but the magnitude is highly uncertain. Precipitation projections for the upstream Indus show increases as well as decreases with large uncertainties related to the projections. Extreme precipitation events are likely to be more severe and occur with higher frequency. For the Indian summer monsoon increases in precipitation totals, precipitation intensity, inter-annual variability in monsoon strength, and inter-daily variability are likely to increase. It is important to note that the current state-of-the-art climate models have significant difficulties in simulating the complex climate in the HKH region. Only a limited number of models can satisfactorily simulate the monsoon dynamics and no single model is able to simulate all important features in the HKH precipitation regimes. However, empirical-statistical downscaling and bias-correction techniques can reduce climate model errors to large extent.

In the past years, much knowledge has been gathered regarding the cryosphere in the HKH region. Glaciers in most of the HKH region are losing mass in response to climate warming, but glaciers in the Karakoram region have been expanding in recent years. The reason for this “Karakoram anomaly” is not yet fully understood. Despite scientific progress, estimates of total ice volume vary considerably because of the difficulties of estimating ice volumes in situ or from remote sensing products. No strong trends in snow cover changes have been observed. Minor increases or decreases have been reported for different areas. Little is known about the distribution of permafrost in the HKH region. Thus its importance for the regional hydrology remains unclear as well. Estimates of future glacier volumes and areas are uncertain and are hampered because modelling of ice flow is restricted to catchment scale studies. However, strong decreases in glacier volume and area are projected for the HKH region as a whole.

As a result of glacier retreat, the number of proglacial lakes is increasing rapidly and existing lakes are increasing in area and volume. The lakes are often dammed by moraines, which can be unstable. Dam failure can result in glacial lake outburst floods (GLOF) which can have devastating downstream effects. Glacial lakes are being monitored more extensively, but proper

mitigation remains challenging. Knowledge regarding permafrost and changes in permafrost in the HKH region is very limited.

## 6.2 Impacts on hydropower

The aim of this report is to establish a state-of-the-art understanding of future climatological and hydrological changes as a basis for future planning of hydropower development in the HKH. Although general statements of the effects of climate change at the river basin scale can be made based on this literature review, it is very important to note that the effects of climate change on hydrology in the larger HKH region are highly variable in space and time. Therefore it is highly recommended that this first phase assessment be expanded and intensified to include detailed studies of catchments which are candidates for hydropower development.

Continued warming and projected changes in monsoon patterns are likely to cause increases in flow during low flow periods of the year. This is due to earlier onset and longer lasting of the snow and glacier melting processes. Increases in low flows and more evenly distributed flows will be beneficial for the generation of hydropower throughout the year.

Precipitation intensity increases are likely for most parts of the Indus, Ganges and Brahmaputra basins. Increases in peak flows are very likely and pose risks to hydropower plants that can be damaged by floods, and also have reduced lifespans as a result of increased sedimentation. Again it is important to note that projections of precipitation intensity changes show large spatial variation, and catchment scale analysis is indispensable.

Total water availability in the Indus, Ganges and Brahmaputra basins are expected to increase as a result of increased flows during the first half of the 21<sup>st</sup> century. This will stimulate hydropower development. But climate change projections become more uncertain on the long run and therefore also the hydrological projections. Increases in melt water are projected for the first half of the 21<sup>st</sup> century in the HKH region. However, during the second half of the 21<sup>st</sup> century decreasing glacier melt is expected, with further decreases in ice volume and area. The projected timing of such a turnaround is highly variable and dependent on the specific climate change scenario and location in the HKH. Climate models project a large range of possible futures, especially for the amount of precipitation. A continued increase in precipitation can be expected for the upstream Ganges and Brahmaputra basins. The range in projections however is very large and very uncertain. Spatial variation in the projections is also very large. Climate models project partly increasing precipitation and partly decreasing precipitation for the upper Indus basin. With the contribution of glacier melt expected to decrease at the end of the 21<sup>st</sup> century, this makes the hydrological future in the Indus highly uncertain. These large uncertainties may be a risk for hydropower development. Thorough climate change impact analysis for hydrology at catchment scale may narrow down these basin-wide uncertainties. The large range in projections stresses the importance of using an ensemble of climate models covering the range of projections when performing a climate change impact study in the HKH region.

Glacial lake outburst floods (GLOF) have proven to be a serious risk for hydropower sites and cannot be disregarded. As inventories of glacial lakes are improving, more and more information becomes available on the risks of GLOFs. It is recommendable to do extensive risk analyses of glacial lakes before selection of possible hydropower development sites.

In summary, consistent trends of climate change related impacts on hydrology in the HKH region are recognized, but detailed analyses at catchment scale remains necessary for proper assessment of climate change induced hydrological risks for candidate hydropower development sites. These analyses should also consider other factors influencing suitability for hydropower development, such as health, safety and security, environmental and social factors.

### **6.3 Limitations in our understanding**

A lack of knowledge is a major limitation in reducing the large uncertainty pertaining to the present climatic and hydrological conditions in the HKH region and to future predictions.

Quantification and prediction of precipitation, but in particular high altitude precipitation and its spatial distribution is problematic. Meteorological ground stations are sparse and existing gridded meteorological products yield inconsistent simulations of past climate. Combining ground station data with weather model data may increase accuracy of precipitation estimates.

Components of the water balance and hydrological processes in the HKH are also not yet satisfactorily quantified. Examples are water losses through sublimation of snow and ice and losses to deep groundwater. Although huge progress has been made in recent years to gain knowledge about the state of the cryosphere in the HKH region, large knowledge gaps are still present. The distribution of permafrost and its role in the hydrological cycle remains unclear. Similarly, estimates of the ice volume are uncertain. The distribution of snow can be mapped well using remote sensing, but snow depth and snow water equivalent is difficult to assess. The amount of water stored in seasonal snow, which is important for assessing hydropower potential, is difficult to assess.

Prediction of changes in the climate of the HKH is very poor or non-existent and yet forms an important basis for future predictions of the cryosphere and hydrology of the region. Present climate models indicate different trajectories of future climate change, with especially large uncertainty in future precipitation. It is expected that climate modeling will improve in future and the accuracy of predictions will improve, but this will take time.

Even if climate predictions are improved, the response of the cryosphere to climate change is not fully understood, making future predictions of the cryosphere uncertain. It is for example very difficult to determine how fast glaciers, with long delays in responding to changes in climate, will respond in the long run.

### **6.4 Research proposal**

This review gives a comprehensive overview of the state of climate change impacts at regional and basin scale. As such it has given us good insight in the shortcomings in understanding of relevant natural processes, but also shortcomings in models, in situ measurements, technologies in general. Due to the large spatial variation in findings it is important to follow up on these findings on smaller scales.

In the sections above it is shown that research questions vary from the general (eg. how to improve broad scale climate modeling for the region) to the specific (e.g. future sedimentation and its role in hydropower plant longevity). The research needs also vary in degree of importance of their role to improve effectiveness in hydropower development.

It is recommended that ICIMOD jointly with StatKraft develop a research program that focuses more strongly on the understanding of impacts of climate change at catchment level and sub-basin level, and specifically in those catchments/sub-basins which are candidates for hydropower development. Such a joint research programme will have to be based on a well thought through design to address the spectrum of research requirements that became apparent in this review.

## 8 References

- Andermann, C., L. Longuevergne, S. Bonnet, A. Crave, P. Davy, and R. Gloaguen (2012), Impact of transient groundwater storage on the discharge of Himalayan rivers, *Nat. Geosci.*, 5(2), 127–132, doi:10.1038/ngeo1356.
- Archer, D. (2003), Contrasting hydrological regimes in the upper Indus Basin, *J. Hydrol.*, 274(1-4), 198–210, doi:10.1016/S0022-1694(02)00414-6.
- Archer, D. R., and H. J. Fowler (2004), Spatial and temporal variations in precipitation in the Upper Indus Basin, global teleconnections and hydrological implications, *Hydrol. Earth Syst. Sci.*, 8(1), 47–61, doi:10.5194/hess-8-47-2004.
- Asif, M. (2009), Sustainable energy options for Pakistan, *Renew. Sustain. Energy Rev.*, 13(4), 903–909, doi:10.1016/j.rser.2008.04.001.
- Azam, M. F. et al. (2012), From balance to imbalance: A shift in the dynamic behaviour of Chhota Shigri glacier, western Himalaya, India, *J. Glaciol.*, 58(208), 315–324, doi:10.3189/2012JoG11J123.
- Azam, M. F., P. Wagnon, C. Vincent, A. Ramanathan, A. Mandal, and J. G. Pottakkal (2014a), Processes governing the mass balance of Chhota Shigri Glacier (Western Himalaya, India) assessed by point-scale surface energy balance measurements, *Cryosph. Discuss.*, 8(3), 2867–2922, doi:10.5194/tcd-8-2867-2014.
- Azam, M. F., P. Wagnon, C. Vincent, A. Ramanathan, A. Linda, and V. B. Singh (2014b), Reconstruction of the annual mass balance of Chhota Shigri glacier, Western Himalaya, India, since 1969, *Ann. Glaciol.*, 55(66), 69–80, doi:10.3189/2014AoG66A104.
- Bajracharya, S. R., and B. Shrestha (2011), *The status of glaciers in the Hindu Kush-Himalayan region.*, Kathmandu.
- Bajracharya, S. R., P. K. Mool, and B. R. Shrestha (2007), *Impact of climate change on Himalayan glaciers and glacial lakes: Case studies on GLOF and associated hazards in Nepal and Bhutan.*, Kathmandu.
- Bajracharya, S. R., S. B. Maharjan, F. Shrestha, W. Guo, S. Liu, W. Immerzeel, and B. Shrestha (2015), The glaciers of the Hindu Kush Himalayas: current status and observed changes from the 1980s to 2010, *Int. J. Water Resour. Dev.*, 31, 161–173, doi:10.1080/07900627.2015.1005731.
- Bamber, J. L., and A. Rivera (2007), A review of remote sensing methods for glacier mass balance determination, *Glob. Planet. Change*, 59(1-4), 138–148, doi:10.1016/j.gloplacha.2006.11.031.
- Barlow, M., M. Wheeler, B. Lyon, and H. Cullen (2005), Modulation of Daily Precipitation over East Africa by the Madden – Julian Oscillation, *Mon. Weather Rev.*, 133, 3579–3594, doi:10.1175/JCLI-D-13-00693.1.
- Basnett, S., A. V. Kulkarni, and T. Bolch (2013), The influence of debris cover and glacial lakes on the recession of glaciers in Sikkim Himalaya, India, *J. Glaciol.*, 59(218), 1035–1046, doi:10.3189/2013JoG12J184.
- Bernhardt, M., and K. Schulz (2010), SnowSlide: A simple routine for calculating gravitational snow transport, *Geophys. Res. Lett.*, 37(11), n/a–n/a, doi:10.1029/2010GL043086.
- Berthier, E., Y. Arnaud, R. Kumar, S. Ahmad, P. Wagnon, and P. Chevallier (2007), Remote sensing estimates of glacier mass balances in the Himachal Pradesh (Western Himalaya, India), *Remote Sens. Environ.*, 108(3), 327–338, doi:10.1016/j.rse.2006.11.017.
- Bhagat, R. M., V. Kalia, C. Sood, P. K. Mool, and S. R. Bajracharya (2004), *Inventory of glaciers and glacial lakes and the identification of potential glacial lake outburst floods (GLOFs) affected by global warming in the mountains of the Himalayan region: Himachal Pradesh Himalaya, India.*, Kathmandu, Nepal.
- Bhambri, R., T. Bolch, P. Kawishwar, D. P. Dobhal, D. Srivastava, and B. Pratap (2013),

- Heterogeneity in glacier response in the upper Shyok valley, northeast Karakoram, *Cryosph.*, 7(5), 1385–1398, doi:10.5194/tc-7-1385-2013.
- Bhambri, R., M. Mehta, D. P. Dobhal, and A. K. Gupta (2015), *Glacial lake inventory of Uttarakhand*, edited by K. Kumar, WADIA Institute of Himalayan Geology.
- Bhutiyan, M. R. (1999), Mass-balance studies on Siachen Glacier in the Nubra valley, Karakoram Himalaya, India, *J. Glaciol.*, 45, 112–118.
- Bhutiyan, M. R., V. S. Kale, and N. J. Pawar (2007), Long-term trends in maximum, minimum and mean annual air temperatures across the Northwestern Himalaya during the twentieth century, *Clim. Change*, 85(1-2), 159–177, doi:10.1007/s10584-006-9196-1.
- Bocchiola, D., G. Diolaiuti, a. Soncini, C. Mihalcea, C. D'Agata, C. Mayer, a. Lambrecht, R. Rosso, and C. Smiraglia (2011), Prediction of future hydrological regimes in poorly gauged high altitude basins: the case study of the upper Indus, Pakistan, *Hydrol. Earth Syst. Sci.*, 15(7), 2059–2075, doi:10.5194/hess-15-2059-2011.
- Boe, J., L. Terray, F. Habets, and E. Martin (2007), Statistical and dynamical downscaling of the Seine basin climate for hydro-meteorological studies, *Int. J. Climatol.*, 27, 1643–1655, doi:10.1002/joc.
- Bolch, T. (2007), Climate change and glacier retreat in northern Tien Shan (Kazakhstan/Kyrgyzstan) using remote sensing data, *Glob. Planet. Change*, 56(1-2), 1–12, doi:10.1016/j.gloplacha.2006.07.009.
- Bolch, T., M. Buchroithner, T. Pieczonka, and A. Kunert (2008), Planimetric and volumetric glacier changes in the Khumbu Himal, Nepal, since 1962 using Corona, Landsat TM and ASTER data, *J. Glaciol.*, 54(187), 592–600, doi:10.3189/002214308786570782.
- Bolch, T. et al. (2012), The state and fate of Himalayan glaciers, *Science* (80- ), 336, 310–314.
- Bookhagen, B. (2012), Hydrology: Himalayan groundwater, *Nat. Geosci.*, 5(2), 97–98, doi:10.1038/ngeo1366.
- Bookhagen, B., and D. W. Burbank (2010), Toward a complete Himalayan hydrological budget: Spatiotemporal distribution of snowmelt and rainfall and their impact on river discharge, *J. Geophys. Res.*, 115(F3), 1–25, doi:10.1029/2009JF001426.
- Bordoy, R., and P. Burlando (2013), Bias Correction of Regional Climate Model Simulations in a Region of Complex Orography, *J. Appl. Meteorol. Climatol.*, 52(1), 82–101, doi:10.1175/JAMC-D-11-0149.1.
- Bordoy, R., and P. Burlando (2014), Stochastic downscaling of precipitation to high-resolution scenarios in orographically complex regions: 1. Model evaluation, *Water Resour. Res.*, 50(November 2012), 540–561, doi:10.1002/2012WR013289.
- Brock, B. W., C. Mihalcea, M. P. Kirkbride, G. Diolaiuti, M. E. J. Cutler, and C. Smiraglia (2010), Meteorology and surface energy fluxes in the 2005–2007 ablation seasons at the Miage debris-covered glacier, Mont Blanc Massif, Italian Alps, *J. Geophys. Res.*, 115(D9), D09106, doi:10.1029/2009JD013224.
- Brown, R. D. (2000), Northern Hemisphere Snow Cover Variability and Change, 1915–97, *J. Clim.*, 13(13), 2339–2355, doi:10.1175/1520-0442(2000)013<2339:NHSCVA>2.0.CO;2.
- Brun, F., M. Dumont, P. Wagnon, E. Berthier, M. F. Azam, J. M. Shea, P. Sirguey, A. Rabatel, and A. Ramanathan (2015), Seasonal changes in surface albedo of Himalayan glaciers from MODIS data and links with the annual mass balance, *Cryosph.*, 9(1), 341–355, doi:10.5194/tc-9-341-2015.
- Cannon, F., L. M. V. Carvalho, C. Jones, and B. Bookhagen (2014), Multi-annual variations in winter westerly disturbance activity affecting the Himalaya, *Clim. Dyn.*, 44(1-2), 441–455, doi:10.1007/s00382-014-2248-8.
- Che, T., L. Xiao, and Y.-A. Liou (2014), Changes in Glaciers and Glacial Lakes and the Identification of Dangerous Glacial Lakes in the Pumqu River Basin, Xizang (Tibet), *Adv. Meteorol.*, 2014, 1–8, doi:10.1155/2014/903709.

- Choudhury, N. (2010), *Sustainable dam development in India between global norms and local practices*, Bonn.
- Christensen, J. H., and O. B. Christensen (2002), Severe summertime flooding in Europe, *Nature*, 421(February), 805–806.
- Collier, E., and W. W. Immerzeel (2015), High-resolution modeling of atmospheric dynamics in the Nepalese Himalaya, *J. Geophys. Res. Atmos.*, 1–15, doi:10.1002/2015JD023266.Received.
- Dobhal, D. P., and M. Mehta (2010), Surface morphology, elevation changes and Terminus retreat of Dokriani Glacier, Garhwal Himalaya: implication for climate change, *Himal. Geol.*, 31(1), 71–78.
- Dobhal, D. P., M. Mehta, and D. Srivastava (2013), Influence of debris cover on terminus retreat and mass changes of Chorabari Glacier, Garhwal region, central Himalaya, India, *J. Glaciol.*, 59(217), 961–971, doi:10.3189/2013JoG12J180.
- Ducharme, P., A. Houdayer, Y. Choquette, B. Kapfer, and J. P. Martin (2015), Numerical Simulation of Terrestrial Radiation over a Snow Cover, *J. Atmos. Ocean. Technol.*, 32(8), 1478–1485, doi:10.1175/JTECH-D-14-00100.1.
- Dyrgerov, M. B., and M. F. Meier (2005), *Glaciers and the changing earth system: A 2004 snapshot*, Boulder.
- Eden, J. M., and M. Widmann (2014), Downscaling of GCM-Simulated Precipitation Using Model Output Statistics, *J. Clim.*, 27(1), 312–324, doi:10.1175/JCLI-D-13-00063.1.
- Eden, J. M., M. Widmann, D. Grawe, and S. Rast (2012), Skill, Correction, and Downscaling of GCM-Simulated Precipitation, *J. Clim.*, 25(11), 3970–3984, doi:10.1175/JCLI-D-11-00254.1.
- Ferraris, L., S. Gabellani, N. Reborra, and A. Provenzale (2003), A comparison of stochastic models for spatial rainfall downscaling, *Water Resour. Res.*, 39(12), n/a–n/a, doi:10.1029/2003WR002504.
- Forsythe, N., H. J. Fowler, S. Blenkinsop, A. Burton, C. G. Kilsby, D. R. Archer, C. Harpham, and M. Z. Hashmi (2014), Application of a stochastic weather generator to assess climate change impacts in a semi-arid climate: The Upper Indus Basin, *J. Hydrol.*, 517, 1019–1034, doi:10.1016/j.jhydrol.2014.06.031.
- Fowler, H. J., and D. R. Archer (2006), Conflicting Signals of Climatic Change in the Upper Indus Basin, *J. Clim.*, 19(17), 4276–4293, doi:10.1175/JCLI3860.1.
- Fowler, H. J., S. Blenkinsop, and C. Tebaldi (2007), Linking climate change modelling to impacts studies : recent advances in downscaling techniques for hydrological modelling, *Int. J. Climatol.*, (September), 1547–1578, doi:10.1002/joc.
- Frey, H., H. Machguth, M. Huss, C. Huggel, S. Bajracharya, T. Bolch, A. Kulkarni, A. Linsbauer, N. Salzmann, and M. Stoffel (2014), Estimating the volume of glaciers in the Himalayan-Karakoram region using different methods, *Cryosph.*, 8(6), 2313–2333, doi:10.5194/tc-8-2313-2014.
- Fujita, K., and T. Nuimura (2011), Spatially heterogeneous wastage of Himalayan glaciers, *Proc. Natl. Acad. Sci.*, 108(34), 14011–14014, doi:10.1073/pnas.1106242108.
- Fujita, K., and A. Sakai (2014), Modelling runoff from a Himalayan debris-covered glacier, *Hydrol. Earth Syst. Sci.*, 18(7), 2679–2694, doi:10.5194/hess-18-2679-2014.
- Fujita, K., F. Nakazawa, and B. Rana (2001a), Glaciological observations on Rikha Samba Glacier in Hidden Valley, Nepal Himalayas, 1998 and 1999, *Bull. Glaciol. Res.*, 18(2901), 31–35.
- Fujita, K., T. Kadota, B. Rana, R. B. Kayastha, and Y. Ageta (2001b), Shrinkage of Glacier AX010 in Shorong region, Nepal Himalayas in the 1990s, *Bull. Glacier Res.*, 18, 51–54.
- Fujita, K., R. Suzuki, T. Nuimura, and A. Sakai (2008), Performance of ASTER and SRTM

- DEMs, and their potential for assessing glacial lakes in the Lunana region, Bhutan Himalaya, *J. Glaciol.*, 54(185), 220–228, doi:10.3189/002214308784886162.
- Gardelle, J., Y. Arnaud, and E. Berthier (2011), Contrasted evolution of glacial lakes along the Hindu Kush Himalaya mountain range between 1990 and 2009, *Glob. Planet. Change*, 75(1-2), 47–55, doi:10.1016/j.gloplacha.2010.10.003.
- Gardelle, J., E. Berthier, and Y. Arnaud (2012), Slight mass gain of Karakoram glaciers in the early twenty-first century, *Nat. Geosci.*, 5(5), 322–325, doi:10.1038/ngeo1450.
- Gardelle, J., E. Berthier, Y. Arnaud, and A. Kääb (2013), Region-wide glacier mass balances over the Pamir-Karakoram-Himalaya during 1999&ndash;2011, *Cryosph.*, 7(4), 1263–1286, doi:10.5194/tc-7-1263-2013.
- Gardner, A. S. et al. (2013), A Reconciled Estimate of Glacier Contributions to Sea Level Rise: 2003 to 2009, *Science (80-. )*, 340(6134), 852–857, doi:10.1126/science.1234532.
- Giorgi, F., C. Jones, and G. R. Asrar (2009), Addressing climate information needs at the regional level: the CORDEX framework, *Bull. - World Meteorol. Organ.*, 58(3), 175–183.
- Gobiet, A., M. Suklitsch, and G. Heinrich (2015), The effect of empirical-statistical correction of intensity-dependent model errors on the temperature climate change signal, *Hydrol. Earth Syst. Sci.*, 19, 1–12, doi:10.5194/hess-19-1-2015.
- Govindha Raj, B. K., V. K. Kumar, and R. S.N. (2013), Remote sensing-based inventory of glacial lakes in Sikkim Himalaya: semi-automated approach using satellite data, *Geomatics, Nat. Hazards Risk*, 4(3), 241–253, doi:10.1080/19475705.2012.707153.
- Gruber, S. (2012), Derivation and analysis of a high-resolution estimate of global permafrost zonation, *Cryosphere*, doi:10.5194/tc-6-221-2012.
- Gurung, D. R., A. Giriraj, K. S. Aung, B. Shrestha, and A. V Kulkarni (2011), *Snow-cover mapping and monitoring in the Hindu Kush-Himalayas*.
- Häusler, H., and D. Leber (1998), *Final report of Raphstreng Tsho Outburst Flood Mitigatory Project (Lunana, Northwestern Bhutan) Phase I*, Vienna, Austria.
- Häusler, H., D. Leber, M. Schreilechner, R. Morawetz, H. Lentz, S. Skuk, M. Meyer, C. Janda, and E. Burgschwaiger (2000), *Final report of Raphstreng Tsho Outburst Flood Mitigatory Project (Lunana, Northwestern Bhutan) Phase II*, Vienna, Austria.
- Hewitt, K. (2005), The Karakoram Anomaly? Glacier Expansion and the “Elevation Effect,” Karakoram Himalaya, *Mt. Res. Dev.*, 25(4), 332–340, doi:10.1659/0276-4741(2005)025[0332:TKAGEA]2.0.CO;2.
- Heynen, M., F. Pellicciotti, and M. Carenzo (2013), Parameter sensitivity of a distributed enhanced temperature-index melt model, *Ann. Glaciol.*, 54(63), 1–11, doi:10.3189/2013AoG63A537.
- Hock, R. (2003), Temperature index melt modelling in mountain areas, *J. Hydrol.*, 282(1-4), 104–115, doi:10.1016/S0022-1694(03)00257-9.
- Hubbard, A., I. Willis, M. Sharp, D. Mair, P. Nienow, B. Hubbard, and H. Blatter (2000), Glacier mass-balance determination by remote sensing and high-resolution modelling, *J. Glaciol.*, 46(154), 491–498, doi:10.3189/172756500781833016.
- Huss, M., G. Jouvett, D. Farinotti, and a. Bauder (2010), Future high-mountain hydrology: a new parameterization of glacier retreat, *Hydrol. Earth Syst. Sci.*, 14(5), 815–829, doi:10.5194/hess-14-815-2010.
- Immerzeel, W. (2008), Historical trends and future predictions of climate variability in the Brahmaputra basin, *Int. J. Climatol.*, 28, 243–254, doi:10.1002/joc.
- Immerzeel, W. W., and M. F. P. Bierkens (2012), Asia’s water balance, *Nat. Geosci.*, 5(12), 841–842, doi:10.1038/ngeo1643.
- Immerzeel, W. W., P. Droogers, S. M. de Jong, and M. F. P. Bierkens (2009), Large-scale monitoring of snow cover and runoff simulation in Himalayan river basins using remote

- sensing, *Remote Sens. Environ.*, 113(1), 40–49, doi:10.1016/j.rse.2008.08.010.
- Immerzeel, W. W., L. P. H. van Beek, M. Konz, A. B. Shrestha, and M. F. P. Bierkens (2011), Hydrological response to climate change in a glacierized catchment in the Himalayas, *Clim. Change*, 110, 721–736, doi:10.1007/s10584-011-0143-4.
- Immerzeel, W. W., F. Pellicciotti, and A. B. Shrestha (2012), Glaciers as a Proxy to Quantify the Spatial Distribution of Precipitation in the Hunza Basin, *Mt. Res. Dev.*, 32(1), 30–38, doi:10.1659/MRD-JOURNAL-D-11-00097.1.
- Immerzeel, W. W., F. Pellicciotti, and M. F. P. Bierkens (2013), Rising river flows throughout the twenty-first century in two Himalayan glacierized watersheds, *Nat. Geosci.*, 6(8), 1–4, doi:10.1038/ngeo1896.
- Immerzeel, W. W., P. D. A. Kraaijenbrink, J. M. Shea, A. B. Shrestha, F. Pellicciotti, M. F. P. Bierkens, and S. M. de Jong (2014a), High-resolution monitoring of Himalayan glacier dynamics using unmanned aerial vehicles, *Remote Sens. Environ.*, 150, 93–103, doi:10.1016/j.rse.2014.04.025.
- Immerzeel, W. W., L. Petersen, S. Ragetti, and F. Pellicciotti (2014b), The importance of observed gradients of air temperature and precipitation for modeling runoff from a glacierized watershed in the Nepalese Himalayas, *Water Resour. Res.*, doi:10.1002/2013WR014506.
- Ives, J. D., R. B. Shrestha, and P. K. Mool (2010), *Formation of Glacial Lakes in the Hindu Kush-Himalayas and GLOF Risk Assessment*, Kathmandu.
- Jacob, T., J. Wahr, W. T. Pfeffer, and S. Swenson (2012), Recent contributions of glaciers and ice caps to sea level rise, *Nature*, 482(7386), 514–518, doi:10.1038/nature10847.
- Jain, S. K., A. Goswami, and A. K. Saraf (2009), Role of Elevation and Aspect in Snow Distribution in Western Himalaya, *Water Resour. Manag.*, 23(1), 71–83, doi:10.1007/s11269-008-9265-5.
- Jamie Carter, Keil Schmid, Kirk Waters, L. B., and J. H. Brian Hadley, Rebecca Mataosky (2012), Lidar 101 : An Introduction to Lidar Technology , Data , and Applications, *NOAA Coast. Serv. Cent.*, (November), 76.
- Kääb, A., E. Berthier, C. Nuth, J. Gardelle, and Y. Arnaud (2012), Contrasting patterns of early twenty-first-century glacier mass change in the Himalayas, *Nature*, 488(7412), 495–498, doi:10.1038/nature11324.
- Kadota, T. (1994), *Report for the field investigation on the Tsho Rolpa glacier lake, Rolwaling valley. WECS Report No. 551*, Kathmandu, Nepal.
- Karma, Y. Ageta, N. Naito, S. Iwata, and H. Yabuki (2003), Glacier distribution in the Himalayas and glacier shrinkage from 1963 to 1993 in the Bhutan Himalayas, *Bull. Glaciol. Res.*, 20, 29–40.
- Kaur, R., D. Saikumar, A. V. Kulkarni, and B. S. Chaudhary (2009), Variations in snow cover and snowline altitude in Baspa Basin, *Curr. Sci.*, 96(9), 1255–1258.
- Kay, A. L., H. N. Davies, V. A. Bell, and R. G. Jones (2008), Comparison of uncertainty sources for climate change impacts: flood frequency in England, *Clim. Change*, 92, 41–63, doi:10.1007/s10584-008-9471-4.
- Khattak, M. S., M. S. Babel, and M. Sharif (2011), Hydro-meteorological trends in the upper Indus River basin in Pakistan, *Clim. Res.*, 46(2), 103–119, doi:10.3354/cr00957.
- Koul, M. N., and R. K. Ganjoo (2010), Impact of inter- and intra-annual variation in weather parameters on mass balance and equilibrium line altitude of Naradu Glacier (Himachal Pradesh), NW Himalaya, India, *Clim. Change*, 99(1-2), 119–139, doi:10.1007/s10584-009-9660-9.
- Kripalani, R. H., A. Kulkarni, and S. S. Sabade (2003), Western Himalayan snow cover and Indian monsoon rainfall: A re-examination with INSAT and NCEP/NCAR data, *Theor. Appl. Climatol.*, 74(1-2), 1–18, doi:10.1007/s00704-002-0699-z.

- Krishna, A. P. (2005), Snow and glacier cover assessment in the high mountains of Sikkim Himalaya, *Hydrol. Process.*, 19(12), 2375–2383, doi:10.1002/hyp.5890.
- Krishna Kumar, K., S. K. Patwardhan, a. Kulkarni, K. Kamala, K. Koteswara Rao, and R. Jones (2011), Simulated projections for summer monsoon climate over India by a high-resolution regional climate model (PRECIS), *Curr. Sci.*, 101(3), 312–326.
- Kumar, V., G. Venkataramana, and K. a. Høgda (2011), Glacier surface velocity estimation using SAR interferometry technique applying ascending and descending passes in Himalayas, *Int. J. Appl. Earth Obs. Geoinf.*, 13(4), 545–551, doi:10.1016/j.jag.2011.02.004.
- Leander, R., and T. A. Buishand (2007), Resampling of regional climate model output for the simulation of extreme river flows, *J. Hydrol.*, 332, 487–496, doi:10.1016/j.jhydrol.2006.08.006.
- Leber, D., H. Hausler, M. Brauner, and D. Wangda (2002), *Glacier Lake Outburst Flood Mitigation Project Phase III (2000-2002)*, Vienna, Austria.
- Lejeune, Y., Y. L'Hôte, and P. Chevallier (2003), Instrumentation et constitution d'une base de données météorologiques et nivologiques dans les Andes, station Charquini, 4795 m, Bolivie.,
- Lejeune, Y., L. Bouilloud, P. Etchevers, P. Wagnon, P. Chevallier, J.-E. Sicart, E. Martin, and F. Habets (2007), Melting of Snow Cover in a Tropical Mountain Environment in Bolivia: Processes and Modeling, *J. Hydrometeorol.*, 8(4), 922–937, doi:10.1175/JHM590.1.
- LIGG, WECS, and NEA (1988), *Expedition to Glaciers and Glacier Lakes in the Pumqu (Arun) and Poiqu (Bhote-Sun Kosi) River Basins, Xizang (Tibet) China. Report on First Expedition to Glaciers and Glacier Lakes in the Pumqu (Arun) and Poiqu (Bhote-Sun Kosi) River Basins, Xizang (Tibet)*, Beijing.
- Löffler-Mang, M., and J. Joss (2000), An Optical Disdrometer for Measuring Size and Velocity of Hydrometeors, *J. Atmos. Ocean. Technol.*, 17(2), 130–139, doi:10.1175/1520-0426(2000)017<0130:AODFMS>2.0.CO;2.
- Lu, A., S. Kang, Z. Li, and W. H. Theakstone (2010), Altitude effects of climatic variation on Tibetan plateau and its vicinities, *J. Earth Sci.*, 21(2), 189–198, doi:10.1007/s12583-010-0017-0.
- Lutz, A. F., W. W. Immerzeel, A. Gobiet, F. Pellicciotti, and M. F. P. Bierkens (2013), Comparison of climate change signals in CMIP3 and CMIP5 multi-model ensembles and implications for Central Asian glaciers, *Hydrol. Earth Syst. Sci.*, 17(9), 3661–3677, doi:10.5194/hess-17-3661-2013.
- Lutz, A. F., W. W. Immerzeel, A. B. Shrestha, and M. F. P. Bierkens (2014), Consistent increase in High Asia's runoff due to increasing glacier melt and precipitation, *Nat. Clim. Chang.*, 4, 587–592, doi:10.1038/NCLIMATE2237.
- Maraun, D. et al. (2010), Precipitation downscaling under climate change: recent developments to bridge the gap between dynamical models and the end user, *Rev. Geophys.*, 48(RG3003), 1–34.
- Marzeion, B., A. H. Jarosch, and M. Hofer (2012), Past and future sea-level change from the surface mass balance of glaciers, *Cryosph.*, 6(6), 1295–1322, doi:10.5194/tc-6-1295-2012.
- Matsuo, K., and K. Heki (2010), Time-variable ice loss in Asian high mountains from satellite gravimetry, *Earth Planet. Sci. Lett.*, 290(1-2), 30–36, doi:10.1016/j.epsl.2009.11.053.
- Maurer, E. P., and D. W. Pierce (2014), Bias correction can modify climate model simulated precipitation changes without adverse effect on the ensemble mean, *Hydrol. Earth Syst. Sci.*, 18(3), 915–925, doi:10.5194/hess-18-915-2014.
- Maussion, F., D. Scherer, T. Mölg, E. Collier, J. Curio, and R. Finkelburg (2014), Precipitation Seasonality and Variability over the Tibetan Plateau as Resolved by the High Asia Reanalysis, *J. Clim.*, 27(5), 1910–1927, doi:10.1175/JCLI-D-13-00282.1.

- Meehl, G. A., C. Covey, T. Delworth, M. Latif, B. McAvaney, J. F. B. Mitchell, R. J. Stouffer, and K. E. Taylor (2007), The WCRP CMIP3 multimodel dataset: A New Era in Climate Change Research, *Bull. Am. Meteorol. Soc.*, 88(September), 1382–1394.
- Ménégoz, M., H. Gallée, and H. W. Jacobi (2013), Precipitation and snow cover in the Himalaya: From reanalysis to regional climate simulations, *Hydrol. Earth Syst. Sci.*, doi:10.5194/hess-17-3921-2013.
- Mihalcea, C., C. Mayer, G. Diolaiuti, A. Lambrecht, C. Smiraglia, and G. Tartari (2006), Ice ablation and meteorological conditions on the debris-covered area of Baltoro glacier, Karakoram, Pakistan, *Ann. Glaciol.*, 43(1), 292–300, doi:10.3189/172756406781812104.
- Molden, D. J., R. A. Vaidya, A. B. Shrestha, G. Rasul, and M. S. Shrestha (2014), Water infrastructure for the Hindu Kush Himalayas, *Int. J. Water Resour. Dev.*, 30(1), 60–77, doi:10.1080/07900627.2013.859044.
- Mool, P. K. (2005), *Monitoring of glaciers and glacial lakes from 1970s to 2000 in Poiqu Basin, Tibet Autonomous Region, PR China.*, Kathmandu, Nepal.
- Mool, P. K., and S. R. Bajracharya (2003), *Inventory of glaciers, glacial lakes and the identification of potential glacial lake outburst floods (GLOFs) affected by global warming in the mountains of Himalayan region: Tista Basin, Sikkim Himalaya, India.*, Kathmandu, Nepal.
- Mool, P. K., T. Kadota, P. Pokharel, and S. Joshi (1993), *Report on the field investigation on the Tsho Rolpa glacier lake, Rolwaling valley. WECS Report No. 436*, Kathmandu, Nepal.
- Mool, P. K., D. Wangda, S. R. Bajracharya, K. Kunzang, D. R. Gurung, and S. P. Joshi (2001a), *Inventory of glaciers, glacial lakes and glacial lake outburst floods. Monitoring and early warning systems in the Hindu Kush-Himalayan Region: Bhutan*, ICIMOD, Kathmandu, Nepal.
- Mool, P. K., S. R. Bajracharya, and S. P. Joshi (2001b), *Inventory of glaciers, glacial lakes and glacial lake outburst floods. Monitoring and early warning systems in the Hindu Kush-Himalayan Region: Nepal.*, ICIMOD, Kathmandu, Nepal.
- Mool, P. K. et al. (2011), *Glacial Lakes and Glacial Lake Outburst Floods in Nepal*, Kathmandu.
- Moron, V., A. W. Robertson, M. N. Ward, and O. Ndiaye (2008), Weather Types and Rainfall over Senegal. Part II: Downscaling of GCM Simulations, *J. Clim.*, 21(2), 288–307, doi:10.1175/2007JCLI1624.1.
- Moss, R. H. et al. (2010), The next generation of scenarios for climate change research and assessment., *Nature*, 463(7282), 747–56, doi:10.1038/nature08823.
- Mukhopadhyay, B., and A. Khan (2014a), A quantitative assessment of the genetic sources of the hydrologic flow regimes in Upper Indus Basin and its significance in a changing climate, *J. Hydrol.*, 509, 549–572, doi:10.1016/j.jhydrol.2013.11.059.
- Mukhopadhyay, B., and A. Khan (2014b), Rising river flows and glacial mass balance in central Karakoram, *J. Hydrol.*, 513, 192–203, doi:10.1016/j.jhydrol.2014.03.042.
- Mukhopadhyay, B., and A. Khan (2015), A reevaluation of the snowmelt and glacial melt in river flows within Upper Indus Basin and its significance in a changing climate, *J. Hydrol.*, 527, 119–132, doi:10.1016/j.jhydrol.2013.11.059.
- Negi, H. S., N. K. Thakur, R. Kumar, and M. Kumar (2009), Monitoring and evaluation of seasonal snow cover in Kashmir valley using remote sensing, GIS and ancillary data, *J. Earth Syst. Sci.*
- Negi, H. S., S. K. Singh, A. V. Kulkarni, and B. S. Semwal (2010), Field-based spectral reflectance measurements of seasonal snow cover in the Indian Himalaya, *Int. J. Remote Sens.*, 31(9), 2393–2417, doi:10.1080/01431160903002417.
- Nepal, S., P. Krause, W.-A. Flügel, M. Fink, and C. Fischer (2014), Understanding the hydrological system dynamics of a glaciated alpine catchment in the Himalayan region using the J2000 hydrological model, *Hydrol. Process.*, 28(3), 1329–1344,

doi:10.1002/hyp.9627.

- Nicholson, L., and D. I. Benn (2006), Calculating ice melt beneath a debris layer using meteorological data, *J. Glaciol.*, *52*(178), 463–470, doi:10.3189/172756506781828584.
- Nie, Y., Q. Liu, and S. Liu (2013), Glacial Lake Expansion in the Central Himalayas by Landsat Images, 1990–2010, *PLoS One*, *8*(12), e83973, doi:10.1371/journal.pone.0083973.
- Nuimura, T., K. Fujita, S. Yamaguchi, and R. R. Sharma (2012), Elevation changes of glaciers revealed by multitemporal digital elevation models calibrated by GPS survey in the Khumbu region, Nepal Himalaya, 1992–2008, *J. Glaciol.*, *58*(210), 648–656, doi:10.3189/2012JoG11J061.
- Nuimura, T. et al. (2015), The GAMDAM glacier inventory: a quality-controlled inventory of Asian glaciers, *Cryosph.*, *9*(3), 849–864, doi:10.5194/tc-9-849-2015.
- Palazzi, E., J. Von Hardenberg, and A. Provenzale (2013), Precipitation in the Hindu-Kush Karakoram Himalaya : Observations and future scenarios, *J. Geophys. Res. Atmos.*, *118*, 85–100, doi:10.1029/2012JD018697.
- Palazzi, E., J. von Hardenberg, S. Terzago, and A. Provenzale (2014), Precipitation in the Karakoram-Himalaya: a CMIP5 view, *Clim. Dyn.*, 21–45, doi:10.1007/s00382-014-2341-z.
- Pellicciotti, F., B. Brock, U. Strasser, P. Burlando, M. Funk, and J. Corripio (2005), An enhanced temperature-index glacier melt model including the shortwave radiation balance: development and testing for Haut Glacier d’Arolla , Switzerland, *J. Glaciol.*, *51*(175), 573–587.
- Pellicciotti, F., C. Buergi, W. W. Immerzeel, M. Konz, and A. B. Shrestha (2012), Challenges and Uncertainties in Hydrological Modeling of Remote Hindu Kush–Karakoram–Himalayan (HKH) Basins: Suggestions for Calibration Strategies, *Mt. Res. Dev.*, *32*(1), 39–50, doi:10.1659/MRD-JOURNAL-D-11-00092.1.
- van Pelt, S. C., J. J. Beersma, T. a. Buishand, B. J. J. M. van den Hurk, and P. Kabat (2012), Future changes in extreme precipitation in the Rhine basin based on global and regional climate model simulations, *Hydrol. Earth Syst. Sci.*, *16*(12), 4517–4530, doi:10.5194/hess-16-4517-2012.
- Pepin, N. et al. (2015), Elevation-dependent warming in mountain regions of the world, *Nat. Clim. Chang.*, *5*, 424–430, doi:10.1038/nclimate2563.
- Pfeffer, W. T. et al. (2014), The Randolph Glacier Inventory: a globally complete inventory of glaciers, *J. Glaciol.*, *60*(221), 537–552, doi:10.3189/2014JoG13J176.
- Piani, C., G. P. Weedon, M. Best, S. M. Gomes, P. Viterbo, S. Hagemann, and J. O. Haerter (2010), Statistical bias correction of global simulated daily precipitation and temperature for the application of hydrological models, *J. Hydrol.*, *395*(3-4), 199–215, doi:10.1016/j.jhydrol.2010.10.024.
- Prasch, M., W. Mauser, and M. Weber (2013a), Quantifying present and future glacier melt-water contribution to runoff in a central Himalayan river basin, *Cryosph.*, *7*(3), 889–904, doi:10.5194/tc-7-889-2013.
- Prasch, M., W. Mauser, and M. Weber (2013b), Quantifying present and future glacier melt-water contribution to runoff in a central Himalayan river basin, *Cryosph.*, *7*(3), 889–904, doi:10.5194/tc-7-889-2013.
- Prudhomme, C., N. Reynard, and S. Crooks (2002), Downscaling of global climate models for flood frequency analysis: where are we now?, *Hydrol. Process.*, *16*(6), 1137–1150, doi:10.1002/hyp.1054.
- Pu, Z., and L. Xu (2009), MODIS/Terra observed snow cover over the Tibet Plateau: Distribution, variation and possible connection with the East Asian Summer Monsoon (EASM), *Theor. Appl. Climatol.*
- Puri, V. M. K., R. K. Singh, D. Srivastava, C. V. Sangewar, S. Swaroop, and C. K. Gautam (1999), Inventory of the Himalayan glaciers: A contribution to the International Hydrological

- Programme. No. 34., in *Geological survey of India*, edited by M. K. Kaul and V. M. K. Puri, pp. 1–14, Calcutta, India.
- Rabatel, A., J.-P. Dedieu, and C. Vincent (2005), Using remote-sensing data to determine equilibrium-line altitude and mass-balance time series: validation on three French glaciers, 1994–2002, *J. Glaciol.*, *51*(175), 539–546, doi:10.3189/172756505781829106.
- Racoviteanu, A. E., M. W. Williams, and R. G. Barry (2008), Optical Remote Sensing of Glacier Characteristics: A Review with Focus on the Himalaya, *Sensors*, *8*(5), 3355–3383, doi:10.3390/s8053355.
- Racoviteanu, A. E., R. Armstrong, and M. W. Williams (2013a), Evaluation of an ice ablation model to estimate the contribution of melting glacier ice to annual discharge in the Nepal Himalaya, *Water Resour. Res.*, *49*(9), 5117–5133, doi:10.1002/wrcr.20370.
- Racoviteanu, A. E., R. Armstrong, and M. W. Williams (2013b), Evaluation of an ice ablation model to estimate the contribution of melting glacier ice to annual discharge in the Nepal Himalaya, *Water Resour. Res.*, *49*(9), 5117–5133, doi:10.1002/wrcr.20370.
- Radić, V., A. Bliss, A. C. Beedlow, R. Hock, E. Miles, and J. G. Cogley (2014), Regional and global projections of twenty-first century glacier mass changes in response to climate scenarios from global climate models, *Clim. Dyn.*, *42*(1-2), 37–58, doi:10.1007/s00382-013-1719-7.
- Ragetti, S., and F. Pellicciotti (2012), Calibration of a physically based, spatially distributed hydrological model in a glacierized basin: On the use of knowledge from glaciometeorological processes to constrain model parameters, *Water Resour. Res.*, *48*, W03509, doi:10.1029/2011WR010559.
- Ragetti, S., F. Pellicciotti, R. Bordoy, and W. W. Immerzeel (2013), Sources of uncertainty in modeling the glacio-hydrological response of a Karakoram watershed to climate change, *Water Resour. Res.*, *49*, 1–19, doi:10.1002/wrcr.20450.
- Ragetti, S., F. Pellicciotti, W. W. Immerzeel, E. Miles, L. Petersen, M. Heynen, J. M. Shea, D. Stumm, S. Joshi, and A. B. Shrestha (2015), Unraveling the hydrology of a Himalayan watershed through integration of high resolution in-situ data and remote sensing with an advanced simulation model, *Adv. Water Resour.*, *78*, 94–111, doi:10.1016/j.advwatres.2015.01.013.
- Raina, V. K. (2009), *Himalayan glaciers: a state-of-art review of glacial studies, glacial retreat and climate change*.
- Rajbhandari, R., a. B. Shrestha, a. Kulkarni, S. K. Patwardhan, and S. R. Bajracharya (2014), Projected changes in climate over the Indus river basin using a high resolution regional climate model (PRECIS), *Clim. Dyn.*, doi:10.1007/s00382-014-2183-8.
- Ramesh, K. V., and P. Goswami (2014), Assessing reliability of regional climate projections: the case of Indian monsoon., *Nat. Sci. reports*, *4*, 4071, doi:10.1038/srep04071.
- Randhawa, S. S., R. K. Sood, B. P. Rathore, and A. V. Kulkarni (2005), Moraine-dammed lakes study in the Chenab and the Satluj River basins using IRS data., *J. Indian Soc. Remote Sens.*, *33*(2), 285–290.
- Rangwala, I., and J. R. Miller (2012), Climate change in mountains: A review of elevation-dependent warming and its possible causes, *Clim. Change*, *114*, 527–547, doi:10.1007/s10584-012-0419-3.
- Rasul, G. (2014), Why Eastern Himalayan countries should cooperate in transboundary water resource management, *Water Policy*, *16*(1), 19, doi:10.2166/wp.2013.190.
- Reynolds, J. M. (1999), Glacial hazard assessment at Tsho Rolpa, Rolwaling, Central Nepal, *Q. J. Eng. Geol.*, *302*, 209–214.
- Richardson, S. D., and J. M. Reynolds (2000), An overview of glacial hazards in the Himalayas, *Quat. Int.*, *65/66*, 31–47.
- Roohi, R., R. Ashraf, R. Naz, S. A. Hussain, and M. H. Chaudhry (2005), *Inventory of glaciers*

and glacial lakes outburst floods (GLOFs) affected by global warming in the mountains of Himalayan region, Indus Basin, Pakistan Himalaya., Kathmandu, Nepal.

- Rupa Kumar, K., A. K. Sahai, K. Krishna Kumar, S. K. Patwardhan, P. K. Mishra, J. V. Revadekar, K. Kamala, and G. B. Pant (2006), High-resolution climate change scenarios for India for the 21st century, *Curr. Sci.*, 90(3), 334–345.
- Sah, M., G. Philip, P. K. Mool, S. R. Bajracharya, and B. Shrestha (2005), *Inventory of glaciers and glacial lakes and the identification of potential glacial lake outburst floods (GLOFs) affected by global warming in the mountains of Himalayan region: Uttaranchal Himalaya, India.*, Kathmandu, Nepal.
- Schaner, N., N. Voisin, B. Nijssen, and D. P. Lettenmaier (2012), The contribution of glacier melt to streamflow, *Environ. Res. Lett.*, 7, 034029, doi:10.1088/1748-9326/7/3/034029.
- Scherler, D., B. Bookhagen, and M. R. Strecker (2011a), Spatially variable response of Himalayan glaciers to climate change affected by debris cover, *Nat. Geosci.*, 4(3), 156–159, doi:10.1038/ngeo1068.
- Scherler, D., B. Bookhagen, and M. R. Strecker (2011b), Spatially variable response of Himalayan glaciers to climate change affected by debris cover, *Nat. Geosci.*, 4(3), 156–159, doi:10.1038/ngeo1068.
- Schmidli, J., C. Frei, and P. L. Vidale (2006), Downscaling from GCM precipitation: a benchmark for dynamical and statistical downscaling methods, *Int. J. Climatol.*, 26(5), 679–689, doi:10.1002/joc.1287.
- Schneider, U., A. Becker, P. Finger, A. Meyer-Christoffer, M. Ziese, and B. Rudolf (2013), GPCP's new land surface precipitation climatology based on quality-controlled in situ data and its role in quantifying the global water cycle, *Theor. Appl. Climatol.*, 26, doi:10.1007/s00704-013-0860-x.
- Shaman, J., and E. Tziperman (2005), The Effect of ENSO on Tibetan Plateau Snow Depth: A Stationary Wave Teleconnection Mechanism and Implications for the South Asian Monsoons, *J. Clim.*, 18(12), 2067–2079, doi:10.1175/JCLI3391.1.
- Sharif, M., D. R. Archer, H. J. Fowler, and N. Forsythe (2013), Trends in timing and magnitude of flow in the Upper Indus Basin, *Hydrol. Earth Syst. Sci.*, 17(4), 1503–1516, doi:10.5194/hess-17-1503-2013.
- Sharmila, S., S. Joseph, a. K. Sahai, S. Abhilash, and R. Chattopadhyay (2015), Future projection of Indian summer monsoon variability under climate change scenario: An assessment from CMIP5 climate models, *Glob. Planet. Change*, 124, 62–78, doi:10.1016/j.gloplacha.2014.11.004.
- Shea, J. M., W. W. Immerzeel, P. Wagnon, C. Vincent, and S. Bajracharya (2015), Modelling glacier change in the Everest region, Nepal Himalaya, *Cryosph.*, 9(3), 1105–1128, doi:10.5194/tc-9-1105-2015.
- Shrestha, M., L. Wang, T. Koike, Y. Xue, and Y. Hirabayashi (2012), Modeling the Spatial Distribution of Snow Cover in the Dudhkoshi Region of the Nepal Himalayas, *J. Hydrometeorol.*, 13(1), 204–222, doi:10.1175/JHM-D-10-05027.1.
- Shrestha, M., T. Koike, Y. Hirabayashi, Y. Xue, L. Wang, G. Rasul, and B. Ahmad (2015), Integrated simulation of snow and glacier melt in water and energy balance-based, distributed hydrological modeling framework at Hunza River Basin of Pakistan Karakoram region, *J. Geophys. Res. Atmos.*, 120(10), 4889–4919, doi:10.1002/2014JD022666.
- Singh, K., P. Datt, and V. Sharma (2011), Snow depth and snow layer interface estimation using Ground Penetrating Radar, *Curr. Sci. ...*, 100(10).
- Singh, K. K., A. Kumar, A. V Kulkarni, P. Datt, S. K. Dewali, V. Kumar, and R. Chauhan (2015), Snow depth estimation in the Indian Himalaya using multi-channel passive microwave radiometer, *Curr. Sci.*, 108(5), 942.
- Singh, P., and S. K. Jain (2002), Snow and glacier melt in the Satluj River at Bhakra Dam in the western Himalayan region, *Hydrol. Sci. J.*, 47(1), 93–106,

doi:10.1080/02626660209492910.

- Soncini, A., D. Bocchiola, G. Confortola, A. Bianchi, R. Rosso, C. Mayer, A. Lambrecht, E. Palazzi, C. Smiraglia, and G. Diolaiuti (2015), Future Hydrological Regimes in the Upper Indus Basin: A Case Study from a High-Altitude Glacierized Catchment, *J. Hydrometeorol.*, 16(1), 306–326, doi:10.1175/JHM-D-14-0043.1.
- Sperber, K. R., and H. Annamalai (2014), The use of fractional accumulated precipitation for the evaluation of the annual cycle of monsoons, *Clim. Dyn.*, 43(12), 3219–3244, doi:10.1007/s00382-014-2099-3.
- Sperber, K. R., H. Annamalai, I. S. Kang, A. Kitoh, A. Moise, A. Turner, B. Wang, and T. Zhou (2013), The Asian summer monsoon: An intercomparison of CMIP5 vs. CMIP3 simulations of the late 20th century, *Clim. Dyn.*, 41(9-10), 2711–2744, doi:10.1007/s00382-012-1607-6.
- Strozzi, T., A. Kouraev, A. Wiesmann, U. Wegmüller, A. Sharov, and C. Werner (2008), Estimation of Arctic glacier motion with satellite L-band SAR data, *Remote Sens. Environ.*, 112(3), 636–645, doi:10.1016/j.rse.2007.06.007.
- Sund, M., T. R. Lauknes, and T. Eiken (2014), Surge dynamics in the Nathorstbreen glacier system, Svalbard, *Cryosph.*, 8(2), 623–638, doi:10.5194/tc-8-623-2014.
- Surendra, K. C., S. K. Khanal, P. Shrestha, and B. Lamsal (2011), Current status of renewable energy in Nepal: Opportunities and challenges, *Renew. Sustain. Energy Rev.*, 15(8), 4107–4117, doi:10.1016/j.rser.2011.07.022.
- Suzuki, R., K. Fujita, and Y. Ageta (2007), Spatial distribution of thermal properties on debris-covered glaciers in the Himalayas derived from ASTER data, *Bull. Glaciol. Res.*, 24, 13–22.
- Tahir, A. A., P. Chevallier, Y. Arnaud, and B. Ahmad (2011), Snow cover dynamics and hydrological regime of the Hunza River basin, Karakoram Range, Northern Pakistan, *Hydrol. Earth Syst. Sci.*, 15(7), 2275–2290, doi:10.5194/hess-15-2275-2011.
- Taylor, K. E., R. J. Stouffer, and G. A. Meehl (2012), An Overview of CMIP5 and the Experiment Design, *Bull. Am. Meteorol. Soc.*, 93(4), 485–498, doi:10.1175/BAMS-D-11-00094.1.
- Terink, W., R. Hurkmans, R. Uijlenhoet, and P. Torfs (2010), Bias correction of downscaled precipitation and temperature reanalysis data for the Rhine Basin, *Hydrol. Earth Syst. Sci.*, 14, 687–703.
- Themeßl, M. J., A. Gobiet, and A. Leuprecht (2011a), Empirical-statistical downscaling and error correction of daily precipitation from regional climate models, *Int. J. Climatol.*, 31(10), 1530–1544, doi:10.1002/joc.2168.
- Themeßl, M. J., A. Gobiet, and A. Leuprecht (2011b), Empirical-statistical downscaling and error correction of daily precipitation from regional climate models, *Int. J. Climatol.*, 31(10), 1530–1544, doi:10.1002/joc.2168.
- Themeßl, M. J., A. Gobiet, and G. Heinrich (2011c), Empirical-statistical downscaling and error correction of regional climate models and its impact on the climate change signal, *Clim. Change*, 112(2), 449–468, doi:10.1007/s10584-011-0224-4.
- Uddin, S. N., R. Taplin, and X. Yu (2007), Energy, environment and development in Bhutan, *Renew. Sustain. Energy Rev.*, 11(9), 2083–2103, doi:10.1016/j.rser.2006.03.008.
- Ukita, J. et al. (2011), Glacial lake inventory of Bhutan using ALOS data: Methods and preliminary results, *Ann. Glaciol.*, 52(58), 65–71, doi:10.3189/172756411797252293.
- Vaidya, R. (2012), Water and Hydropower in the Green Economy and Sustainable Development of the Hindu Kush-Himalayan Region., *Hydro Nepal J. Water, Energy Environ.*, (10), 11–19.
- Veettil, B. K., N. Bianchini, A. M. de Andrade, U. F. Bremer, J. C. Simões, and E. de Souza Junior (2015), Glacier changes and related glacial lake expansion in the Bhutan Himalaya, 1990–2010, *Reg. Environ. Chang.*, doi:10.1007/s10113-015-0853-7.

- Viste, E., and A. Sorteberg (2015), Snowfall in the Himalayas: an uncertain future from a little-known past, *Cryosph.*, 9(3), 1147–1167, doi:10.5194/tc-9-1147-2015.
- Vuuren van, D. P. et al. (2011a), The representative concentration pathways: an overview, *Clim. Change*, 109(1-2), 5–31, doi:10.1007/s10584-011-0148-z.
- Vuuren van, D. P. et al. (2011b), The representative concentration pathways: an overview, *Clim. Change*, 109(1-2), 5–31, doi:10.1007/s10584-011-0148-z.
- Wagnon, P. et al. (2007), Four years of mass balance on Chhota Shigri Glacier, Himachal Pradesh, India, a new benchmark glacier in the western Himalaya, *J. Glaciol.*, doi:10.3189/002214307784409306.
- Wagnon, P. et al. (2013), Seasonal and annual mass balances of Mera and Pokalde glaciers (Nepal Himalaya) since 2007, *Cryosph.*, doi:10.5194/tc-7-1769-2013.
- Wang, W., Y. Xiang, Y. Gao, A. Lu, and T. Yao (2015), Rapid expansion of glacial lakes caused by climate and glacier retreat in the Central Himalayas, *Hydrol. Process.*, 29(6), 859–874, doi:10.1002/hyp.10199.
- Wilcke, R. A. I., T. Mendlik, and A. Gobiet (2013), Multi-variable error correction of regional climate models, *Clim. Change*, 120(4), 871–887, doi:10.1007/s10584-013-0845-x.
- Wu, L., T. Che, R. Jin, X. Li, T. Gong, and Y. Xie (2005), *Inventory of glaciers, glacial lakes and the identification of potential glacial lake outburst floods (GLOFs) affected by global warming in the mountains of Himalayan region: Pumqu, Rongxer, Poiqu, Zangbuqin, Jilongcangbu, Majiacangbu, Daoliqu, and Jiazha*, Kathmandu, Nepal.
- Xiang, Y., Y. Gao, and T. Yao (2014), Glacier change in the Poiqu River basin inferred from Landsat data from 1975 to 2010, *Quat. Int.*, 349, 1–10, doi:10.1016/j.quaint.2014.03.017.
- Yang, W., T. Yao, B. Xu, G. Wu, L. Ma, and X. Xin (2008), Quick ice mass loss and abrupt retreat of the maritime glaciers in the Kangri Karpo Mountains, southeast Tibetan Plateau, *Chinese Sci. Bull.*, 53(16), 2547–2551, doi:10.1007/s11434-008-0288-3.
- Yao, T. et al. (2012), Different glacier status with atmospheric circulations in Tibetan Plateau and surroundings, *Nat. Clim. Chang.*, doi:10.1038/nclimate1580.
- Zemp, M. et al. (2013), Reanalysing glacier mass balance measurement series, *Cryosph.*, 7(4), 1227–1245, doi:10.5194/tc-7-1227-2013.
- Zhang, G. et al. (2013a), Energy and mass balance of Zhadang glacier surface, central Tibetan Plateau, *J. Glaciol.*, 59(213), 137–148, doi:10.3189/2013JoG12J152.
- Zhang, G., T. Yao, H. Xie, W. Wang, and W. Yang (2015), An inventory of glacial lakes in the Third Pole region and their changes in response to global warming, *Glob. Planet. Change*, 131, 148–157, doi:10.1016/j.gloplacha.2015.05.013.
- Zhang, T., C. Xiao, W. Colgan, X. Qin, W. Du, W. Sun, Y. Liu, and M. Ding (2013b), Observed and modelled ice temperature and velocity along the main flowline of East Rongbuk Glacier, Qomolangma (Mount Everest), Himalaya, *J. Glaciol.*, 59(215), 438–448, doi:10.3189/2013JoG12J202.
- Zhao, L., R. Ding, and J. C. Moore (2014), Glacier volume and area change by 2050 in high mountain Asia, *Glob. Planet. Change*, 122, 197–207, doi:10.1016/j.gloplacha.2014.08.006.